NASA Innovative Advanced Concepts (NIAC) Phase II
80HQTR20NOA01-20NIAC-A2

GRAVITY OBSERVATION AND DARK ENERGY DETECTION EXPLORER IN THE SOLAR SYSTEM

FINAL REPORT

NIAC Fellow, Nan Yu[1]
Study Participants: Rashied Amini[1], Phil Bull[1], Yanbei Chen[3], Sheng-wey Chiow[1], Curt J. Cutler[1], Olivier Doré[1], Jérôme Gleyzes[1], Jeffrey B. Jewell[1], Holger Müller[2], Kristofer M. Pardo[4], Jason Rhodes[1], Ashmeet Singh[5], and Slava Turyshev[1]

[1]*Jet Propulsion Laboratory, California Institute of Technology, 4800 Oak Grove Drive, Pasadena, CA 91109-0899, USA*

[2]*University of California, Berkeley, CA*

[3]*California Institute of Technology, Pasadena, CA*

[4]*University of Southern California, Los Angeles, CA*

[5]*Whitman College, Walla Walla, WA*

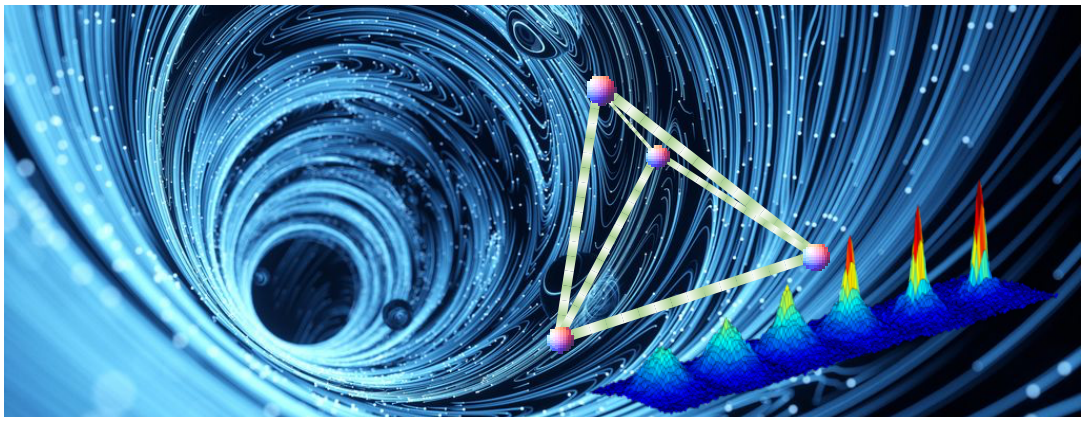

The Gravity Probe and Dark Energy Detection Mission (GDEM) mission is a proposed ambitious multi-science mission in gravity and dark energy measurements using a tetrahedral spacecraft formation 1 AU from the Sun. Leveraging atomic drag-free test masses, the atom interferometer quantum sensor approach, and laser ranging for precise measurements, the mission will focus on the scalar force gradient tensor's trace, unaffected by standard gravitational forces. This scientifically and technologically feasible 3-year mission in the solar system promises to provide significant evidence of the cubic Galileon field as a possible source for dark energy and a model agnostic test of the gravity inverse square law in general. At the same time, it provides a rich set of measurement data for mid-band gravitational wave detection, dark matter detection, precise measurements of solar gravity and detection of unknown solar system bodies.

Jet Propulsion Laboratory
4800 Oak Grove Drive MS 298-310, Pasadena, CA 91109-8099
nan.yu@jpl.nasa.gov

June 25, 2024

EXECUTIVE SUMMARY:

Understanding the accelerating expansion of the universe and the nature of dark energy, which constitutes ~70% of the universe's mass-energy, is a fundamental challenge in cosmology and fundamental physics in general. This accelerating expansion contradicts quantum field theory, indicating that solutions might lie outside Einstein's general theory of relativity (GR), the century old theory of gravity which underpins cosmology. The cosmological constant problem, still unsolved, can be addressed by invoking light scalar fields that interact with normal matter. These fields are thought to be as light as the Hubble scale ($H_0 \approx 10^{-33}$ eV) and interact with standard model particles and fields with a strength comparable to gravity. Such characteristics are essential for these fields to significantly impact the universe's evolution and address the discrepancies in the cosmological constant.

To overcome the challenges of understanding and detecting the light scalar fields introduced by dark energy, in our NIAC Phase II study we examined the use of a tetrahedral spacecraft formation in unperturbed heliocentric orbits for detecting small spatial variations in the gravitational field, particularly in the gravity gradient tensor (GGT) trace. This configuration's high sensitivity, potentially reaching ~O(10^{-24} s^{-2}), allows for probing new physics, such as deviations from general relativity that could manifest in a non-zero trace of the GGT.

This report summarizes results of our NIAC Phase II study focusing on a mission design that will be able to detect potential new physics by precisely measuring the trace of the GGT using a tetrahedral formation of spacecraft on heliocentric orbits. The objective is to observe a non-zero trace and small spatial changes in the gravitational field, which might indicate deviations from GR, with the potential to detect effects predicted by recent cosmological models. The feasibility of achieving the required sensitivity to measure the trace of the GGT is demonstrated, along with a discussion on the impact of the tetrahedral formation's dynamical behavior on measurement quality.

The Gravity Probe and Dark Energy Detection Mission (GDEM) mission involves placing four spacecraft in a tetrahedral formation on elliptical heliocentric orbits. This configuration is designed to maximize the sensitivity and spatial resolution of the GGT measurements in a flexible formation configuration. GDEM's feasibility has been supported by technological advancements in spacecraft formation flying, laser interferometric ranging techniques, the development of robust data analysis methods, and in particular atomic test mass-based quantum inertial sensor technology. Implementation of the GDEM is enabled by 1) Precise formation flying in a tetrahedral configuration for optimal sensitivity with flexible formation flight. 2) Precision laser ranging to accurately measure the distances between spacecraft. 3) Use of atom-wave interferometry (AI) to correct for local non-gravitational disturbances and enhance the precision of gravitational measurements. 4) Sagnac interferometry for accurately determining the angular velocity of the formation, essential for maintaining the tetrahedral configuration and interpreting the gravitational data.

We reached or exceeded all objectives set for our Phase II study: We studied the trace of GGT, utilizing precision laser ranging for inter-satellite measurements and atom-wave interferometry to counter non-gravitational disturbances. We have improved and validated the use of AI techniques for high-precision gravitational measurements and their role in enabling the measurements of non-gravitational forces. Our approach includes developing analytical models and formulating observational equations specifically for measuring the GGT's trace within this formation. We developed comprehensive analytical models to interpret the GGT data accurately and efficiently. We also investigated the impact of the tetrahedral formation's dynamical behavior, as its orientation and shape evolve over the orbits. Additionally, we highlight Sagnac interferometry's role in enhancing

measurement accuracy, surpassing other navigational techniques in determining the formation's angular frequency relative to an inertial frame. We simulated mission performance and demonstrating the feasibility of the tetrahedral spacecraft formation and measurement techniques. In additional to the GGT trace measurements for detecting signs of dark energy scalar field, we explored use of the GDEM measurement data for other science analyses including mid-band gravitational wave detection, dark matter detection, as well as precision Newtonian gravity measurements in general in the solar system.

Under the Phase II NIAC program, we confirmed the feasibility of the tetrahedron-based technique for direct detection of the small forces in the solar system beyond the current levels of sensitivity by 6 orders of magnitude, yielding technology readiness level (TRL) of TRL 3. Our tetrahedron architecture with all internal measurements allows most flexible mission design and optimization. We investigated different ways to deploy and utilize AI quantum sensors for spacecraft drag reduction and/or removal. A simpler concept of implementation of atomic test masses away from spacecraft in space vacuum was formulated and space environment impact has been shown not a showstopper.

In this Report we describe the mission architecture and the relevant technology steps, which we can begin today, that would allow the launch of a GDEM pathfinder mission by 2028-2030 and the full science mission in 10 years following the completion of other major dark energy missions in development and operation today. The GDEM CONOPS could use multiple small satellites that will rely on the use of AI technologies to operate interdependently. Further mission development will allow us build in mission flexibility, reduce risk, and drive down mission cost.

We used physics-based analytical tools to define the trajectories around the Sun. We addressed the position, navigation, and timing (PNT) requirements by extending the capabilities of the NASA's Deep Space Network (DSN) to include Sagnac interferometry. The design of the spacecraft (s/c) utilized a concurrent engineering methodology tool yielding a robust design.

AI quantum sensor performances are based on advanced operation concepts with high atom flux sources, large momentum transfer, and longer interrogation times afforded in space microgravity environment. The proof of concept of these advanced technical approaches have been demonstrated in laboratory setting. What is needed is to have space environmental to have full advanced AI capability and feasibility demonstration in space. NASA CAL has already pioneered cold atom experiments in space on ISS and AI demonstration. Other AI based space instrument/mission concepts are in active development. GDEM mission can heavily leverage on these developments in time for the mission implementation.

We concluded that most of the technologies for GDEM mission either already exist (rideshare/cluster launch, space laser interferometry, RF/optical comm, all at TRL9), are at intermediate levels of readiness: swarm operations (TRL5), terabit onboard processing (either FPGA or GPU, TRL 9/7), CONOPS (TRL7), or in active developments in at NASA and around the world. What is missing is the system approach to assemble all these technologies for autonomous operations in deep space (TRL3). There is a clear path on how to close this gap, maturing the GDEM concept to TRL 4-5.

This GDEM architecture design may lead to a reduction of the mission's cost in many ways: 1) It cuts the cost of mission by enabling broad choices of funding, building, deploying, operating, and analyzing system elements. 2) It delivers economies of scale in an architecture relying on duplicative production to minimize recurring costs. 3) It applies maturing technologies to allow autonomous mission execution, eliminating the need for operator-intensive mission management, and (4)

It reduces launch costs by relying on "rideshare" opportunities to launch the spacecraft, avoiding the costs of large, dedicated launchers.

The results of our NIAC Phase II study are encouraging as they lead to a realistic design for a mission that will be able to detect new forces in the solar system. The spacecraft tetrahedral configuration and measurement techniques of GDEM, specifically precision laser ranging and atom-interferometry, will allow reaching the target sensitivity of $\sim O(10^{-24}\,s^{-2})$ for GGT detection. It could allow exploration of new physics in the solar system relying on the GDEM capabilities within the next decade relying on new and extant technologies. The architecture and mission concepts for a mission to the GDEM, at this early stage, are promising and should be explored further.

TABLE OF CONTENTS:

1 INTRODUCTION

1.1 Mission Objectives and Science Significance

The accelerating expansion of the universe presents a significant challenge in cosmology, particularly in understanding the physical nature of 'dark energy', which accounts for nearly 70% of the universe's total mass-energy. This phenomenon challenges current quantum field theory, which predicts a significantly higher density of dark energy than observed. Addressing this "cosmological constant problem", likely requires a paradigm shift in gravitational theory (Copeland et al., 2006). Current research suggested solutions may involve light scalar fields, with masses at or below the Hubble scale ($H_0 \approx 10^{-33}$ eV). These fields are theorized to interact with standard model particles with a gravitational-strength coupling. Such interactions could crucially modify the large contributions of the standard model vacuum to the cosmological constant, offering a plausible resolution to this fundamental issue in physics.

Light scalar fields coupling to matter with gravitational strength can introduce 'fifth forces'. However, their effects must be significantly suppressed in the solar system, consistent with current technological and experimental limits, to avoid contradicting established tests of General Relativity. Some dark energy theories address this by implementing environment-dependent interactions between matter and dark energy fields, a process known as screening. This method adjusts the coupling strength in areas of high matter density (Joyce, et al., 2015). Detecting such a coupling would be a groundbreaking discovery, opening new avenues for exploring dark energy and understanding the cosmos.

Screening mechanisms in scalar field theories fall into two categories: those dependent and those independent of local mass densities. Theories like chameleon and symmetron, relying on local mass densities, exhibit a 'thin shell effect' where only an object's very outer layer interacts with dark energy fields (Joyce, et al., 2015), diminishing the overall dark energy impact and allowing gravity to dominate. Precision lab experiments can detect this short-range force, especially in atoms where the thin shell exceeds their radius, leading to partial unscreening. Recent advancements have significantly narrowed the parameter spaces for these models. Moreover, conducting these experiments in space's microgravity could further refine our understanding of thin shell models (Chiow and N. Yu., 2018).

The Vainshtein screening mechanism, involving a 'Galileon' field, represents a distinct category of scalar field theories. Characterized by highly nonlinear equations of motion, its nonlinearity strength is determined by a coupling constant r_c. The Galileon force diminishes like gravity ($1/r^2$) far from matter but weakens more slowly ($1/r^{1/2}$ for cubic Galileon) near it. The expansive Vainshtein radius, spanning hundreds of parsecs, makes ground lab tests unfeasible. Experimental

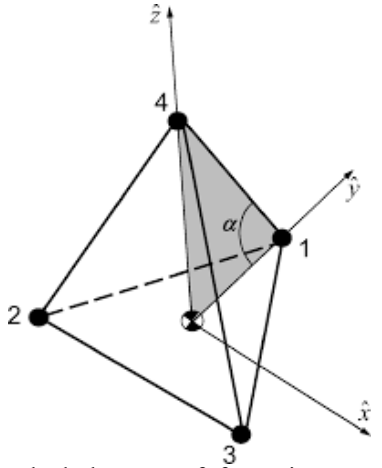

Figure 1. Tetrahedral spacecraft formations on stable heliocentric orbits are used for precise measurements of the gravity gradient tensor (GGT), potentially revealing new physics through observable deviations from general relativity. We aim to detect GGT traces with a sensitivity of $O(10^{-24}\,s^{-2})$, aligning with predictions from recent cosmological models.

constraints on r_c are currently limited to lunar laser ranging and gravitational wave observations.

In cosmology, the Galileon concept has emerged as a compelling theoretical framework, particularly as a potential explanation for dark energy. Originating from the idea of modifying gravity, Galileons are a class of scalar fields that arise in the context of higher-dimensional theories and possess certain symmetries. These fields have been studied for their unique properties and interactions that do not arise in standard models of particle physics or general relativity.

The appeal of the Galileon concept lies in its ability to potentially explain the accelerated expansion of the universe without invoking the dark energy concept in the more traditional sense. Instead, the modifications to gravity introduced by Galileon fields could account for the observations attributed to dark energy. The Galileon model proposes that these fields can affect the cosmic expansion rate and structure formation in the universe, providing an alternative route to understanding cosmic acceleration.

Galileons are particularly interesting because they generally lead to self-accelerating solutions without the need for fine-tuning, addressing some of the naturalness problems associated with the cosmological constant. Furthermore, they have been found to evade common issues like ghost instabilities, which often plague other modified gravity theories. Their interactions are designed to become significant on large scales, such as cosmic scales, while remaining unnoticeable at shorter distances, making them consistent with solar system tests of gravity. However, the Galileon concept is not without challenges and remains an active area of investigation. Precise measurements and observations, particularly those concerning the growth of cosmic structures and the expansion history of the universe, are crucial for testing the viability of Galileon models and understanding their implications for cosmology. High-precision measurements of the gravitational field could offer invaluable data to test Galileon theories and further our understanding of the dark energy.

In our NIAC study, we focus on detecting the Galileon dark energy field within the Vainshtein model as a benchmark science scenario, using the solar system as a laboratory. Our mission concept entails using a tetrahedral spacecraft formation, about 1 AU from the Sun, for precise measurements of the scalar force gradient tensor's trace, unaffected by the stronger, traceless gravitational field (Figure 1). We employ the novel and enabling atomic test masses and atom interferometers for accurate inertial referencing, and laser ranging interferometers for connecting spacecraft and measuring differential gradient forces.

- The initial motivation for the NIAC study was the direct detection of dark energy, a compelling and mysterious force driving the accelerated expansion of the universe. However, throughout Phase I of the research, it became evident that the mission concept and science products have the potential to be much broader and more diverse than initially anticipated. This realization expanded the science scope of the mission significantly in Phase II study.
- The mission's potential was extended to include formulating more model-agnostic Inverse Square Law (ISL) measurements. These measurements are critical in testing the variations or deviations from the traditional Newtonian gravity, which could provide insights into new physics or modifications of gravity at different scales. This approach allows the mission to remain flexible and adaptable to various theoretical frameworks, rather than being tightly bound to specific models of dark energy or modified gravity.
- Additionally, the expanded scope includes probing for dark matter, another elusive aspect of the universe that, much like dark energy, remains one of the great mysteries in modern astrophysics. Understanding dark matter is crucial for comprehending the structure and evolution of the universe, and direct detection or improved constraints can significantly advance the field.

The mission also aims to contribute to gravitational wave (GW) astronomy by providing measurements that could complement observations from current and future gravitational wave detectors. This could open new windows into studying cosmic events and testing the GR.

- The expansion of the mission concept to include precision Newtonian gravity measurements within the solar system marks a significant advancement in the GDEM's scientific capabilities. These measurements are crucial for a refined understanding of the gravitational forces that govern planetary and satellite dynamics, interactions between solar system bodies, and the behavior of space debris and minor bodies. By providing accurate measurements of gravitational fields, GDEM aims to test and potentially refine our understanding of general relativity, as well as explore alternative theories of gravity that might arise in different regimes or scales.

This evolution from a singular focus on direct dark energy detection to a versatile mission capable of addressing a wide array of astrophysical and cosmological phenomena reflects the dynamic and iterative nature of scientific inquiry. What starts as a pursuit to answer a specific question often unfolds into a journey uncovering a range of scientific opportunities and mysteries.

The Gravity Observation and Dark Energy Detection Explorer (GDEM) is thus envisioned as a pioneering mission. Its comprehensive approach in measuring various aspects of gravitational physics is indeed unique and sets a new precedent in space missions dedicated to fundamental physics. The ambitious nature of GDEM, coupled with its potential to provide unprecedented insights into dark energy, dark matter, gravitational waves, and the laws of gravity, underscores its significance as a next-generation mission in fundamental physics and cosmology, complementing traditional astrophysical telescope-based observational approaches. Its development represents a bold step into the future of deep space exploration and scientific discovery.

1.2 Phase I Study – Key Points

The main objective of our Phase I effort was the development of the overall mission concept with atom interferometer sensor as the enabling technology Details of the results can be found in the Phase I final report (Yu et al., 2018). The key findings are summarized below as the starting point in the Phase II study:

- Recognizing the challenges of detecting the dark energy force that is 10 orders of magnitude smaller than that of the gravitational force in the solar system, we have formulated an overall measurement strategy by focusing on the trace of GGT with the overwhelming gravitation field GGT vanishing to zero. It becomes a more general search of a violation of the inverse square law of the Newtonian gravity.
- For the precision GGT measurements, we proposed to use atomic test masses and atom interferometer quantum sensors for acceleration measurements, leveraging their measurement sensitivity and accuracy over traditional bulk proof mass schemes. Our analyses showed that, with the advanced atom interferometer schemes, we will be able to meet the science measurement requirements.
- For the GGT differential measurements between the long baseline spacecraft, we developed the concept of tetrahedral satellite measurement formation that offer the most robust formation-flying configuration with minimal number of spacecraft. The tetrahedral formation allows the determination of GGT in any orientation so minimal formation maintenance is necessary.

- To mitigate the s/c self-gradient drag forces, we investigated the feasibility of operating the atomic test mass far away from spacecraft in space vacuum and identified key space environment factors to address.
- Based on the science requirements and accelerometer instrument capabilities, we did preliminary trade off studies for optical science signal detection for the given instrument sensitivity and determine the tetrahedral formation should be flown around about 1 AU from the Sun.
- We developed the corresponding requirements for the inter-satellite ranging requirements in turns of the Doppler and absolute range measurements.
- It also became clear in Phase I study that the inter-satellite measurements can be used and analyzed for other important science investigations such as gravitational wave detection at the mid-band.
- The Phase I study concluded with a viable measurement scheme and the "GODDESS" mission concept[1] going forward for further studies.

1.3 Approach for Phase II

During Phase II, we expanded the science scope for the GDEM and continued to explore the topics for a robust concept, including refinement of the mission architectures by taking them through simulations and design trades. Specifically, we considered the following eight major topics:

1. We investigated the science operations in support of the primary objectives of high-precision measurements of the race of the GGT. For that, we confirmed the feasibility for a sensitivity level of $O(10^{-24}\ s^{-2})$ to detect potential new physics through the trace of the GGT.
2. We studied a science measurement configuration comprising a four small spacecraft, each moving at a slightly different trajectory but each on a highly eccentric heliocentric orbit. We analyzed tetrahedral spacecraft formation, its dynamical behavior, and conditions for an optimal tetrahedral configuration of four spacecraft in elliptical orbits around the Sun.
3. We considered precision laser ranging for accurate inter-satellite measurements and clearly defined the critical roles of AI to correct local non-gravitational disturbances.
4. We determined the feasibility of operating the AI in space vacuum for mitigating the atomic test mass drag requirements and long-boom implementation trade study.
5. We developed models for relevant observables and formulated observational equations, particularly utilizing laser ranging and Sagnac interferometry. In fact, we identified and utilized Sagnac interferometry as a key capability for measuring the angular frequency of the tetrahedron's rotation with high accuracy. We investigated the effect of the tetrahedron's evolving orientation and shape on the quality of scientific measurements.
6. We established preliminary mission and instrument requirements necessary to measure the trace of the GGT and validate the feasibility of the mission objectives.
7. We studied mission design: i) flight system and science requirements; ii) key mission, system, operations concepts, and technology drivers; iii) description of mission and small craft concepts to enable GDEM; and iv) study instruments and systems for the GDEM spacecraft, including power, comm, navigation, propulsion, pointing, and coronagraph.
8. We conducted trade studies with a set of key driving parameters: a) heliocentric distance along the GDEM, b) telescope aperture, c) integration time, d) detector type and sensitivity, etc.

[1] The mission naming of "GODDESS" has been changed to GDEM in the Phase II study.

9. We identified the cost drivers and how to make the concept affordable – specifically to look into small low-cost spacecraft without precision drag-free control, launch service by adopting "rideshare" principles, eliminate/reduce the need for formation maintenance, and distribute the cost among many stakeholders over the program life cycle.

1.4 Phase II Result Highlights

We now have a good understanding of the GDEM performance from the tetrahedral formation configuration (Turyshev et al., 2023). We reduced the space environmental concern of operating atomic quantum sensors in open space vacuum (Chiow et al. 2023). We identified i) key mission requirements; ii) novel and unique means to obtain a high-precision measurements of the trace of the GGT; iii) new robust formation architecture of interplanetary spacecraft. The Phase II work extended the results of the Phase I effort with the necessary refinements. To date, all results look promising with no obvious showstoppers. Scientific objectives are achievable. Technological considerations with regards to mission architecture, instruments, comm, etc. also look feasible. We now understand better the complexities of developing and operating GDEM mission to provide high-precision gravity measurements. The cost of such a mission is beyond the Phase II effort and will be assessed in post-phase II efforts.

The key results are summarized below:

1. The Phase II study confirmed the GDEM mission capable of multi-science exploration. We not only validated the mission architecture that can meet the requirements for detecting Galileon dark energy field forces, but it can also make statements and new limits on the other dark energy thin shell models. Furthermore, we estimated the gravitational wave detection sensitivity and explored the possibility of dark matter detection.
2. The GDEM mission architecture was formulated that included its orbit choice and design, science measurement payload concept for optical interferometer ranging and atom interferometer accelerometers, as well as notional launch configuration, options, and requirements.
3. Mission architecture based on a tetrahedral spacecraft in which 4 small s/c follow nearly identical heliocentric orbits with nominal separation of 1000 km at about 1 AU distance. The eccentricity was selected to provide spatial modulation of the dark energy forces while still allow formation spacecraft free flying with minimal maintenance.
4. Detailed analysis of the error budget due to the nonlinearity of the gravity gradient in the solar system has been mitigated through the total internal measurements and modeling such that the error is no longer a dominating issue.
5. Estimates of the laser interferometer link budget with a given laser transmitters similar to those in the LISA mission.
6. Detailed analysis and estimates of the solar UV radiation ionization effects on atomic test masses in space vacuum and the finding that the UV ionization and resulting atom loss and phase shifts have minimal impact on the performance of the atom interferometers,
7. Recognized and addressed the impact of second-order tidal effects on measurements. The study's findings emphasize the importance of considering these effects for improving experimental accuracy, contributing to a more robust and reliable mission design.
8. Development of analytical expressions that capture the complex dynamics of a tetrahedral spacecraft formation in nearby elliptic heliocentric orbits. We studied systematic volume collapses of the tetrahedral formation during each orbital transition, that significantly influencing

measurement sensitivity and precision. Accordingly, developed strategies for maintaining formation stability and measurement accuracy.

9. Advanced the measurement concept maturity by the use of Sagnac observables, a significant improvement over traditional measurement techniques. The integration of these observables helps in accurately accounting for and correcting rotational discrepancies, enhancing the overall measurement precision.
10. As a result of the realization of Sagnac observables from the closed loop inter-satellite laser interferometers for the rotational effects, we eliminated the needs for direct inter-satellite atom interferometer differential measurements and associated implementation challenges.
11. Tackled the challenges of significant angular variations between spacecraft due to the formation's evolution. The necessity for gimbals with wide articulation ranges was identified, leading to the development of appropriate techniques for continuous and stable operation.
12. Overall, we validated the feasibility of a tetrahedral satellite constellation to achieve high-precision measurements of the gravitational field, aiming for a sensitivity in measuring the trace of the GGT on the order of ~(10^{-24} s^{-2}). We concluded the feasibility of the GDEM within current technological capabilities, with the potential to uncover non-Einsteinian gravitational physics and revolutionize our understanding of gravitational phenomena.

The rest of the Final Report is structured as follows: In Section 2 we briefly describe the science motivations for the mission focusing on direction detection of dark energy. In Section 3, we describe the enabling technologies and innovations relevant to the mission concept and measurement approach. Section 4 presents the overall mission concept and measurement requirements. In Section 5, we describe the mission designs and analysis and their significances as well as possible data analysis for other science investigations. The result concludes with Section 6 summarizing the results we obtained during Phase II. We also present recommendations and approach for transition strategy to realize missions to GDEM.

2 SEARCHING FOR NEW PHYSICS IN THE SOLAR SYSTEM

2.1 Why Do We Need GDEM?

Einstein's general relativity has passed stringent tests via solar system observations and lab experiments, showing no violations. For dark energy scalar field models to align with these observations, they must incorporate a screening mechanism. These models predict a dark energy force on non-cosmological scales, like the solar system, that is significantly weaker than gravity—estimated to be ten orders of magnitude (10^{10} times) weaker (Berezhiani et al., 2003).

However, the gravitational force's strength, defined by the gravitational constant *G*, is only accurate to five decimal places. Detecting a smaller deviation directly off the gravitational force would not be possible without a much more precise determination of G or M*G product. It also necessitates strategies to distinguish the weak dark energy force from the dominant gravitational forces, alongside a thorough understanding of screening mechanisms and the influence of matter on the dark energy field.

Our NIAC study concentrates on developing a mission concept that significantly reduces gravity effects, utilizing innovative atom interferometer force sensors. We're investigating differential measurement setups to minimize gravitational influences while preserving potential dark energy signals. This mission concept has undergone thorough science and engineering feasibility analyses. To further aid the study, concurrently, funded internally by JPL and outside the NIAC scope, we

advanced our understanding of how the Vainshtein field is affected by solar system bodies. This research aims to pinpoint where dark energy force might be detectable (Andrews, Chu & Trodden, 2013). The findings inform our mission design, helping us determine the most effective spacecraft orbits and measurement configurations.

GDEM is conceived as complementary to the observational cosmology in fully deciphering the nature of dark energy, even as we expect a wealth of data from upcoming dark energy telescopes. Recognizing that a comprehensive understanding of dark energy's inherent properties might require direct measurement approaches, the GDEM aims to measure the trace of the GGT to detect possible signs of new physics. This is particularly pertinent in exploring theories where dark energy is hypothesized as a new field, providing a direct window into its effects beyond the capabilities of telescopic observations.

2.2 Why Now?

The 2020s and early 2030s will see the culmination of surveys by a number of telescopes that are either partially or wholly motivated by understanding dark energy. These include the European Space Agency's Euclid mission, NASA Nancy Grace Roman Space Telescope in space, and the NSF/DOE Vera Rubin Observatory and DOE's Dark Energy Spectroscopic Instrument on the ground. These observatories will collect an immense amount of data that allows for indirect measurement of the consequences of dark energy on the growth of cosmic structure and the expansion history of the universe. Collectively, these experiments will beat down statistical errors in astrophysical dark energy measurements. These observatories are also designed to minimize systematic errors in the very demanding measurements of galaxy shapes, positions, and motions required for astrophysically-derived constraints on dark energy. However, it is possible that while error bars on dark energy models will be greatly reduced, the true underlying nature of dark energy will remain a mystery after the completion of the planned surveys from these telescopes. In that case, further astrophysical statistical constraining power from new missions or surveys is unlikely to lead to an ultimate understanding of dark energy. A new, direct measurement approach may be needed.

As observational tools reach their limits in providing a comprehensive understanding of the nature of dark energy, the scientific community is beginning to acknowledge the need for a direct measurement probe like GDEM. The end of this decade may herald the call for such direct detection experiments, necessitating readiness in technology and methodology.

Concurrently, the rapid development and maturation of new quantum sensors and clocks, notably atom interferometers, present a timely opportunity. These advancements are revolutionizing the precision and capabilities of measurement tools, making them increasingly viable for space missions aimed at testing fundamental physics. The synergy between the need for direct detection and the advent of advanced quantum sensors signifies that the time is ripe to start formulating and developing the necessary technologies for such missions.

Preparing for GDEM entails a focused development of these technologies over the next decade. This involves not only advancing the individual components like atom interferometers but also integrating them into a cohesive and robust space-based measurement system. It's about ensuring that when the scientific call for direct detection experiments becomes urgent, the technological groundwork is well laid out, tested, and ready for deployment. Therefore, GDEM is a proactive step in aligning emerging technologies with the anticipated directions of cosmological research. This strategic approach aims to position GDEM at the forefront of the next significant leap in understanding the universe's fundamental mysteries.

Our analysis for the GDEM suggests that it is a viable mission that could be developed and implemented in the foreseeable future. This optimism is grounded in the current technological landscape and scientific understanding, which collectively provide a strong foundation for the mission's success. Key factors supporting the feasibility and the timeliness of GDEM include:

- Quantum sensing technologies around atomic clocks and quantum sensors has gone through an incredibly intense and productive period, now laboratory demonstrations have shown unprecedented precisions and enabling capabilities. Terrestrial instruments have begun deployed in field applications. NASA and other space agencies around world are beginning to recognize and embracing the quantum sensing capabilities, with QS technology demon mission being developed both in NASA and Europe. As a result, more and more efforts are now in maturing the technologies and infusing into space applications. At the same time, research and innovations from university research continue produce more advanced methodology and techniques leading to further measurement capabilities.
- Several critical technologies that are integral to the mission are either already mature or are advancing rapidly. These include laser interferometer ranging for precision inter-satellite measurements; small spacecraft utilizations and affordable space access facilitated by ridesharing options; formation flights and constellation maintenance.
- The significance of complete understanding the nature of dark energy, together with the GDEM multi-science capabilities, can draw shared costs in various aspects, including the development of flight prototypes. The collaborative nature of space missions today, including partnerships between NASA divisions, agencies, academia, and the private sector, allows for the sharing of resources, knowledge, and infrastructure, significantly reducing individual stakeholder costs. This collaborative approach extends to the sharing of technological developments and operational strategies, further enhancing the mission's feasibility.

In summary, the convergence of a deep understanding of the necessary space experimental physics, the maturity and rapid development of key technological components, and the potential for shared interests and resources makes GDEM a feasible and timely endeavor. These factors position us well to undertake this ambitious mission to probe the fundamental nature of dark energy and potentially unveil new physics in the next decade. The mission is a unique opportunity to investigate dark energy and other cosmic phenomena within this decade, making it a relevant and timely project.

2.3 Searching for New Physics with the Trace of the GGT

2.3.1 Science motivation and challenges

Einstein's General Theory of Relativity (GR), which has been the primary framework for understanding gravity for over a century, is facing new challenges due to emerging cosmological data. These data hint at potential discrepancies in GR's description of gravitational phenomena, particularly on cosmological scales. Advanced theories that propose modifications to GR introduce scalar fields, predicting phenomena such as violations of the Equivalence Principle and alterations in cosmic-scale dynamics. However, GR's predictions have been largely untested on these scales, despite being robust in other contexts, like the detection of gravitational waves (GW) and the study of black holes.

As a result, the gravitational field equations of GR[2] (with R^{mn} and T^{mn} being the Ricci and the stress-energy tensors, correspondingly, and Λ being the cosmological constant)

$$R^{mn} - \tfrac{1}{2}g^{mn}R + g^{mn}\Lambda = \frac{8\pi G}{c^4}T^{mn} \tag{1}$$

are expected to be modified or else augmented. There is a possibility that the deviation may come not from invalidity of GR but would be due to new fields that will interact with baryonic matter in a novel way, leading to new forces that justifies the importance of experimental validation, particularly in space-based environments, thus providing the motivation for new fundamental physics missions (Yu et al., 2018, Yu et al., 2019).

Considering non-relativistic Newtonian approximation of (1), this equation collapses to

$$\nabla^2 U = 4\pi G\rho, \tag{2}$$

where ρ is the density of matter within the solar system with U being the gravitational potential.

In the solar systems environment, we observe that in the vacuum outside the Sun and away from other celestial bodies (i.e., planetary system, asteroids, etc.) $\rho = 0$. But that space is not perfectly empty as there is dust and particles present. Cosmic dust particles range in size from a few molecules to 100 μm, such as micrometeoroids (Jorgensen, 2021). Based on its location, cosmic dust is classified as intergalactic (between galaxies), interstellar (within galaxies, between stars), interplanetary (within a solar system, e.g., zodiacal cloud), and circumplanetary (e.g., planetary rings). Dark energy is also expected to produce small deviation in the solar system dynamics.

In the solar system two types of dust are of relevance – interplanetary and interstellar. The density of the interplanetary dust was observed to be $\leq 8 \times 10^{-21}$ kg m^{-3} (Jorgensen, 2021), which contributes up to $4\pi G\rho \simeq 6.71 \times 10^{-30}$ s^{-2} to the right-hand side of Eq. (2). The presence of the interstellar dust in interplanetary space with the density of $(2.1 \pm 0.6)\times 10^{-24}$ kg m^{-3} (Kruger, 2015), contributes to Poisson Eq. (2) with the magnitude of $4\pi G\rho \simeq 1.76\times 10^{-33}$ s^{-2}.

The particle content within the interplanetary medium decreases with the square of the distance from the Sun, averaging ~ 5 particles/cm^3 near Earth, but can spike up to 40 particles/cm^3 during specific solar events like coronal mass ejections. Then, taking 40 protons to be the source of the density, we estimate that they would contribute up to $4\pi G\cdot 40\cdot 1.67\times 10^{-21}$ km/m$^3 \simeq 5.67\times 10^{-29}$ s^{-2} to Eq. (2). Although these contributions are very small (see Table 1) they are detected with interplanetary spacecraft thus providing the motivation to search for other small deviations.

Thus, in the solar system, the presence of interplanetary and interstellar dust and the interplanetary medium contributes to the gravitational potential, albeit minimally. These contributions, while small, are important for detecting deviations from expected gravitational behavior.

Among the plausible mechanisms to explain dark energy, modified gravity theories offer an intriguing deviation from GR. To do that, some of such theories introduce a screening mechanism that depends on the environmental density. Screening mechanisms in physics are fundamentally categorized into two types: those dependent on local mass densities and those that are not. Scalar field theories such as chameleon and symmetron are examples of the former. These theories exhibit a unique 'thin shell effect' where only the outermost layer of a substantial object interacts with dark energy fields. This selective interaction causes the dark energy force to be predominantly confined to this thin outer layer, reducing its overall observable impact.

[2] We use the Einstein summation convention with Greek indices are $(m,n) \in [0,1,2,3]$.

As a result, gravitational forces typically overshadow dark energy interactions in most observable phenomena. Despite this, the presence of the short-range dark energy force could still be detected through precision experiments in laboratory settings. Unlike classical gravity theories that fail solar system tests, these screened theories can effectively mask their non- GR behavior in high-density regions, such as our solar system, thus providing an optimal testing ground (Bartlett, 2021). By observing gravitational dynamics and interactions in such settings, one can tease out the subtle signatures of these modified gravity theories, thus broadening our understanding of gravitational physics beyond GR (Sakstein, 2018, 2020).

In contrast, the Vainshtein screening mechanism follows a distinct approach. This mechanism involves the Vainshtein scalar field, which is mediated by a nonlinear 'Galileon' field. The nonlinearity of this field's equation of motion is characterized by a coupling constant, r_c. The Galileon force behaves similarly to gravity, $1/r^2$, at large distances from matter but diminishes much more gradually ($1/\sqrt{r}$ for a cubic Galileon) when closer to matter. The Vainshtein radius, particularly for the Sun, is around 100 parsecs, within which the gravitational force does not follow the inverse square law (ISL) but is instead inversely proportional to the square root of the distance (Adelberger, 2003). Direct detection of these deviations would effectively test the ISL, with the solar system serving as an optimal testing ground.

Table 1. Contributions of various sources to the Poisson equation.

Source	Density, $[\mathrm{kg\,m^{-3}}]$	Value, $4\pi G\rho$
Interplanetary dust	$\leq 8 \times 10^{-21}$	$6.71 \times 10^{-30}\ \mathrm{s^{-2}}$
Interstellar dust	$(2.1 \pm 0.6) \times 10^{-24}$	$1.76 \times 10^{-33}\ \mathrm{s^{-2}}$
Interplanetary medium	$\leq 6.69 \times 10^{-20}$	$5.67 \times 10^{-29}\ \mathrm{s^{-2}}$
Dark energy, $\Omega_{\mathrm{DE}} \simeq 0.7$	$\sim 5.95 \times 10^{-27}$	$-5.56 \times 10^{-36}\ \mathrm{s^{-2}}$

The enormity of the Vainshtein radius makes it impractical to test this scalar field in terrestrial laboratory settings. Currently, the experimental limits on r_c are constrained by tests of gravity's inverse square law, including lunar laser ranging and the analysis of gravitational wave propagation (Sakstein, 2018; Creminelli & Vernizzi, 2017; Crisostomi & Koyama, 2018). In cosmology, the Galileon field is considered a theoretically robust candidate for explaining the dark energy field.

The cubic Galileon model (Andrews, 2013), with its Vainshtein screening mechanism, offers an alternative explanation to deviations from Newtonian gravity, distinct from chameleon and symmetron models. The model, which does not exhibit thin shell effects, alters Newtonian gravity over long distances. Within the Sun's Vainshtein radius, its force behaves differently from the standard $1/r^2$ law. For effective testing, the measurement sensitivity requirement is around $10^{-24}\ \mathrm{s^{-2}}$.

Dark energy, if related to the cosmological constant model, has a unique characteristic wherein its pressure $p = -\rho$. Given the Universe's critical density of $\rho_c \approx 0.85 \times 10^{-26}\ \mathrm{kg/m^3}$ and dark energy contributing to ~70% of this ($\Omega_{\mathrm{DE}} \simeq 0.7$), if U signifies the gravitational potential due to dark energy and the Laplacian, ∇^2, indicates spatial variations, then the resulting contribution to Eq. (2) is $4\pi G\Omega_{\mathrm{DE}}\rho_{\mathrm{crit}} \simeq -5.56\times10^{-36}\ \mathrm{s^{-2}}$. This very small value underscores the subtle effect of dark energy on gravitational potential, confirming its broad yet delicate impact, particularly in driving the universe's accelerated expansion.

Dark energy, particularly in the cosmological constant model, also impacts gravitational potential, although its effects are subtle and challenging to observe directly with current technology. The values associated with dark energy's effects, are extremely small and lie beyond the current

detection capabilities of modern instruments. Given the present state of technology, these minute effects might remain unobservable in any direct manner.

The exploration of these subtle phenomena, potentially indicative of new physics beyond GR, is driving the need for innovative missions and experiments in fundamental physics. It is the goal of GDEM to expand our understanding of gravitational physics, considering the complex interplay of dark energy, modified gravity theories, and the cosmological constant in shaping the universe's dynamics, through precision measurements in the solar system.

2.3.2 Innovative approaches and significance

We explored a measurement concept using new sensor technologies and innovative approaches to address the challenges in detecting dark energy. The first major innovation is employing atom-wave interferometry (AI), a novel technology for measuring weak forces using laser-cooled ultra-cold atoms. Already proven in research labs and finding commercial use for terrestrial gravity measurements, we aim to adapt AI for open space operations. This involves using freely floating atomic test mass particles in space vacuum, rather than in enclosed vacuum chambers, to enhance AI sensitivity in microgravity and reduce spacecraft self-gravity gradient forces.

AI leverages the quantum wave nature of atoms, using light-pulse atom optics to manipulate atom waves in matter wave interferometers. The sensitivity of these interferometers, dependent on the lengths of their arms, needs to be significantly extended for dark energy detection. Using atoms in open space circumvents the constraints of vacuum enclosure sizes on spacecraft, enabling increased measurement sensitivity vital for detecting Galileons in the solar system.

The second innovation lies in our measurement scheme, designed to suppress gravity force interference by exploiting the unique properties of non-Newtonian gravitational forces. Newtonian gravity has a zero trace of the field gradient tensor in space, unlike deviations expected from dark energy forces. This difference allows for high suppression of gravity-induced systematic effects and enables model-independent identification of dark energy signatures. This trace method doesn't require precise knowledge of gravitational force strengths.

Furthermore, we identified a practical constellation configuration to make the trace value determination independent of the measurement orientation relative to mass distributions. By designing the spacecraft constellation tetrahedrally (as seen in Figure 2) and conducting simultaneous differential measurements across six arms, we can determine the local trace of the force field gradient tensor, irrespective of the constellation's orientation in the solar system.

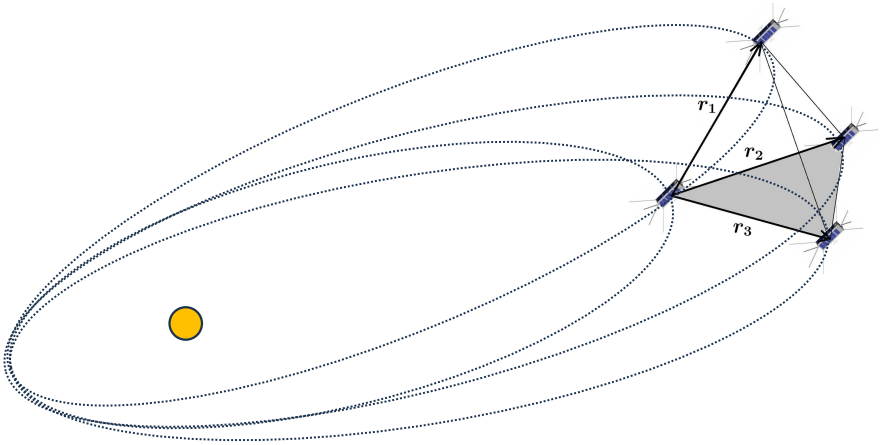

Figure 2. Tetrahedral spacecraft formation on nearby heliocentric orbits.

Spacecraft formations and/or distributed space systems allow measurements not possible with single spacecraft. For fundamental physics missions, observable field parameters related to the gravitational field may exhibit subtle variations in space and time. Thus, understanding of the processes within the field requires accurate and precise observations and analysis of both the temporal and spatial variations.

A tetrahedron formation has the advantage that four spacecraft with variable separations are the minimum needed to resolve a three-dimensional structure, at least to the lowest order in the physical field gradients. The tetrahedral configuration is a special geometric arrangement that has been proposed for multiple spacecraft formations, primarily due to its inherent stability and symmetry properties. When discussing spacecraft in such configurations, they can be seen as vertices of a tetrahedron moving in space.

As we will see, it is possible to investigate this prediction at very high accuracy using a configuration of satellites in heliocentric orbit. These satellites would be flying in close formation, typically separated by a few thousand kilometers or less, as they follow individual, undisturbed eccentric orbit around the Sun. Relying solely on observations that can be performed within the constellation (and specifically not relying on precision astrometry or high accuracy radio navigation, as neither methods are sufficiently accurate for this experiment) it is possible to reconstruct the trace[GTT].

For this, GDEM utilizes intersatellite range data and accelerations in the form of corresponding second time derivatives. There are, however, difficulties that must be overcome. We recognize that the tetrahedron may also undergo rotation, which implies that the computed accelerations must be decoupled from pseudo-accelerations implied by a rotating reference frame. In the absence of an accurate external reference, these accelerations must be measured in-constellation. To allow for such measurements, we introduce a generalized Sagnac-type observable, which, in principle, can be measured at the required accuracy using the same laser ranging equipment (perhaps with modest modifications) that is already be available on board for range measurements.

3 ENABLING TECHNOLOGY AND INNOVATIVE APPROACHES

3.1 Atomic Test Mass and Atom Interferometers

3.1.1 Drag-free requirements for gravity measurements

The unique measurement requirements and challenges for gravity measurements, particularly for a mission like GDEM, revolve around achieving extreme precision and stability in a dynamic space environment. One critical aspect is minimizing non-gravitational forces such as solar radiation pressure, magnetic fields, and atmospheric drag, which can perturb the spacecraft and affect the accuracy of gravity measurements. This leads to the necessity of a “drag-free” system, where the test masses can freely fall under the influence of gravity without the effects of these external forces, including craft mass self-gradient forces.

SEARCH FOR NEW PHYSICS WITH TETRAHEDRAL FORMATIONS

Key technical aspects guiding GDEM mission design

- **Atom-wave Interferometers (AI):**
  - We use AI to maintain stable, drag-free conditions for each s/c. AI is to adjust for non-grav forces: solar rad pressure, outgassing, attitude control, etc.
  - We assume AI can correct any local non-grav disturbances, maintaining stability to within ~1e-15 m/s^2/$\sqrt{\text{Hz}}$ of differential acceleration.

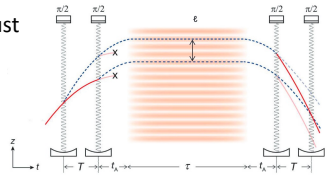

- **Precision Laser Ranging Systems:**
  - Their role: i) To measure range changes between s/c pairs. ii) By measuring in multiple directions, they can isolate the trace[Grav. Gradient Tensor].
  - Specifically, we rely on laser ranging to measure the range and to compute range-rate between any pair of spacecraft at nominal separation of 1,000 km.
  - We assume each s/c is equipped with i) 3 small telescopes (~5cm aperture), ii) 3 precision gimbals capable of a wide angular articulations in 2D.
  - We assume a LISA-class laser ranging system with sensitivity of 30 pm/$\sqrt{\text{Hz}}$.
  - Our objectives is to identify the range of angular articulation, pointing knowledge and stability needed to support the science operations.

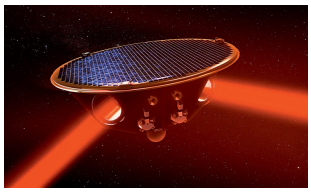

- **Tetrahedral Configuration:**
  - To ensure that gravitational effects are sampled in 4 non-coplanar directions.
  - Tetrahedral formation established by 4-spacecraft on nearby elliptic orbits.
  - We study dynamical behavior of such a configuration, its evolution, rotation, and elastic properties.
  - Our objective is to i) express trace of gravity gradient tensor via inter-satellite range measurements, and computed quantities, such as range-rates and range-accelerations, and ii) show that this mission is enabled by a set of local differential measurements done at the local tetrahedral coordinate frame.

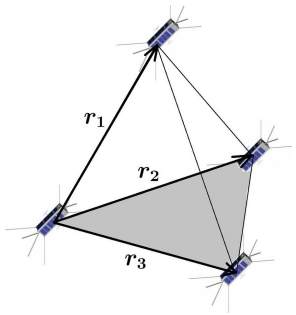

- **Sagnac Interferometers (SI):**
  - SI on any 3 non-coplanar triangles at any vertex can determine 3 components of the angular velocity, **Ω**, to measure elastic rotation to high-precision.
  - We assume that SI can measure optical path differences (OPD) between co- and contra-propagating beams at 30 pm/$\sqrt{\text{Hz}}$, which is compatible with LISA.
  - SI allows determining the angular velocity of the tetrahedron with respect to the solar system barycentric (SSB) coordinate reference frame.

GDEM targets a detection sensitivity of $\sim 10^{-24}/s^2$ for gravity gradients.

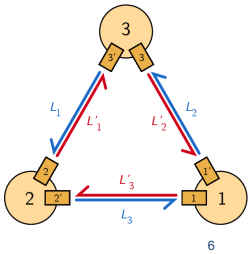

6

Figure 3. Key technical aspects guiding GDEM mission design.

Typically, in gravity missions like GDEM, the measurement requirements are extremely stringent, often requiring the detection of accelerations as small as 10^{-15} m/s^2 or even lower. To achieve this, drag-free control systems must maintain the spacecraft and test masses in a pure gravitational orbit, compensating for non-gravitational forces to an exceptionally high degree of accuracy.

In the case of LISA, the drag-free requirement is particularly demanding due to the need to detect gravitational waves over vast distances. The test masses, typically 1.96 kg gold-platinum cubes, must be isolated from all external forces except gravity, necessitating spacecraft following the test mass to a positional accuracy on the order of nanometers and control forces that are less than 10^{-14} N. LISA's drag-free technology uses capacitive sensing to detect the position of the test mass relative to the spacecraft, and micro-Newton thrusters to adjust the spacecraft's position continuously. The challenge lies not only in the precision of the measurements and control but also in maintaining this over the years-long mission duration in the deep space environment. Typically,

only one direction along the laser ranging interferometer was precisely measured and controlled. This limits the formation flying and its angular working ranging.

The atomic test mass concept introduces atoms as inertial references. In this approach, clouds of ultra-cold atoms (often rubidium or cesium for technical convenience) are used as test masses. The atoms are cooled to temperatures just above absolute zero and placed in a state of free fall within the spacecraft. The cooling is entirely through interaction with laser without any cryogenic system used. Their positions and velocities are then measured using atom interferometry, which involves precisely manipulating and measuring the wave properties of atoms using laser light. This technique can achieve acceleration sensitivities on the order of 10^{-12}-10^{-15} m/s^2 or better, with the potential for further improvement as the technology matures.

The advantage of atomic test masses lies in their uniformity and quantum nature, allowing for extremely precise measurements that are largely free from the biases and noise associated with classical test masses. Identical atomic particle test masses can be regenerated and reset to new starting points. However, challenges include the need for ultra-high vacuum conditions, sophisticated laser systems to cool and manipulate the atoms, and systematic control of the atomic system. Additionally, the technology must be ruggedized and automated for operation in the space environment, where traditional laboratory conditions cannot be replicated.

As a result, the quantitative and technological focus for GDEM lies in use of atomic test masses and atom interferometry for achieving and maintaining the necessary isolation from non-gravitational forces, precision measurement of test mass position and acceleration. These efforts are driving forward the capabilities for precision tests of general relativity, detection of dark energy, gravitational wave detection, and other fundamental physics objectives.

3.1.2 Light pulsed atom interferometer

Laser cooling and atom trapping techniques form the core of our atomic sensors, capitalizing on both the quantized atomic internal energy structure and the wave characteristics of atoms. Typical atomic quantum sensors work with cold atomic sources, laser-cooled to micro-Kelvin and below, all the way to pico-Kelvin when combined with more sophisticated cooling schemes. At these extremely low temperatures, atoms exhibit pronounced quantum wave behaviors, appearing more as diffuse 'fuzzy balls' than distinct particles. At the certain conditions, atom clouds cross a density threshold where the atomic clouds transition into a quantum state called Bose-Einstein Condensate (BEC). This process generates ultra-cold atom clouds at temperatures only a billionth of a degree above absolute zero, and notably, it achieves this without cryogenic cooling.

These cold atom-wave packets are crucial for constructing matter-wave interferometers, where we employ laser pulses as atom optics. This setup mirrors the principles of optical Mach-Zehnder interferometers, which use beam-splitters and mirrors, but with a key distinction: in atom interferometers, the roles of light and matter are inverted. This inversion results in interferometry with massive particles rather than massless photons. As a result, atom interferometers are intrinsically highly sensitive to inertial forces/gravity, small motional changes, particularly accelerations.

The acceleration sensitivity per measurement (often referred as shot in light pulsed schemes) for an AI can be quantified by the expression:

$$\delta a = \frac{\delta \phi}{n k_{\text{eff}} T^2}$$

where $\delta\phi$ is the phase resolution of an AI, n is the number of photon momentum pairs exchanged between light and atom during one beamsplitter (a large-momentum-transfer beamsplitter), k_{eff} is the effective wave number of the AI laser; T is the time interval between laser pulses.

The phase resolution δϕ is fundamentally constrained by quantum projection noise of atoms, which scales as $1/\sqrt{N}$, where N is the number of independent atoms. For instance, with N=10^6 and using a 780 nm AI laser (k_{eff} =4π/780nm) for rubidium (Rb) atoms, the acceleration sensitivity becomes δa= 62/(nT^2) pm/s^2, where T is in seconds. This formula highlights the exquisite sensitivity of AI to weak forces, particularly in microgravity environments in space. Here, longer intervals T between laser pulses can be achieved, significantly enhancing the AI's capability to detect minute accelerations. This makes AI an extremely powerful tool for measuring weak forces in space applications.

For GDEM and similar demanding space applications, long interrogation times T are essential. The thermal velocity and expansion of typical cold atom clouds are insufficient for these purposes. Instead, a much colder atomic sample, such as a Bose-Einstein Condensate (BEC), is required to achieve the necessary long interrogation times and heightened AI sensitivities.

Even at nK or pK temperature, atoms still have finite velocities and spread. The residual atom velocity spread will limit the longest interrogation possible. In this regard, BEC is not only a fascinating quantum state with large numbers of atoms but also an ideal source for ultra-cold atoms. For example, a point-like ^{87}Rb atom cloud, if not cooled to a BEC, will expand to a 6 mm radius ball in one second at a photon-recoil temperature of 360 nK, which is the lowest achievable temperature without using BEC. These extended clouds necessitate larger laser beams for effective manipulation, bigger vacuum chambers for containment, and are more vulnerable to spatial systematic errors, which are critical in precision metrology.

In contrast, a BEC source can provide atom clouds of much lower temperatures, around 10 nK or even less. This drastic temperature reduction minimizes the expansion rate of the atom cloud, facilitating better control for precision measurements. Moreover, recent advancements have introduced delta-kick cooling in BEC generators, which effectively localizes the atoms spatially, leading to effective temperatures in the picokelvin (pK) range. Such ultra-cold temperatures achieved by BEC significantly improve the performance of atom interferometers by allowing for extended interrogation times and reducing potential systematic errors, making them highly suitable for sensitive applications like those planned in the GDEM mission.

The second key to AI used for the precision measurements in GDEM is the number of photon momentum exchange with atoms. Typical photon momentum exchanges are two with Raman based AI method. In order to increase the number of photon momentum transfer, various so-called large momentum transfer (LMT) schemes have be developed and demonstrated in the labs, up to several hundreds [LMT]. The AI interferometer sensors used in GDEM will have to implement one LMT scheme with n>100.

3.1.3 Atomic test mass for drag-free measurements

In the GDEM, the use of atomic test masses plays a crucial role in achieving the high precision required for the mission's objectives. The mission aims to measure relative accelerations between spacecraft over extended periods, which is key to detecting subtle effects from the Sun's Vainshtein field. This necessitates the use of stable, long-term inertial references, for which atom interferometer emerges as the enabling technology in this context.

AI technology, akin to atomic clocks, provides the necessary stability for extended durations, a fact well-demonstrated by terrestrial gravity measurements on Earth. In the space environment,

the sensitivity of AI is expected to improve due to longer interrogation times, and its inherent long-term stability is anticipated to ensure a constant noise spectral density down to very low frequencies. This makes AI an ideal choice for the precise measurements required by GDEM.

The role of AI in GDEM represents a significant departure from traditional drag-free flight methods, such as those utilized in the LISA mission. Rather than caging a bulk test mass and using micro-thrusters to maintain alignment, AI in GDEM measures the relative acceleration between ultracold atoms and the spacecraft. In this setup, atoms serve as instantaneous inertial references. This method achieves drag-free measurements by continuously refreshing and repositioning atomic samples, thereby minimizing the relative motion between the atomic test mass cloud and the spacecraft during each measurement cycle.

To truly realize drag-free measurements, any test masses operated inside spacecraft has to also address the spacecraft self-gravity field gradient (gravity field due to the spacecraft mass itself). This is because the presence of a self-gravity force will be position dependent under a gradient, translating the position noises to the corresponding acceleration noises. Conventional approach would involve carefully arranging the spacecraft's mass distribution to reduce its self-gravity gradient and keep the relative position between the test mass and spacecraft fixed as much as possible, as in the LISA drag-free flight approach. This approach requires sophisticated drag-free flight with sensors and micro thrusters and fuels. It also does not work well with atom interferometers as AI would need to extend to meters for long interrogation times.

To mitigate this constraint and remove the drag-free flight of spacecraft requirement all together, we had proposed and investigated placing the atomic test mass outside the spacecraft away from the spacecraft mass as in Phase I report [Phase I]. This is possible because we use atomic particles as test masses and deep space provide a good vacuum environment for disturbance-free life of the atomic particles. Unshielded solar radiations turned out not a showstopper (discussed later in the report.) Self-gradient forces due to the spacecraft mass die down fast while moving away from it. When it is far enough from the spacecraft mass, sufficiently small gradient force can be achieved. Estimates show that one will need to operate the atomic test massed 100 m away from spacecraft to allow μm position displacement jitter (comparing with LISA of nm displacement jitter requirement.) This distance is challenging for rigid mechanical boom structure but possible with optical metrology. It is also possible to use trailing daughter spacecraft to provide the needed retroreflecting optics to operate the atom interferometer at the distance from the mother spacecraft.

3.2 Measurement Strategy – Tracelessness Test for the Unknown Force

The cubic Galileon model, featuring the Vainshtein screening mechanism, diverges from the thin shell effects seen in chameleon and symmetron models. It alters Newtonian gravity over long distances. Specifically, beyond the Vainshtein radius (about 100 pc for the Sun), the Galileon field exerts a force adhering to the inverse square law (ISL). However, within this radius, the force deviates from the ISL, following as $1/\sqrt{r}$ pattern. This characteristic makes direct detection of the Galileon force viable through tests of the ISL. Success hinges on the anticipated signal size, instrument sensitivity, and suppression of systematic effects.

For GDEM's conceptual design, we estimate the Galileon signal from the Sun, the solar system's most massive body, while initially disregarding other planetary influences (which can impact local Galileon forces). Based on the coupling constant r_c=6000 Mpc, the solar Galileon acceleration near 1 AU is approximately 10^{-13} m/s^2, compared to the Sun's gravitational acceleration of about 6×10^{-3} m/s^2 at the same distance (White, 2020]. The Galileon force is this ~ 10 orders of magnitude

weaker than gravity for solar system bodies, explaining the lack of observed deviations from Newtonian gravity.

Our approach circumvents these issues by testing the tracelessness of the gravity gradient tensor (GGT). The trace of this tensor is invariably zero in vacuum, a unique property of 1/r potentials satisfying the ISL. In contrast, the Galileon force, with its as $1/\sqrt{r}$ dependence, produces a non-zero trace of the same magnitude as its force gradient. Measuring the local gradient tensor's trace strategically bypasses gravitational nuisances, requiring no precise knowledge of mass distribution or the gravitational constant *G*. Furthermore, the trace's rotational invariance simplifies the orientation requirements for the measurement instrument.

There are locations where gravitational forces or gradients balance out between celestial bodies such as Lagrange points. The exact positions, directions, and their tolerances again are tied to the GM products. There are regions of interests as the gravitational force or gradient strengths are greatly reduced. We have looked at these special regions for possibly more advantageous science measurements. The initial investigations indicated that there are no strong advantages of insisting measurements in these regions.

3.3 Robust Measurement Configuration

To accurately measure the trace of the gravitational gradient tensor, three orthogonal gravity gradiometers onboard a spacecraft constellation are utilized. Each gradiometer measures one principal diagonal component of the tensor, with the trace derived from the sum of these components. Precision is paramount; each measurement must be accurate to one part in 10^{10} to ensure an overall trace accuracy of 10^{-10}, crucial for detecting the Galileon signal.

This necessitates precise alignment and positioning of the gradiometers, demanding strict orthogonality and overlapping central points. Such precision is challenging due to the required spacecraft formation and trajectory control relative to solar bodies. For instance, at 1 AU from the Sun, any misalignment in the gradiometers—beyond 10^{-10} radians—could significantly impact measurement accuracy, introducing errors that could mask the Galileon signal. Current technologies like star-trackers and laser ranging systems struggle to achieve this level of precision, making accurate trace measurement a complex task.

A more robust and effective measurement approach for the gravitational gradient tensor involves leveraging the natural trajectories of spacecraft in an appropriate constellation – an equilateral tetrahedral formation of four spacecraft. This method is less sensitive to changes in the constellation's orientation. By measuring differential accelerations along six directions—each corresponding to lines connecting pairs of spacecraft—a complete and unique determination of the symmetric 3x3 gradient tensor is achievable (Yu, 2018). Consequently, its trace can be accurately measured.

In this setup, the critical factor is the relative angles between these measurement lines. Although these angles require stringent precision, they can be accurately determined through high-precision laser ranging and tracking to measure the distances between spacecraft. It's important to note that while the overall orientation and shape of the constellation dynamically change, affecting the tensor elements, these changes do not impact the measurement of the trace. Thus, the detection of unknown forces remains unaffected.

The overall measurement scheme hinges on three key elements: high-precision laser ranging, inertial reference for orientation stability, and precise trace determination systematics. For GDEM, the constellation dynamics involve managing a tetrahedral formation of spacecraft in a heliocentric orbit. This requires counteracting both gravitational influences from celestial bodies and non-

gravitational forces like solar radiation pressure to maintain the formation's stability. The mission aims to ensure this stability with precision $<10^{-15}$ m/s^2 to enable accurate gravitational measurements.

Over time, formation changes are inevitable due to gravitational perturbations and other external forces. To maintain the integrity and precision of the constellation, the mission can implement formation-keeping strategies. These strategies will use occasional micro-thruster maneuvers to achieve positional accuracy on the order of picometers, allowing the formation to adapt while maintaining measurement precision and sensitivity. On the other hand, most of the formation changes are periodical with the solar orbit. Science measurements can be achieved with most of the orbit period, relaxing the micro thruster requirements for simplicity and cost savings.

Nevertheless, it is to be emphasized that the impact of proper spacecraft formation on the science objectives of the mission is profound (Turyshev et al., 2024). Maintaining formation stability is crucial for precise gravity measurements. The constellation must retain its shape and orientation accurately to measure components of the GGT with the aimed sensitivity goals approaching ~10^{-24} s^{-2}. Additionally, the ability to adapt the formation is vital for meeting diverse scientific objectives, including investigating dark energy, dark matter, detecting gravitational waves, and conducting precision Newtonian gravity measurements within the solar system. Each of these objectives requires different formation configurations and sensitivities, making the dynamic control of the constellation a critical aspect of the mission's success.

3.4 Laser Interferometric Ranging

To measure the trace of GGT, GDEM using a tetrahedral constellation of spacecraft and relies on atom interferometers (AI) and laser ranging interferometers (LRI), adapted to measure the force gradient tensor's trace over significant distances. The challenge of large spatial separation between spacecraft is addressed by linking spacecraft through laser interferometry. This integration effectively forms an extended gradiometer for differential measurements.

The LRI's primary role is tracking relative spacecraft accelerations by analyzing the rate of Doppler shift changes. This technique is like the one used in the LISA mission for gravitational wave detection but differs in its measurement objective. While LISA searches for time-varying signals within a specific frequency band, this mission aims to average single measurement values to a DC trace value over the mission's duration to the first order, and search for the spatial variation of such a value as a function of the distance to the Sun. The sensitivity of these measurements is directly proportional to the baseline length between spacecraft pairs.

A secondary, yet just as crucial function of the LRI is conducting absolute distance measurements between spacecraft. Given the requirement of ten-digit precision for each gradient measurement and the angular determination requirements, the baseline length must be determined with comparable precision. This precision is essential because the gradient value is calculated by dividing the differential acceleration measurement by the baseline length. Additionally, precise determination of the tetrahedron configuration's geometric angles is necessary for accurate trace calculation, achievable through exact measurement of all tetrahedron side lengths.

In the context of a 1000 km baseline in the GDEM mission, the ranging accuracy needs to be finer than 30 pm, both for determining gradiometer baselines and calculating relative angles. With an anticipated gravity gradient signal of approximately 10^{-14} /s² at 1 AU and a differential gravity acceleration of about 10^{-8} m/s² for this baseline, the mission aims to detect a Galileon signal smaller than 10^{-18} m/s². Over an estimated 3-year mission duration, the required acceleration measurement sensitivity is projected to be $1x10^{-14}$ m/s²/Hz$^{1/2}$, similar to that of the LISA's LRI sensitivity goals.

3.5 Sagnac Interferometer Measurements

Direct intersatellite differential measurements alone do not provide the GGT, and its resultant trace does not automatically zero out when the tetrahedral constellation is rotating around the Sun. Relying solely on inter-satellite distances presents challenges due to neglect of the constellation's rotational dynamics, which induce fictitious forces. In a typical gradiometer-like measurement in orbit, one often tried to use a tilting mirror to compensate the rotation. In GDEM, however, by incorporating Sagnac-type observables, we can accurately address and correct these rotational discrepancies through the LRI measurements.

Sagnac observables utilize the high-precision LRI instruments discussed above to detect all components of 3D angular velocity by observing phase shifts in light beams traveling in opposite directions within a loop. These instruments are crucial in measuring the angular velocity of the tetrahedron relative to the solar system barycentric (SSB) frame.

Employing Sagnac interferometers aligned along any three non-coplanar triangles within the tetrahedron enables the determination of the three components of angular velocity, ω. This provides a comprehensive, high-precision measure of the tetrahedron's rotation as the spacecraft move in their nearby elliptic orbits. Sagnac observables can measure optical path differences between co- and contra-propagating beams of any triangle to an accuracy of approximately 30 pm/$\sqrt{\text{Hz}}$, compatible with the LISA mission requirements. We demonstrate that the optical path difference, provided by Sagnac interferometry, allows for determining the angular frequency at which the tetrahedral formation rotates relative to the inertial SSB coordinate reference frame. Turyshev et al. (2024) have shown that the Sagnac observable is a mission-enabling capability, offering the ability to measure the angular frequency of tetrahedral rotation relative to an inertial reference frame with much higher accuracy than other modern navigational techniques.

3.6 Choice of Baseline Length

In the context of space-based gravitational gradient measurements, extending the baseline length is beneficial for enhancing fractional precision for a given set of accelerometer/LRI sensitivities. However, as the baseline extends longer, errors of systematic effects such as the curvature of the higher-order gravity field, becomes more pronounced, necessitating a careful trade-off and optimization process. In addition, propagation delay and laser beam divergence and corresponding technical challenges become more severe.

Gravitational gradients, ideally properties of single spatial points, are measured over finite distances. In this setup, using long baselines for improved measurement sensitivity and precision means the measured value represents an average near the baseline's midpoint. However, when spacecraft follow their individual trajectories, these midpoints may not align at a single spatial point. Ignoring these displacements can lead to substantial errors in trace calculation due to the presence of higher-order derivatives of the gravitational potential.

One mitigation to this error is to have some first order knowledge of the solar gravitational field and apply it to correct the know non-linearity. This can be done by knowing to the first order where the measurement is carried out relative to the Sun. NASA DSN (Deep Space Network) spacecraft tracking capability should give the position of the constellation in the solar system. On the other hand, as shown in (Turyshev et al., 2024), these higher order considerations can be included in the GGT trace recovery data analysis through the total internal measurements without the need of DSN. In fact, the internal data measurements can be used for determining the measurement location in the solar system when a higher order nonspherical gravitational potential is used, leading to a potentially novel way for solar system spacecraft navigation.

The choice of baseline length for inter-spacecraft separation is critical, influenced by several factors: 1) anticipated inter-spacecraft dynamics, 2) the technology selected for necessary measurements, and 3) mission-related constraints. As the constellation orbits heliocentrically, the relative motion of the spacecraft introduces variability in these distances, necessitating a carefully designed optomechanical system (telescopes, gimbals, detectors, etc.) for observations. This dynamic also causes differential rotation that must be countered by the three gimbals on each spacecraft to prevent the telescopes from colliding. Moreover, formation changes might lead to the collapse of the tetrahedral volume, requiring a temporary cessation of observations to reposition the spacecraft and restart the experiment. Additionally, smaller separations decrease the sensitivity to the GGT, whereas larger separations enhance the detection of differential gravitational signals from standard gravity (Turyshev et al., 2024). Thus, the optimal choice for inter-spacecraft separation should result from a multiparametric trade-off that considers the aforementioned factors. In our research, we evaluated several options, including distances of a = 1 AU, 5AU and 10AU, with inter-spacecraft separations of $r_{ij} = 10^3$ km, 10^5 km.

In our study, we considered one of these options, namely a =1 1AU and $r_{ij} = 10^3$ km and considered the reference orbit with the semi-major axis of $a = 1$ AU, eccentricity $e = 0.6$. For such a configuration, the natural orbital frequency is $n = \sqrt{\mu_\odot / a^3} \simeq 1.99 \times 10^{-7}$ s^{-1}. Considering the inter-spacecraft separation of $r_{ij} \sim 10^3$~km, the nominal relative velocities, v_{ij}, and accelerations, a_{ij}, within the constellation are estimated to be

$$v_{ij} \sim n r_{ij} \simeq 0.20 \text{ m/s}, \; a_{ij} \sim n^2 r_{ij} \simeq 3.96 \times 10^{-8} \text{ m/s}^2.$$

We note that, as evidenced by the form, even in this rather simple case, in addition to the natural frequency, n, there will be other frequencies present in v_{ij} and a_{ij}. As a result, as the spacecraft move in their ecliptic orbits around the Sun, the values v_{ij} and a_{ij} will be modulated and amplified, resulting in changes that are small but important to be accounted for when considering a realistic mission architecture. Therefore, below, we use these results as nominal representative values when addressing the error budget and mission design.

3.7 Choice of Mission Trajectories

In the context of detecting Galileon gradient signals, the scaling behavior of these signals relative to distance from the Sun plays a critical role. As the spacecraft moves along an elliptical orbit with an eccentricity of e = 0.6 and a semi-major axis of a = 1 AU, the Galileon signal's intensity changes inversely with the square root of the distance from the Sun (~$1/r^{1/2}$). This variability in signal strength, along with the changing ratio of Galileon to gravitational signals across the orbit, is a key factor in choosing this specific orbital configuration.

Considering a larger semi-major axis, such as 10 AU, would result in a significantly longer orbital period, extending the mission duration beyond practical limits. Such an extension would impact both the cost and feasibility of the mission, making it less desirable for achieving timely scientific objectives.

Furthermore, the operational logistics and variability in gravitational corrections also play a significant role. With increasing distance from the Sun, systematic errors associated with measurements decrease, allowing for the use of longer baselines to enhance instrument sensitivity and signal-to-noise ratio (SNR). This improvement in SNR reaches a point where further increases in distance present challenges in maintaining long-baseline laser ranging interferometry, managing time delay noise, and addressing mission-related constraints.

When systematic errors are minimized using the correction coefficient method, proximity to the Sun could be technically advantageous. However, challenges such as intense solar radiation, interference from solar wind particles, and significant gravitational influences from inner planets, which alter the assumed 1/r potential, need careful consideration.

Operating the mission outside the ecliptic plane aligns better with the assumptions of a single mass source (the Sun) and the 1/r potential used in calculations. The complexities introduced by multiple gravitational sources and the high nonlinearity of the Galileon field's equations was explored through numerical simulations. These are critical for refining mission design, suggesting that an orbit at 1 AU outside the ecliptic plane is currently the most viable option due to these dynamics.

Exploring regions with multiple gravitational sources might offer advantages once a better understanding of the Galileon field's behavior in such environments is achieved. In areas where gravitational gradients from two sources are comparable, the Galileon field's response could significantly alter the total field's Laplacian, presenting an opportunity for missions to modulate the Galileon signal by periodically moving between regions dominated by one gravitational source and regions where two sources contribute equally.

4 SCIENCE TRACEABILITY MATRIX AND MEASUREMENT REQUIREMENTS

4.1 Measurement of Gradient Tensor and Trace

Gravitational gradiometry, central to GDEM, involves measuring the second derivatives of the gravitational potential, U. This process, known as gradiometry, measures the gradients of the gravitational acceleration vector, **a**, which is expressed in terms of the gravitational constant, G, and the density of the matter distribution. These measurements form the GGT, a second-order tensor field with nine components, reflecting the spatial variations of the gravitational field.

SEARCH FOR NEW PHYSICS WITH TETRAHEDRAL FORMATIONS

Gravity gradient tensor

- **Newtonian acceleration** $\mathbf{a} = \boldsymbol{\nabla} U = -G \int \rho(\mathbf{x}') d^3\mathbf{x}' \frac{(\mathbf{x}-\mathbf{x}')}{|\mathbf{x}-\mathbf{x}'|^3}$
- **Gravity gradient tensor (GGT):** $\mathbf{T} \equiv T^{ab} = \nabla_a a_b = \nabla_a \nabla_b U = G \int \frac{\rho(\mathbf{x}') d^3\mathbf{x}'}{|\mathbf{x}-\mathbf{x}'|^3} \left(3\mathbf{n}^a\mathbf{n}^b - \mathbf{I}^{ab}\right)$
- **Newtonian potential:** $U(\mathbf{r}) = \frac{\mu_\odot}{r}\left[1 - \sum_{n=1}^{\infty} \left(\frac{R_\odot}{r}\right)^{2n} J_{2n} P_{2n}(\cos\theta)\right]$
- **Solar GGT:** $\mathbf{T} \equiv \nabla_a \nabla_b U = \begin{bmatrix} \partial^2_{11}U & \partial^2_{12}U & \partial^2_{13}U \\ \partial^2_{21}U & \partial^2_{22}U & \partial^2_{23}U \\ \partial^2_{31}U & \partial^2_{31}U & \partial^2_{33}U \end{bmatrix} = -\frac{\mu_\odot}{r^3}\left(\delta^{ab} - 3n^a n^b\right) + \mathcal{O}\left(2.84 \times 10^{-25}\ \mathrm{s}^{-2}\right)$ (from solar J_2)

TABLE II: Contribution of current measurement uncertainties for $a = 1$ AU orbit.

Source	Expresison	Value	Present value
Heliocentric position	$\delta r \simeq (r^4/2\mu_\odot)\delta \mathrm{T_c}$	$\leq 1.89(\delta \mathrm{T_c}/10^{-21}\ \mathrm{s}^{-2})$ km	$\leq$2 m, 2AU
Heliocentric direction	$\delta n^a \simeq (r^3/6\mu_\odot)\delta \mathrm{T_c}$	$\leq 4.21 \times 10^{-9}(\delta \mathrm{T_c}/10^{-21}\ \mathrm{s}^{-2})$ rad	$\leq 6.7 \times 10^{-12}$ rad
Solar constant, $\mu_\odot = GM_\odot$	$\delta\mu_\odot/\mu_\odot \simeq (r^3/2\mu_\odot)\delta \mathrm{T_c}$	$\leq 1.26 \times 10^{-8}(\delta \mathrm{T_c}/10^{-21}\ \mathrm{s}^{-2})$	6×10^{-11}

- **Solar gravity model (must be relativistic):**
  - Newtonian terms: $T_{\mathrm{N}} \sim 2\mu_\odot/\mathrm{AU}^3 \simeq 7.92 \times 10^{-14}\ \mathrm{s}^{-2}$
  - post-Newtonian terms: $T_{\mathrm{pN}} \sim (\tilde{U}/c^2)T_{\mathrm{N}} \simeq (\mu_\odot/c^2\mathrm{AU})T_{\mathrm{N}} \simeq 7.83 \times 10^{-22}\ \mathrm{s}^{-2}$

7

Figure 4. Gravity gradient tensor and the values of relevant quantities in the solar system.

The GGT is more sensitive to nearby mass distributions than gravitational acceleration or potential, as it depends on the inverse-cubed distance from masses (**Error! Reference source not found.**). This sensitivity makes it a powerful tool for studying local gravitational effects. The GGT is symmetric and, in the context of Newtonian physics, trace-free outside mass distributions, meaning the sum of its diagonal elements is zero, i.e., trace[GGT] = 0. This property is essential for testing the presence of new physical laws in the solar system as mentioned before.

In GDEM, the focus is on the solar gravitational potential, U(***r***), especially considering the Sun's axial symmetry and rotation-induced deviations from a spherical configuration. The evaluation of the GGT at approximately 1 AU from the Sun involves considering the solar gravitational constant, μ_S, and solar gravitational moments, J_{2n}. The resulting GGT components are influenced by these factors, with an error term due to the solar gravitational quadrupole.

GDEM's study of the GGT involves complex calculations and considerations, including the spacecraft's precise position relative to the Sun and the fine details of the Sun's gravitational field. These factors are crucial for the mission's goal of detecting subtle gravitational effects, potentially revealing new insights into fundamental physics.

To create a comprehensive science traceability matrix and discuss specific subsystems in a quantitative and contextual manner for the GDEM, we derived and presented a detailed requirement analysis. This analysis relied on the mission's primary scientific objectives, technical challenges, and operational constraints to reach the sensitivity of $\sim O(10^{-24}\ s^{-2})$ in measuring the trace of the trace of the GGT.

4.2 Science Traceability Matrix (STM)

Table 2. GDEM Science Traceability Matrix

Science goals	Science objectives	Science requirements	Measurement requirements	Instrument requirements	Mission requirements
Understand "What are dark matter and dark energy" by "investigating the nature of dark energy" (NRC2010 and 2020 Vision) Test of Fundamental physics and probe new physics (2023 BPS decadal survey)	Determine the validity of models of dark energy as Galileon scalar field Tests of model-independent non-Newtonian gravity through test of Inverse Square Law Test of cosmological gravity on the solar scale Gravitational wave detection in the mid frequency band (0.03 to 1 Hz) Dark matter detection with certain models Precision measurements of solar gravity and possible detection of unknown terrestrial objects	If non-Newtonian gravity force exists, measure at 10sigma of the Vainshtein model predicted strength and spatial distribution in the solar system. If non-Newtonian gravity force does not exist, improves the limit of the solar system-scale gravity Inverse Square Law by a factor of 100 under screening scenarios and model agnostic measurements	Trace of force field gradient tensor at the precision of $1x10^{-24}/s^2$ or one 10^{th} of predicted galileon peak signal strength over mission period Measurements are obtained over designed orbit trajectory with predicted galileon signal strength varying over one decade (10x) Periodical and semi-periodical measurements per optimal trajectory with predicted galileon signal strength varying over one decade (10x) Six nonplanar gravity differential measurements over 1,000 km baseline separation with > 10 mHz bandwidth Inter-spacecraft ranging for Doppler and absolute distance ranging	Averaged gradient measurement sensitivity per each differential measurement at $1x10^{-20}/s2/Hz^{1/2}$ over separation near 1 AU Four (4) simultaneous differential acceleration measurements along the near-regular tetrahedral lines. Local acceleration measurement sensitivity and drag-free control to a precision of $1x10^{-15}\ m/s^2$ Laser ranging interferometer between each spacecraft pair at 30 $pm/Hz^{1/2}$ in measurement band over 10^6 separation Absolute laser distance ranging at the accuracy of < 100 µm over 1,000 km separation in the measurement band	Mission lifetime 5 years Solar elliptic orbit of Semi-major axis of a=1 AU and eccentricity e=0.6 Maintain tetrahedral configuration with volume and locations on the orbit to achieve overall measurement precision as well as its spatial distribution High-capacity terabit onboard processing. Data less than 1 MB/s shall be stored onboard and shall be downloaded on scheduled time. No real-time ground tracking and communication of science data is needed

Here is the summary of top-level requirements:

1. ***Laser Ranging System:***
   - *Contribution to Accuracy:* Precise laser ranging is essential for accurate distance measurements between spacecraft, which is a critical factor in calculating the gravitational tensor.

The higher the precision in distance measurement, the more sensitive and accurate the determination of the GGT trace.

- *Specific Requirement:* Achieving a LISA-class sensitivity of ~30 pm/√Hz or better is crucial to ensure that the minute variations in gravitational forces can be detected and accurately attributed to changes in the GGT trace.
- *Absolute ranging requirement:* To determine the geometry accurately for the derivation of GGT and trace, the LRI shall have the absolute distance ranging accuracy on the order of μm.

2. ***Atom-wave Interferometers (AI):***
   - *Contribution to Accuracy:* AI systems, with their high sensitivity to differential acceleration, are pivotal for maintaining the precise drag-free conditions necessary for accurate gravitational measurements. The stability of these systems directly impacts the mission's ability to detect the subtle signals associated with variations in the GGT trace.
   - *Specific Requirement:* A set of local AI measurements shall determine the drag force on the spacecraft to within approximately ~10^{-15} m/s^2 in all three measurement directions.
3. ***Sagnac Interferometers:***
   - *Contribution to Accuracy:* By accurately measuring the rotational velocity of the spacecraft formation, Sagnac interferometers help maintain the optimal orientation and stability of the tetrahedral configuration. This stability is crucial for consistent and precise gravitational measurements, which are sensitive to changes in the spacecraft's orientation and position.
   - *Specific Requirement:* A sensitivity level of ~30 pm/√Hz allows for high-precision detection of angular velocity, ensuring that the rotational aspects of the spacecraft formation do not introduce errors into the GGT measurements.
4. ***Communication and Data Transmission:***
   - *Contribution to Accuracy:* Efficient and error-free data transmission ensures that the high-volume, high-precision data collected by the spacecraft's instruments is accurately relayed back to Earth for analysis. Any loss or corruption of data could significantly impact the quality and reliability of the GGT measurements.
   - *Specific Requirement:* Robust communication systems with high bandwidth and advanced error correction techniques are necessary to handle and protect the integrity of the large volumes of precise data generated.
5. ***Onboard Processing:***
   - *Contribution to Accuracy:* Advanced onboard processing allows for the real-time or near-real-time analysis of data, quick identification of significant gravitational events, and immediate adjustment of mission parameters. This capability enhances the mission's responsiveness and accuracy in measuring gravitational effects.
   - *Specific Requirement:* High-speed, high-capacity processors capable of handling complex algorithms are needed, possibly incorporating artificial intelligence and machine learning for adaptive and efficient data analysis.
6. ***Power and Thermal Management:***
   - *Contribution to Accuracy:* Stable power supply and thermal conditions are necessary to ensure that all instruments and systems operate within their optimal parameters. Fluctuations in power or temperature can lead to drifts or changes in instrument sensitivity, affecting the accuracy of GGT measurements.

- *Specific Requirement:* Efficient power management systems and precise thermal control mechanisms must be in place to maintain a stable operating environment for all mission-critical components.

By ensuring that each of these subsystems meets its specific requirements and functions optimally, GDEM can achieve the overall mission goal of measuring the trace of the GGT with a sensitivity of ~~10^{-24} 1/s². This sensitivity is crucial for probing new physics and advancing our understanding of the gravitational forces within our solar system and beyond. The integrated performance of all systems and components is essential in reaching the desired level of accuracy and making ground-breaking discoveries in gravitational science.

Table **3**. Top level instrumental requirements for the GDEM mission, along with corresponding symbols from (Turyshev et al., 2024).

Parameter	Symbol	Value
Laser ranging	δr_{4i}	10×10^{-12} m
Range-rates	$\delta \dot{r}_{4i}$	1×10^{-5} m/s
Line-of-sight accelerations	$\delta \ddot{r}_{4i}$	1×10^{-15} m/s^2
AI, as inertial sensor	δf_{4i}	1×10^{-15} m/s^2
Sagnac observable	$\delta \omega$	1.5×10^{-15} s^{-1}

4.3 AI Atomic Test Masses To Remove Non-Gravitational Forces

To ensure GDEM meets its scientific objectives, the mission employs atom interferometry (AI) for drag-free control, targeting a sensitivity level of 10^{-15} m/s^2 to sense and compensate non-gravitational forces such as solar radiation pressure, atmospheric drag, magnetic fields, and thermal forces. This precision is pivotal for maintaining the test masses in a near-perfect free-fall state. Once AI test masses can measure and correct all drag effects, all four spacecraft in the constellation can be treated as drag-free satellites.

Objective for AI Sensitivity: Implement atom interferometry to detect non-gravitational forces at the level of 10^{-15} m/s^2. This sensitivity is essential to ensure that the spacecraft and test masses follow a trajectory influenced solely by gravity. Assuming a measurement time of 100 s, that is, the acceleration sensitivity will be achieved after 100 s of data accumulation, the AI sensitivity is 10^{-14} m/s^2/ $\sqrt{Hz}$ with sufficient data rate. Following is a high-level description and a notional parameter set to achieve such a sensitivity. A Mach-Zehnder AI with large momentum transfer beam splitters of $2n\hbar k$ and an interrogation time T has a per shot acceleration sensitivity of $\delta a = \left(nkT^2C\sqrt{2N}\right)^{-1}$, where C is the fringe contrast and N is the number of participating atoms. Factoring in the measurement cycle time $T_c \geq 2T$, the sensitivity can be reached with T=10 s, n=200 and N=10^8, assume C=0.5.

As mentioned earlier, the self-gravity of the spacecraft is a concern. Ideally, atoms are the test particles freely falling under gravity, undisturbed by drag, radiation pressure, etc. The AI measures the relative acceleration between the atoms and the spacecraft, and thus precisely measures non-gravitational forces that the spacecraft experiences against the totally drag-free atomic test masses. However, the existence of gravitational attraction due the spacecraft mass biases the AI measurements as well as introduces measurement noises due to the position dependent self-gradient. To

reduce the self-gradient noise and the bias error due the craft mass distribution, we baselined approach of operating the atomic test masses over 100 m away from the craft itself.

To further help reduce errors from the self-gradient effects, we investigated and propose an alternative AI measurement mode. For instance, the gravitational acceleration is $3\text{x}10^{-7}$ m/s^2 at a distance 10 m away from a 500 kg spacecraft, which is several orders of magnitude larger than the targeted non-gravitational acceleration sensitivity. Rather than rely on precise modeling of the spacecraft to subtract the self-gravity, the figure-8 double-loop AI scheme described in the following would greatly suppress it with an acceptable degradation of acceleration measurement sensitivity.

While the equivalence principle excludes the possibility to separate gravitational acceleration from platform motion, the scheme exploits the difference in spatial profile of the two. On the one hand, when sufficiently far away from the spacecraft, its gravitational acceleration can be well-modeled as $1/r^2$. On the other hand, platform motion yields a spatially-uniform (position independent) acceleration. We design an AI configuration that suppresses sensitivity to $1/r$ potential while largely maintains sensitivity to uniform acceleration. The configuration is an asymmetric double-loop geometry (figure-8) starting at distance x_0 of the $1/r$ potential, and AI pulses are applied at times $(0, T, 2T + T_2, 2T + 2T_2)$, as depicted in Figure **5**, where $\bar{v}$ is the mean drift velocity of the AI.

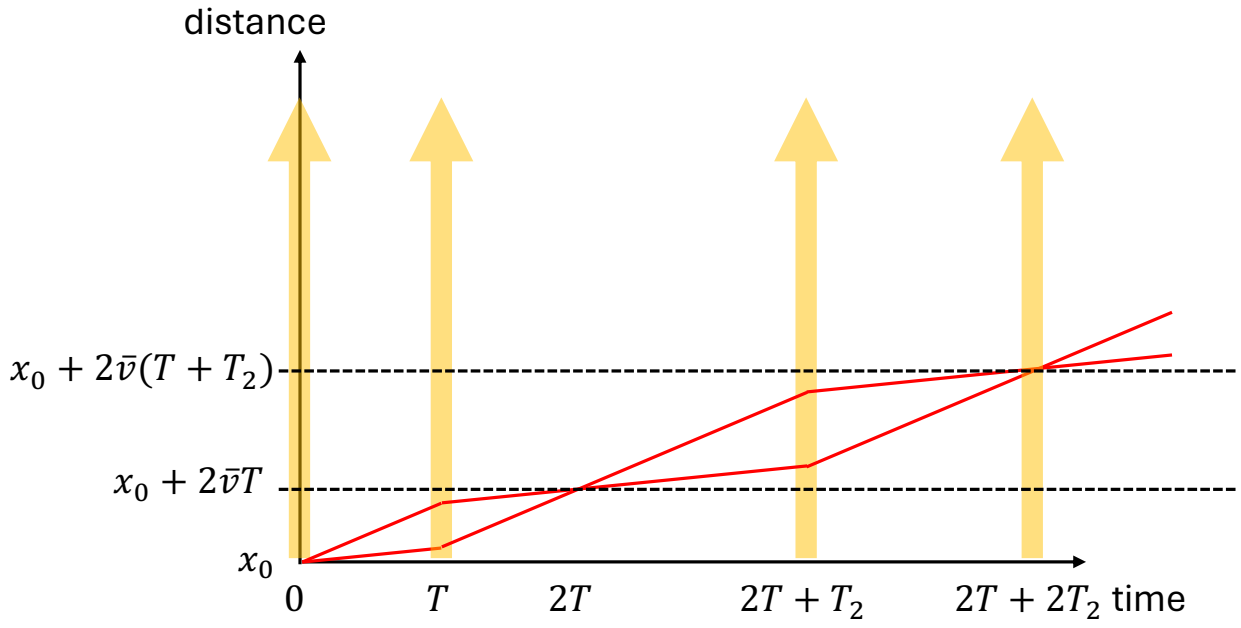

Figure 5. Spacetime diagram of a double-loop AI

It is essentially two back-to-back Mach-Zehnder interferometers of different interrogation times, and the resulting phase is the phase **difference** of such two interferometers. It can be shown that, for a weak potential, the sensitivity to the $1/r$ potential is nulled when $T_2 = T(1 + 2T\bar{v}/x_0)$, and the sensitivity to the uniform acceleration is reduced to $2nk(T_2^2 - T^2) = 2nk(T + T_2)^2((T_2 - T)/(T_2 + T))$. Note that the total interferometer time is $2(T + T_2)$ instead of $2T$.

The targeted sensitivity can be reached with the following parameters: $N = 10^8, n = 100, C = 0.5, x_0 = 10\ m, T = 6\ s, T_2 = 13.2\ s$, and $T_c = 39.4\ s$. The expected sensitivity is $0.8\text{x}10^{-14}$ m/s^2/ $\sqrt{Hz}$. At the end of the interferometer, the distance is 48.4 m away from the spacecraft. Thus, a boom of 50 m length will be sufficient for deploying the retroreflection mirror assembly.

Atomic test masses outside the spacecraft will subject to solar radiations and deep space environment. The main effects are due the residual magnetic field in deep space and the solar radiation. Normal magnetic field strength at 1 AU is about 10s of micro-G, which is not expected to have significant impact to AI measurements. In addition, AI methods such as Bragg diffraction will make the measurement totally insensitive to the magnetic fields.

We have also investigated the solar UV radiation effects on the atomic test masses and atom interferometer operation (Chiow, 2024). A detailed analysis shows the UV ionization on unshielded neutral atoms will have finite ionization cross section. We estimate the ionization rate will be 0.1%/s. The ionized atomic particles will acquire a large momentum that will be fly out of the atomic assembly, resulting a net loss of atom numbers. Within the planned AI interrogation time duration, we have about 1% atom loss, which will have little effect on the atom detection signal to noise ratio.

On the other hand, when ionized atoms transit through the atomic cloud, they will have large cross section of collisions with neutral atomic, inducing large phase shifts. Interesting, we can show that these large phase shifts are exactly cancelled by the propagation phase shift due to the corresponding collisional trajectory change. As a result, the single point collision with ions do not result in a net phase error.

4.4 Laser Ranging Interferometer For Doppler, Ranging And Sagnac Measurements

Objective: GDEM must rely on a high precision range measurement precision at the LISA-level of 30 pm/√Hz and with the absolute distance ranging of μm over 1,000 km spacecraft separation. This level of precision is essential for the accurate determination of distances between spacecraft, which in turn is crucial for maintaining formation, conducting gravitational research, and achieving the mission's scientific objectives.

Technical Approach:

- *Ultra-Stable Lasers:* Lasers with extremely stable frequency and high coherence are required. The stability of the laser's frequency directly impacts the precision of the range measurement, as variations can cause significant errors over the long distances involved. This translates in laser technology capable of achieving stability and coherence at the 10^{-15} level or better.
- *Constellation angular frequency measurements:* To achieve high precision in determining the angular velocity of the tetrahedron's rotation, Sagnac interferometers are used to measure angular frequencies with an accuracy that reaches up to 2.5×10^{-15} rad/s. This exceptional precision is crucial for accurately detecting and compensating for rotational effects within the spacecraft formation. By utilizing Sagnac interferometry, the mission can effectively distinguish and correct for the angular movements, ensuring that the gravity gradient tensor (GGT) measurements are accurate and free from errors induced by the spacecraft's own dynamics.
- *Absolute arranging:* laser arrange in absolute accuracy of μm level has been demonstrated over relative short distances. There are several distinct classes of approaches including frequency scanning, frequency mixing, synthetic wavelengths as well as use of frequency combs and optical cross correlations. While μm level precision is not difficult by itself, the main challenge

is the resolving ambiguities that require signal bandwidths. High time resolving pulses and multiple high bandwidth modulation schemes can be used. A robust and efficient ranging approach and protocol will be developed in the next phase of the study.

- *Precise Optical Path Control:* Ensure that the optical paths within the laser ranging systems and the Sagnac interferometer are controlled and maintained with extreme precision. Any path length instability must be minimized to a scale that does not affect the 10^{-15} rad/s rotational measurement, potentially requiring picometer-level control, specifically around 30 pm/√Hz for laser ranging. For Doppler measurements, precision in the range of millimeters per second is necessary to accurately detect velocity shifts. This level of precision is crucial for maintaining the integrity of laser ranging and Doppler measurements, which are instrumental in achieving the required accuracy for detecting minute rotational movements within the spacecraft formation.

5 THE NEW MISSION ARCHITECTURE FOR FUNDAMENTAL PHYSICS

The innovative features of our work rely on the recognition that placing four spacecraft in a tetrahedral formation on elliptical orbits around the Sun allow to precisely measure GGT trace and detect potential deviations from general relativity. GDEM experiment, aims to reach a sensitivity level of 10^{-24} s^{-2}, by utilizing advanced techniques of laser ranging and atom-wave interferometry for accurate local measurements, and Sagnac interferometry for measuring the tetrahedral rotation. We examined the dynamic behavior of the spacecraft formation, developed analytical models for observables, and outlined mission requirements, ultimately assessing the feasibility of accurately measuring the trace of the GGT and contributing to our understanding of gravitational physics.

5.1 Conceptual Designs For The GDEM Mission

Many studies investigated the science objectives and the technological feasibility of fundamental physics missions, including several NIAC studies. Our work benefited from these earlier studies by allowing us to focus on the GDEM-specific features. Clearly, GDEM stands as a pioneering approach in experimental fundamental physics and astrophysics, particularly in investigating gravitational theories using a satellite formation in heliocentric orbit. The mission involves satellites flying in a tightly coordinated formation, each following its own eccentric orbit around the Sun, typically separated by ~1,000 kilometers. This configuration is critical for the experiment's accuracy and feasibility.

A key aspect of GDEM is its reliance on data collected solely within the satellite constellation, steering clear of traditional methods like precision astrometry or high-accuracy radio navigation due to their insufficient accuracy for this type of experiment. The focus is on using intersatellite range data along with the corresponding accelerations, derived as second time derivatives of these distances. This internal data collection is fundamental in reconstructing the trace of the GTT.

One of the major challenges in this mission is the rotation of the satellite formation, or the tetrahedron. This rotation complicates the measurements as it introduces pseudo-accelerations, which result from the rotating reference frame of the satellites. These pseudo-accelerations need to be accurately distinguished from the actual accelerations to ensure the integrity of the data.

To address this, the mission proposes the use of a generalized Sagnac-type observable. This approach is expected to measure the required data accurately within the constellation itself, thus avoiding the need for external reference systems. Interestingly, the mission plans to utilize the existing laser ranging equipment onboard the satellites for these measurements, potentially

requiring only modest modifications. This use of the laser ranging equipment for both distance and Sagnac-type measurements demonstrates the mission's innovative and efficient use of technology.

We considered the trades between geocentric and heliocentric approaches based on smallsats. The latter option opens the possibility of reaching higher sensitivity. The technology requirements were of a particular interest. As many space systems are now being designed in anticipation of radical changes, focusing on resiliency, adaptability, and disaggregation, we expect major progress in these areas soon, benefiting the GDEM mission.

We approached this study with the topics revolving around autonomy, positioning, navigation, communication, and onboard processing. We will focus on the mission architecture and application of small spacecraft. This includes operations in the tetrahedral spacecraft configuration over the period of 3 years, using cooperative small spacecraft on heliocentric orbits.

5.2 Tetrahedron formation orbit dynamics

The mission architecture we propose is radical, specifically tailored to the mission requirements for the collection of many years of data. This provides the needed CONOPS flexibility described in this report.

GDEM employs a tetrahedral configuration of satellites (Figure 2, Figure 6), which is a central element of its mission design and scientific approach. This geometric arrangement, where four spacecraft are positioned in a tetrahedron, is key for effective measurement of gravitational effects.

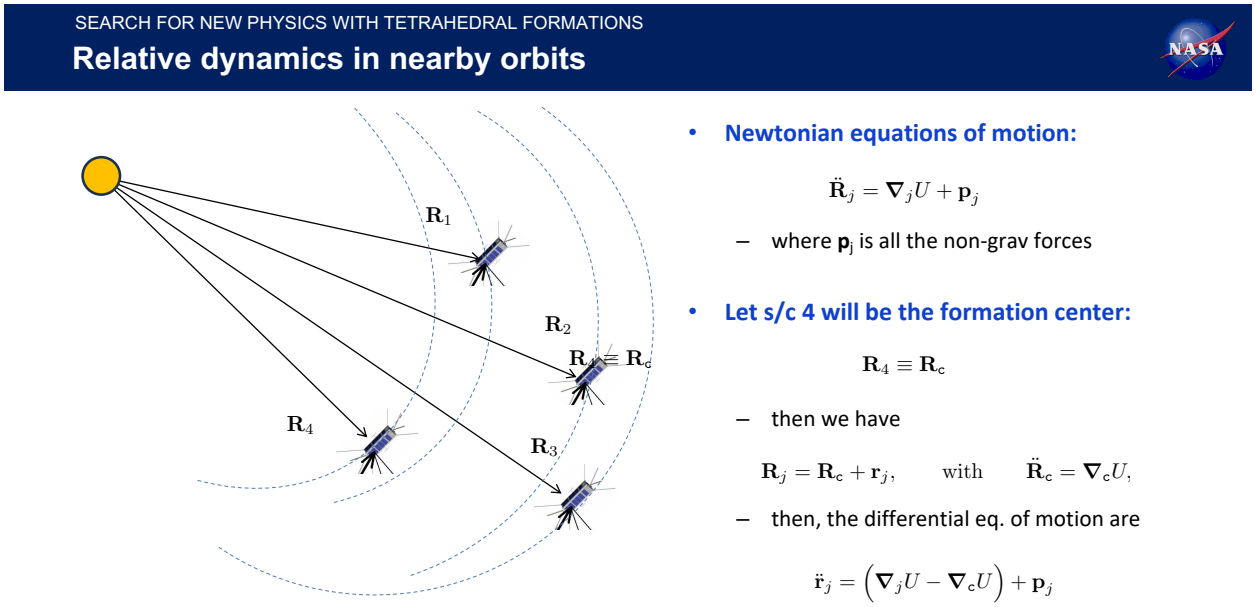

Figure 6. Relative dynamics of spacecraft on nearby heliocentric orbits, thus forming a tetrahedron shown on Figure 1.

The choice of a tetrahedral formation is not arbitrary. It allows for the sampling of gravitational effects in four non-coplanar directions. This is crucial for the mission because it enables the effective nullification or detection of tensor traces, which are important for understanding the gravitational field. Importantly, this benefit is retained regardless of the orientation of the tetrahedron in space, which adds robustness to the measurements and reduces potential complexities related to spacecraft alignment and orientation.

In the context of the GDEM, the tetrahedral formation consists of four spacecraft following nearby elliptical orbits. We delved into the dynamical behavior of such a configuration, exploring how it evolves, rotates, and its elastic properties. Understanding these dynamics will help the mission architecture and design. How the formation changes over time and in response to various gravitational forces will influence the data collected and the interpretations drawn from it. This configuration consists of four spacecraft operating in nearby elliptic heliocentric orbits. For that, we formulated analytical expressions that effectively capture the details of the spacecraft dynamics within an orbital coordinate system introduced at the tetrahedron.

Consider that a constellation of four spacecraft that move around the Sun in a close tetrahedral formation, as seen from the solar system's barycentric coordinate reference system (BCRS), the motion of a j-th spacecraft under the gravitational attraction from the Sun, is governed by the classical equations of motion, where R_j is the position of the spacecraft in the BCRS, U is the solar gravitational potential, and $\boldsymbol{p}_j$ are the accelerations associated with other forces (both of gravitational and non-gravitational nature), spacecraft on-board disturbances, or control inputs. On the other hand, since we have the basic assumption on the drag-free spacecraft behavior, then the $\boldsymbol{p}_j$ would denote the unknown forces that we are interested to detect.

The acceleration of the j-th spacecraft is determined by the gradient of the gravitational potential (U) at the spacecraft's position (j) minus the gradient at the center of mass of the configuration (c), plus any additional perturbative accelerations ($\boldsymbol{p}_j$):

$$\ddot{\mathbf{r}}_j = \left(\nabla_j U - \nabla_c U\right) + \mathbf{p}_j$$

Other gravity forces include that due to the solar quadrupole moment, denoted as (J_2), has a value of 2.21 x 10^{-7} which leads to an acceleration a_{J2} of approximately 4.25 x 10^{-14} m/s²:

$$\delta a_{ij} \simeq a_{J_2}\left(r_{ij}/1\mathrm{AU}\right) \sim 2.84 \times 10^{-19}\ \mathrm{m/s^2}\ \ \Delta\mathrm{GGT}:\ \delta a_{ij}/r_{ij} \sim 2.84 \times 10^{-25}\ \mathrm{s^{-2}}$$

Differential acceleration, give as the difference in the acceleration due to the solar quadrupole moment between two spacecraft (i and j), (δa_{ij}), scales with the ratio of the inter-spacecraft distance (r_{ij}) over 1 AU, resulting in an approximate value of 2.84 x 10^{-19} m/s². This relates to the changes in ΔGGT as $\delta a_{ij}/r_{ij}$, given as below:

$$\delta a_{ij} \simeq a_{J_2}\left(r_{ij}/1\mathrm{AU}\right) \sim 2.84 \times 10^{-19}\ \mathrm{m/s^2}\ \ \Delta\mathrm{GGT}:\ \delta a_{ij}/r_{ij} \sim 2.84 \times 10^{-25}\ \mathrm{s^{-2}}$$

Post-Newtonian terms: Relativistic corrections to the spacecraft's acceleration ($\ddot{\mathbf{r}}_{\mathrm{GR}}$) are accounted for by the post-Newtonian terms. They involve the standard gravitational parameter ($\mu_\odot$) of the Sun, the speed of light (c), and factors of the parameterized post-Newtonian parameters (β and γ), leading to an acceleration of approximately 4.12 x 10^{-10} m/s²:

$$\ddot{\mathbf{r}}_{\mathrm{GR}} = \frac{\mu_\odot}{c^2 r^3}\left\{\left[2(\beta+\gamma)\frac{\mu_\odot}{r} - \gamma\dot{\mathbf{r}}^2\right]\mathbf{r} + 2(1+\gamma)(\mathbf{r}\cdot\dot{\mathbf{r}})\dot{\mathbf{r}}\right\} \simeq 4.12 \times 10^{-10}\ \mathrm{m/s^2}$$

Differential acceleration: The differential acceleration due to post-Newtonian corrections ($\delta a_{ij}^{\mathrm{GR}}$), analogous to the solar quadrupole moment, is given for two spacecraft separated by distance (r_{ij}) at 1 AU, resulting in 2.76 x 10^{-15} m/s². The corresponding impact on the ΔGGT of.

$$\delta a_{ij}^{\mathrm{GR}} = \ddot{\mathbf{r}}_{\mathrm{GR}}\left(r_{ij}/1\mathrm{AU}\right) = 2.76 \times 10^{-15}\ \mathrm{m/s^2}\ \Delta\mathrm{GGT}:\ \delta a_{ij}^{\mathrm{GR}}/r_{ij} \simeq 2.76 \times 10^{-21}\ \mathrm{s^{-2}}$$

Terms due to finite derivatives: The terms resulting from finite differences in the gravitational potential $\left(\nabla_j U - \nabla_c U\right)$ are computed, showing a dependence on the spacecraft's relative positions and incorporating the solar gravitational potential. The expression includes the gravitational

multipole moments $\mathcal{Q}^{<abc>}$ and $\mathcal{Q}^{<abcd>}$, which factor in the spacecraft's relative position vectors and higher-order derivatives, with the remainder term $\mathcal{O}\left(r_j^4/R_c^6\right)$:

$$\left(\nabla_j U - \nabla_c U\right)^a \simeq -\frac{\mu_\odot}{R_c^3}(\delta^{ab} - 3n_c^a n_c^b)r_j^b - \frac{15\mu_\odot}{2R_c^4}\mathcal{Q}^{<abc>}r_j^b r_j^c - \frac{35\mu_\odot}{2R_c^5}\mathcal{Q}^{<abcd>}r_j^b r_j^c r_j^d$$

The $\mathcal{Q}^{<abc>}$ and $\mathcal{Q}^{<abcd>}$ terms are defined as combinations of the spacecraft's relative position unit vectors ($\boldsymbol{n}_c$) and the Kronecker delta (δ^{ab}), representing the trace-free part of the gravitational potential's third and fourth derivatives. These terms encapsulate the complex interactions of the spacecraft with the solar gravitational field and its deviations from a spherically symmetric potential, which are crucial for precise GDEM measurements:

$$\mathcal{Q}^{<abc>} = \left\{n_c^a n_c^b n_c^c - \frac{1}{5}\delta^{ab}n_c^c - \frac{1}{5}\delta^{ac}n_c^b - \frac{1}{5}\delta^{bc}n_c^a\right\},$$

$$\mathcal{Q}^{<abcd>} = \left\{n_c^a n_c^b n_c^c n_c^d - \frac{1}{7}(n_c^a n_c^b \delta^{cd} + n_c^a n_c^c \delta^{bd} + n_c^a n_c^d \delta^{bc} + n_c^b n_c^c \delta^{ad} + n_c^b n_c^d \delta^{ac} + n_c^c n_c^d \delta^{ab}) + \right.$$
$$\left. + \frac{1}{35}(\delta^{ab}\delta^{cd} + \delta^{ac}\delta^{bd} + \delta^{ad}\delta^{bc})\right\}.$$

7. Linearized equations of motion and main contributing forces.

The objective was to investigate the architecture and the anticipated sensitivities in measuring the GGT provided by a tetrahedral spacecraft configuration. For that, it is sufficient to consider only non-relativistic Newtonian approximation GR, which, in this case, collapses to Poisson equation (2), which outside the mass distribution collapses to Laplace equation, which says that GTT is trace-free. This turns out to be the most powerful check for the presence of new physical laws in the solar system. Measurement systems prescribed for GDEM involve assessing GGT between spacecraft pairs connected by laser ranging interferometers across considerable distances, important for reaching the required sensitivity. While like the inter-spacecraft laser ranging in LISA, GDEM's system is tailored for accuracy over these specific distances.

To describe dynamics of the spacecraft within the constellation, we need to choose a reference point which could be either the formation's center or one of the satellites. Such a choice allowed to present spacecraft motion with respect to the reference center.

- Let's evaluate terms:

$$\left(\nabla_j U - \nabla_c U\right)^a \simeq -\frac{\mu_\odot}{R_c^3}(\delta^{ab} - 3n_c^a n_c^b)r_j^b - \frac{15\mu_\odot}{2R_c^4}\mathcal{Q}^{<abc>}r_j^b r_j^c - \frac{35\mu_\odot}{2R_c^5}\mathcal{Q}^{<abcd>}r_j^b r_j^c r_j^d + \mathcal{O}\left(r_j^4/R_c^6\right)$$

- Liner in $\propto r_i$ term:
  differential acceleration: $\delta_1 a_{ij} \simeq 7.93 \times 10^{-8}$ m/s^2 ΔGGT: $\delta_1 a_{ij}/r_{ij} \simeq 7.93 \times 10^{-14}$ s^{-2}
- quadratic in $\propto r_i^2$ term:
  differential acceleration: $\delta_2 a_{ij} \simeq 7.95 \times 10^{-13}$ m/s^2 ΔGGT: $\delta_2 a_{ij}/r_{ij} \simeq 7.95 \times 10^{-19}$ s^{-2}

- cubic in $\propto r_i^3$ term:
  differential acceleration: $\delta_3 a_{ij} \simeq 7.09 \times 10^{-18}$ m/s^2 ΔGGT: $\delta_3 a_{ij}/r_{ij} \simeq 7.09 \times 10^{-24}$ s^{-2}
- Next order term $\propto r_i^4$ contributes ΔGGT: $\delta_4 a_{ij}/r_{ij} \simeq 1.18 \times 10^{-29}$ s^{-2}
- Combining all the terms, we have
  $\mathbf{f}_j = \mathbf{p}_j + \ddot{\mathbf{r}}_{\rm GR} - \frac{15\mu_\odot}{2R_c^4} \mathcal{Q}^{<abc>} r_j^b r_j^c - \frac{35\mu_\odot}{2R_c^5} \mathcal{Q}^{<abcd>} r_j^b r_j^c r_j^d + \mathcal{O}\left(r_j^4/R_c^4\right)$
- Remember GTT: $\mathbf{T} \equiv -\frac{\mu_\odot}{r^3}(\delta^{ab} - 3n^a n^b) + \mathcal{O}(2.84 \times 10^{-25}\ \mathrm{s}^{-2})$
- Observational equation in BCRS: $\ddot{\mathbf{r}}_j = \left(\boldsymbol{\nabla}_j U - \nabla_c U\right) + \mathbf{p}_j \ \Rightarrow\ \ddot{\mathbf{r}}_j = \mathbf{T} \cdot \mathbf{r}_j + \mathbf{f}_j$

Based on these results, we deruved the equation that describes the motion of a spacecraft with the constellation relative to the formation center from the standpoint of the BCRS. As a result, using theyr determied the observational equation needed to determine the GGT:

- Using kinematics, we have $\ddot{\mathbf{r}}_j = \ddot{\mathbf{r}}_j^* + 2\left[\boldsymbol{\omega} \times \dot{\mathbf{r}}_j^*\right] + \left[\boldsymbol{\omega} \times \left[\boldsymbol{\omega} \times \mathbf{r}_j\right]\right] + \left[\dot{\boldsymbol{\omega}} \times \mathbf{r}_j\right]$:

$$\boldsymbol{\omega}_{\rm RIC} \ \rightarrow\ \boldsymbol{\omega} = \boldsymbol{\omega}_{\rm RIC} + \boldsymbol{\omega}_{\rm TCS:}$$

- Equations of motion in an orbital frame:

$$\ddot{\mathbf{r}}_j = \mathbf{T} \cdot \mathbf{r}_j + \mathbf{f}_{j:} \ \Rightarrow\ \ddot{\mathbf{r}}_j^* = \mathbf{T}_c \cdot \mathbf{r}_j + \mathbf{f}_j - \left[\boldsymbol{\omega} \times \left[\boldsymbol{\omega} \times \mathbf{r}_j\right]\right] - \left[\dot{\boldsymbol{\omega}} \times \mathbf{r}_j\right] - 2\left[\boldsymbol{\omega} \times \dot{\mathbf{r}}_j^*\right]$$

rotational matrix: $\boldsymbol{\Omega} = \begin{bmatrix} 0 & -\omega_z & \omega_y \\ \omega_z & 0 & -\omega_x \\ -\omega_y & \omega_x & 0 \end{bmatrix}$, $\boldsymbol{\Omega}^2 =$
$\begin{bmatrix} -\left(\omega_y^2 + \omega_z^2\right) & \omega_x\omega_y & \omega_x\omega_z \\ \omega_x\omega_y & -(\omega_x^2 + \omega_z^2) & \omega_y\omega_z \\ \omega_x\omega_z & \omega_y\omega_z & -\left(\omega_x^2 + \omega_y^2\right) \end{bmatrix}$, $\dot{\boldsymbol{\Omega}} = \begin{bmatrix} 0 & -\dot{\omega}_z & \dot{\omega}_y \\ \dot{\omega}_z & 0 & -\dot{\omega}_x \\ -\dot{\omega}_y & \dot{\omega}_x & 0 \end{bmatrix}$
simplifying the cross-product: $\left[\boldsymbol{\omega} \times \left[\boldsymbol{\omega} \times \mathbf{r}_j\right]\right] = \left(\boldsymbol{\Omega}^2 \cdot \mathbf{r}_j\right)$, $\left[\dot{\boldsymbol{\omega}} \times \mathbf{r}_j\right] = \left(\dot{\boldsymbol{\Omega}} \cdot \mathbf{r}_j\right)$, $\left[\boldsymbol{\omega} \times \dot{\mathbf{r}}_j^*\right] = \left(\boldsymbol{\Omega} \cdot \dot{\mathbf{r}}_j^*\right)$

- Equations of motion in the orbital frame: $\ddot{\mathbf{r}}_j^* = \left\{\mathbf{T}_c - \boldsymbol{\Omega}^2 - \dot{\boldsymbol{\Omega}}\right\}\mathbf{r}_j - 2\left(\boldsymbol{\Omega} \cdot \dot{\mathbf{r}}_j^*\right) + \mathbf{f}_j$
- Same in differential form: $\ddot{\mathbf{r}}_{ij}^* = \left\{\mathbf{T}_c - \boldsymbol{\Omega}^2 - \dot{\boldsymbol{\Omega}}\right\}\mathbf{r}_{ij} - 2\left(\boldsymbol{\Omega} \cdot \dot{\mathbf{r}}_{ij}^*\right) + \mathbf{f}_{ij}$ - key equation in the TCS.

- Equation

$$\ddot{\mathbf{r}}_{ij}^* = \left\{\mathbf{T}_c - \boldsymbol{\Omega}^2 - \dot{\boldsymbol{\Omega}}\right\}\mathbf{r}_{ij} - 2\left(\boldsymbol{\Omega} \cdot \dot{\mathbf{r}}_{ij}^*\right) + \mathbf{f}_{ij}$$

- after e-arranging: $\mathbf{u}_{ij} = \mathbf{M}\mathbf{r}_{ij}$ where $\mathbf{u}_{ij} \equiv \ddot{\mathbf{r}}_{ij}^* + 2\left(\boldsymbol{\Omega} \cdot \dot{\mathbf{r}}_{ij}^*\right) - \mathbf{f}_{ij}$, $\mathbf{M} = \mathbf{T} - \boldsymbol{\Omega}^2 - \dot{\boldsymbol{\Omega}}$.
- Equivalently, in matrix form, at s/c #4: $\mathrm{U} = \mathrm{MR}$

$$\mathbf{U}=\begin{bmatrix} u_{41}^{x} & u_{42}^{x} & u_{43}^{x} \\ u_{44}^{y} & u_{42}^{y} & u_{43}^{y} \\ u_{41}^{z} & u_{42}^{z} & u_{43}^{z} \end{bmatrix},\ \mathbf{M}=\begin{bmatrix} M_{11} & M_{12} & M_{13} \\ M_{21} & M_{22} & M_{23} \\ M_{31} & M_{32} & M_{33} \end{bmatrix},\ \mathbf{R}=\begin{bmatrix} r_{41}^{x} & r_{42}^{x} & r_{43}^{x} \\ r_{41}^{y} & r_{42}^{y} & r \\ r_{41}^{z} & r_{42}^{r} & r_{43}^{r} \end{bmatrix}$$

- Inverse to R :

$$\mathbf{R}^{-1}=\frac{1}{\det(\mathbf{R})}\begin{bmatrix} [\mathbf{r}_{42}\times\mathbf{r}_{43}]^{\mathrm{T}} \\ [\mathbf{r}_{43}\times\mathbf{r}_{41}]^{\mathrm{T}} \\ [\mathbf{r}_{41}\times\mathbf{r}_{42}]^{\mathrm{T}} \end{bmatrix}=\left(\frac{\tilde{\mathbf{n}}_{41}}{r_{41}},\frac{\tilde{\mathbf{n}}_{42}}{r_{42}},\frac{\tilde{\mathbf{n}}_{43}}{r_{43}}\right)$$

- Reciprocal basis: $\tilde{\mathbf{n}}_{41}=\frac{[\mathbf{n}_{42}\times\mathbf{n}_{43}]}{(\mathbf{n}_{41}\cdot[\mathbf{n}_{42}\times\mathbf{n}_{43}])},\ \tilde{\mathbf{n}}_{42}=\frac{[\mathbf{n}_{43}\times\mathbf{n}_{41}]}{(\mathbf{n}_{42}\cdot[\mathbf{n}_{43}\times\mathbf{n}_{41}])},\ \tilde{\mathbf{n}}_{43}=\frac{[\mathbf{n}_{41}\times\mathbf{n}_{42}]}{(\mathbf{n}_{43}\cdot[\mathbf{n}_{41}\times\mathbf{n}_{42}])}$
- as a result: $\mathrm{tr}\,(\mathbf{M})_4=\frac{(\mathbf{u}_{41}\cdot\tilde{\mathbf{n}}_{41})}{r_{41}}+\frac{(\mathbf{u}_{42}\cdot\tilde{\mathbf{n}}_{42})}{r_{42}}+\frac{(\mathbf{u}_{43}\cdot\tilde{\mathbf{n}}_{43})}{r_{43}}$

Using kinematics, the relative acceleration observed in the inertial reference frame in the BCRS can be related to the measurements in the orbiting tetrahedron coordinate system (TCS) as shown in **Error! Reference source not found.**. Thus, in addition to the first two terms containing inertial accelerations, this equation has three other terms due to the non-inertial forces acting on the space-craft in the TCS: the third term is due to the centrifugal force, the fourth term is due to the Euler force, and the last term is due to the Coriolis force.

The observational equation may be solved to determine the trace[GGT], as shown in **Error! Reference source not found.**.

For description of these measurements, an orbital reference frame and appropriate coordinate system were introduced. Such a system is needed to describe the relative dynamics between the spacecraft and the relevant measurements as well as to transform the results between the orbital frame and the BCRS, if needed. The tetrahedral coordinate system (TCS) is given in Figure.

- **Tetrahedral coordinate system:**
  - Coordinate base vectors: $\mathbf{e}_x=\mathbf{n}_{41},\quad \mathbf{e}_z=\frac{[\mathbf{n}_{41}\times\mathbf{n}_{42}]}{|[\mathbf{n}_{41}\times\mathbf{n}_{42}]|},\quad \mathbf{e}_y=[\mathbf{e}_z\times\mathbf{e}_x]$
  - Differential vectors: $\mathbf{r}_{41}=r_{41}(1,0,0)\equiv r_{41}\mathbf{n}_{41},$ $\boldsymbol{\omega}=\boldsymbol{\omega}_{\mathrm{RIC}}+\boldsymbol{\omega}_{\mathrm{TCS}},$
    $\mathbf{r}_{42}=r_{42}(\cos\alpha_{12},\sin\alpha_{12},0)\equiv r_{42}\mathbf{n}_{42},$
    $\mathbf{r}_{43}=r_{43}(\cos\alpha_{13},\sqrt{\sin^2\alpha_{13}-\sin^2\beta_3},\sin\beta_3)\equiv r_{43}\mathbf{n}_{43}.$

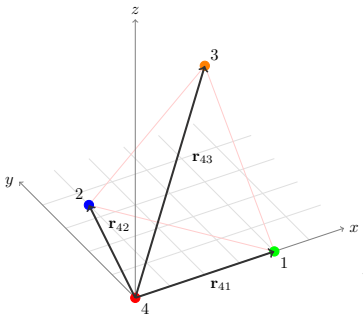

$$\cos\alpha_{12}=\frac{r_{41}^2+r_{42}^2-r_{12}^2}{2r_{41}r_{42}}\qquad \cos\alpha_{13}=\frac{r_{41}^2+r_{43}^2-r_{13}^2}{2r_{41}r_{43}}$$

$$\sin\beta_3=(\mathbf{n}_{43}\cdot[\mathbf{n}_{41}\times\mathbf{n}_{42}])=\pm\frac{6V}{r_{41}r_{42}r_{43}}$$

$$V=\tfrac{1}{12}\left(4r_{41}^2r_{42}^2r_{43}^2-r_{41}^2u^2-r_{42}^2v^2-r_{43}^2w^2+uvw\right)^{\frac{1}{2}},$$

$$u=r_{42}^2+r_{43}^2-r_{23}^2,\qquad v=r_{41}^2+r_{43}^2-r_{13}^2,\qquad w=r_{41}^2+r_{42}^2-r_{12}^2.$$

All relevant vectors are expressed in terms of the intersatellite ranges

Figure 8. The tetrahedral coordinate system (TCS).

Tetrahedral coordinate system is defined as below:

- Coordinate base vectors:

$$\mathbf{e}_x = \mathbf{n}_{41},\ \mathbf{e}_z = \frac{[\mathbf{n}_{41} \times \mathbf{n}_{42}]}{|[\mathbf{n}_{41} \times \mathbf{n}_{42}]|},\ \mathbf{e}_y = [\mathbf{e}_z \times \mathbf{e}_x]$$

- Differential vectors:

$$\mathbf{r}_{41} = r_{41}(1,0,0) \equiv r_{41}\mathbf{n}_{41},$$
$$\mathbf{r}_{42} = r_{42}(\cos\alpha_{12}, \sin\alpha_{12}, 0) \equiv r_{42}\mathbf{n}_{42},$$
$$\mathbf{r}_{42} = r_{42}(\cos\alpha_{12}, \sin\alpha_{12}, 0) \equiv r_{42}\mathbf{n}_{42},$$

Accounting for the fact that angular velocities obey the following relationships:

$$\boldsymbol{\omega} = \boldsymbol{\omega}_{\mathrm{RIC}} + \boldsymbol{\omega}_{\mathrm{TCS}}$$

we have

$$\cos\ \alpha_{12} = \frac{r_{41}^2 + r_{42}^2 - r_{12}^2}{2r_{41}r_{42}}\ \cos\ \alpha_{13} = \frac{r_{41}^2 + r_{43}^2 - r_{13}^2}{2r_{41}r_{43}}$$
$$\sin\ \beta_3 = (\mathbf{n}_{43} \cdot [\mathbf{n}_{41} \times \mathbf{n}_{42}]) = \pm\frac{6V}{r_{41}r_{42}r_{43}}$$

where

$$V = \frac{1}{12}(4r_{41}^2r_{42}^2r_{43}^2 - r_{41}^2u^2 - r_{42}^2v^2 - r_{43}^2w^2 + uvw)^{\frac{1}{2}}$$

and $u = r_{42}^2 + r_{43}^2 - r_{23}^2,\ v = r_{41}^2 + r_{43}^2 - r_{13}^2,\ w = r_{41}^2 + r_{42}^2 - r_{12}^2.$

As a result. all relevant vectors are expressed in terms of the intersatellite ranges.

Using the TCS allow us to present the observational equation in the relevant form, expressing all the quantities involved via a set of local measurement, as shown in Figure 9.

- **Key equation:**

$$\boldsymbol{\omega} = \boldsymbol{\omega}_{\mathrm{RIC}} + \boldsymbol{\omega}_{\mathrm{TCS}};$$

$$\mathrm{tr}(\mathbf{T})_4 \;+\; 2\omega^2 = \\ = \frac{\left(\left(\ddot{\mathbf{r}}^*_{41} + 2[\boldsymbol{\omega}\times\dot{\mathbf{r}}^*_{41}] - \mathbf{f}_{41}\right)\cdot\tilde{\mathbf{n}}_{41}\right)}{r_{41}} + \frac{\left(\left(\ddot{\mathbf{r}}^*_{42} + 2[\boldsymbol{\omega}\times\dot{\mathbf{r}}^*_{42}] - \mathbf{f}_{42}\right)\cdot\tilde{\mathbf{n}}_{42}\right)}{r_{42}} + \frac{\left(\left(\ddot{\mathbf{r}}^*_{43} + [\boldsymbol{\omega}\times\dot{\mathbf{r}}^*_{43}] - \mathbf{f}_{43}\right)\cdot\tilde{\mathbf{n}}_{43}\right)}{r_{43}}$$

- **In the TCS, we have:**

$$\mathrm{tr}(\mathbf{T})_4^{\mathrm{accel}} = \frac{\ddot{r}_{41}}{r_{41}} + \frac{\ddot{r}_{42}}{r_{42}} + \frac{\ddot{r}_{43}}{r_{43}} + \frac{(\sin\alpha_{12})^{\cdot\cdot}}{\sin\alpha_{12}} + \frac{(\sin\beta_3)^{\cdot\cdot}}{\sin\beta_3} + \frac{2\dot{r}_{42}}{r_{42}}\frac{(\sin\alpha_{12})^{\cdot}}{\sin\alpha_{12}} + \frac{2\dot{r}_{43}}{r_{43}}\frac{(\sin\beta_3)^{\cdot}}{\sin\beta_3}$$

$$\mathrm{tr}(\mathbf{T})_4^{\mathrm{forces}} = -\frac{1}{r_{41}}\left\{f_{41x} - f_{41y}\cot\alpha_{12} + \frac{f_{41z}}{\sin\beta_3}\left(\cot\alpha_{12}\sqrt{\sin^2\alpha_{13} - \sin^2\beta_3} - \cos\alpha_{13}\right)\right\} - \\ - \frac{1}{r_{42}\sin\alpha_{12}}\left\{f_{42y} - \frac{f_{42z}}{\sin\beta_3}\sqrt{\sin^2\alpha_{13} - \sin^2\beta_3}\right\} - \frac{f_{43z}}{r_{43}\sin\beta_3}.$$

$$\mathrm{tr}(\mathbf{T})_4^{\mathrm{Cor}} = 2\left\{\frac{\omega_x}{\sin\beta_3}\left\{\sqrt{\sin^2\alpha_{13} - \sin^2\beta_3}\left(\frac{\dot{r}_{43}}{r_{43}} - \frac{(r_{42}\sin\alpha_{12})^{\cdot}}{r_{42}\sin\alpha_{12}}\right) + \left(\sqrt{\sin^2\alpha_{13} - \sin^2\beta_3}\right)^{\cdot}\right\} + \right. \\ + \frac{\omega_y}{\sin\beta_3}\left\{\cos\alpha_{13}\left(\frac{\dot{r}_{41}}{r_{41}} - \frac{\dot{r}_{43}}{r_{43}}\right) + \sqrt{\sin^2\alpha_{13} - \sin^2\beta_3}\left(\frac{(r_{42}\cos\alpha_{12})^{\cdot}}{r_{42}\sin\alpha_{12}} - \cot\alpha_{12}\frac{\dot{r}_{41}}{r_{41}}\right) - (\cos\alpha_{13})^{\cdot}\right\} + \\ \left. + \omega_z\left\{\frac{(r_{42}\cos\alpha_{12})^{\cdot}}{r_{42}\sin\alpha_{12}} - \cot\alpha_{12}\frac{\dot{r}_{41}}{r_{41}}\right\}\right\}.$$

$$\mathrm{tr}(\mathbf{T})_4^{\mathrm{centrif}} = -2\omega^2$$

Figure 9. Expressing all the relevant quantiles via a set of local measurements.

Based on this analysis we were able to formulae a set instrumental requirement for GDEM, as shown in Figure 10. As a result, we were able to express all the quantities involved in the determination of trace of tr(T_4) via two types of observables, namely: i) laser ranging measurements that will provide time series of the inter-satellite ranges, that can be time-differentiated to derives range-rate and line of sight accelerations; and ii) the angular velocity of the non-inertial TCS, ω, with respect to inertial coordinates of the BCRS. Therefore, the knowledge of ω is critical for the success of the experiment.

- **Key equation:**

$$\mathrm{tr}(\mathbf{T})_4 \;+\; 2\omega^2 = \\ = \frac{\left(\left(\ddot{\mathbf{r}}^*_{41} + 2[\boldsymbol{\omega}\times\dot{\mathbf{r}}^*_{41}] - \mathbf{f}_{41}\right)\cdot\tilde{\mathbf{n}}_{41}\right)}{r_{41}} + \frac{\left(\left(\ddot{\mathbf{r}}^*_{42} + 2[\boldsymbol{\omega}\times\dot{\mathbf{r}}^*_{42}] - \mathbf{f}_{42}\right)\cdot\tilde{\mathbf{n}}_{42}\right)}{r_{42}} + \frac{\left(\left(\ddot{\mathbf{r}}^*_{43} + [\boldsymbol{\omega}\times\dot{\mathbf{r}}^*_{43}] - \mathbf{f}_{43}\right)\cdot\tilde{\mathbf{n}}_{43}\right)}{r_{43}}$$

- **Required measurement precision:**

TABLE III: Select set of the GDM mission requirements.

Parameter	Symbol	Value	
Intersatellite range-rate	$\delta\dot{r}_{4i}$	3.2×10^{-5} m/s	← Computed form range data
Line-of-sight acceleration	$\delta\ddot{r}_{4i}$	1×10^{-15} m/s^2	← Computed form range data
Non-gravitational forces	δf_{4i}	1×10^{-15} m/s^2	← Removed with AI
Angular velocity	$\delta\omega$	2.5×10^{-15} s^{-1}	← Provided by Sagnac interferometry
Centrifugal acceleration	$\delta\omega_{\mathrm{CF}}$	2.24×10^{-11} s^{-1}	← DSN navigation or Sagnac

Figure 10. GDEM instrumental requirements.

Below, we will consider two methods to determine the angular velocity of the TCS with respect to the BCRS, including the kinematic determination and that relying on the Sagnac interferometry. For that, we were able to generalize Sagnac observables on the case of an elastic tetrahedron (Figure 11). If precision laser ranging data are available, it enables inertial navigation by providing accurate measurements of the angular velocity vector ω. In other words, Sagnac interferometry conducted along the edges of the three triangles with common vertex within a tetrahedral

configuration, combined with range measurements of the same edges enables determination of ω. This is important for GDEM as it provides critical piece of information needed to determine tr(GTT).

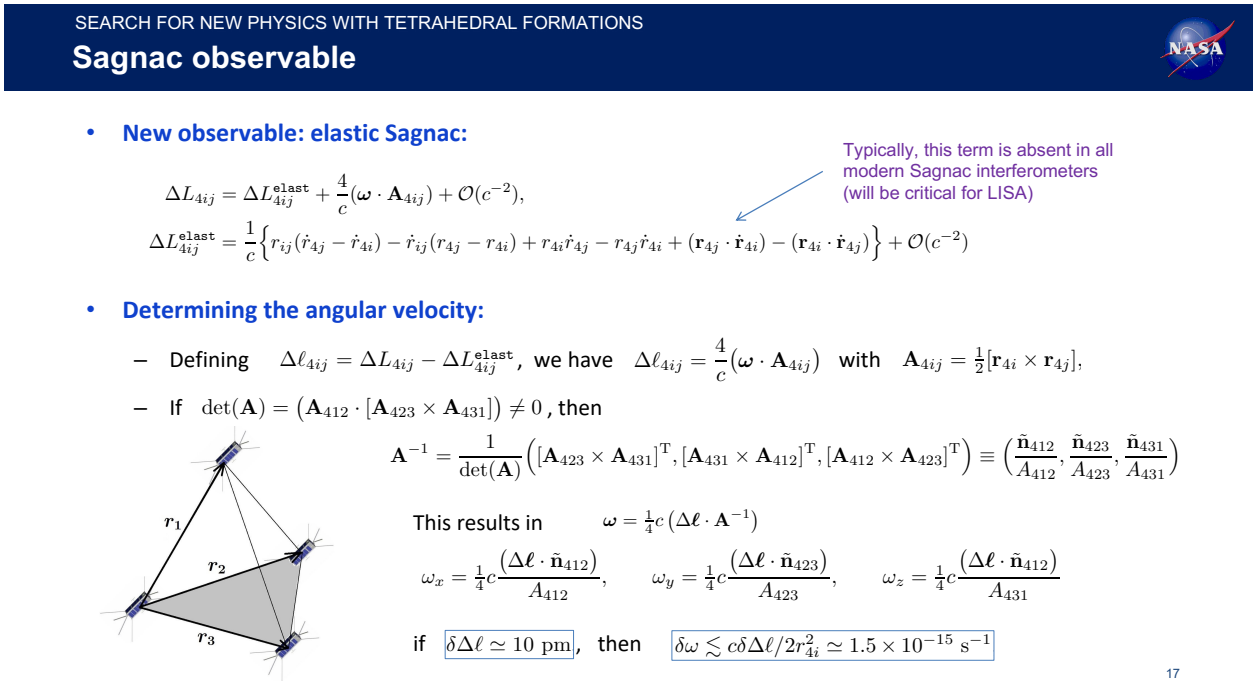

Figure 11. Considering the implementation of the Sagnac observable for GDEM.

An important observation relates to the tetrahedron's volume evolution. Specifically, during each orbital transition, the volume of the tetrahedron, defined by the spacecraft positions, collapses twice. Such changes in the volume can substantially influence the sensitivity and precision of the scientific data that is captured during the mission. We studied the evolution of the distances between the spacecraft in the formation. For orbits with an eccentricity of $e = 0.6$, these inter-spacecraft distances displayed notable variability. We also noted that prior to each of those instances when tetrahedron's volume collapses, the quality of the solution begins to degrade. This may be addressed by resetting the tetrahedral constellation multiple times per orbit, ensuring data quality is maintained across all orbital segments. Consequently, we can gather data throughout crucial orbital segments, particularly at the apogee and perigee, which are vital in the quest for Galileons.

Clearly, many other tetrahedral configurations exist and must be studied and optimized for the ultimate mission. Our choice permits a detailed exploration of a subset of the parameter space without loss of generality, thereby offering valuable insights for the mission design while ensuring computational and analytical efficiency.

The oriented volume of the tetrahedron formed by the four satellites is a fundamental descriptor of its spatial configuration. Using the defined relative vectors $\mathbf{r}_{ij} = \mathbf{r}_j - \mathbf{r}_i$, the volume can be expressed in terms of the scalar triple product. Using the specific values, one can compute the magnitude and sign of the volume, which respectively give the volume's size and the orientation (chirality) of the tetrahedral configuration:

$$V = \tfrac{1}{6}(\mathbf{r}_{41}\cdot[\mathbf{r}_{42}\times\mathbf{r}_{43}]) \equiv \tfrac{1}{6}\det\Big[\mathbf{r}_{41},\mathbf{r}_{42},\mathbf{r}_{43}\Big] = -\tfrac{1}{6\sqrt{2}}\ell_0^3\frac{(1+e)^2\cos^2\nu}{(1+e\cos\nu)^2}.$$

Figure 12 shows the characteristic behavior of the volume that takes four principal values, namely at perigee, $\nu = 0$, it has its nominal value; at $\nu = \frac{\pi}{2}, \frac{3\pi}{2}$ it collapses to zero; and at $\nu = \pi$ it reaches its maximal value, all given below

$$V(0) = \frac{1}{6\sqrt{2}}\ell_0^3, \qquad V(\tfrac{\pi}{2}, \tfrac{3\pi}{2}) = 0, \qquad V(\pi) = \frac{1}{6\sqrt{2}}\ell_0^3 \frac{(1+e)^2}{(1-e)^2}.$$

Note that for $e = 0.6$, as the vehicles move on their orbits between perigee and apogee, the volume increases by a factor of $(1 + e)^2/(1 - e)^2 = 16$, as shown in Figure 12(left).

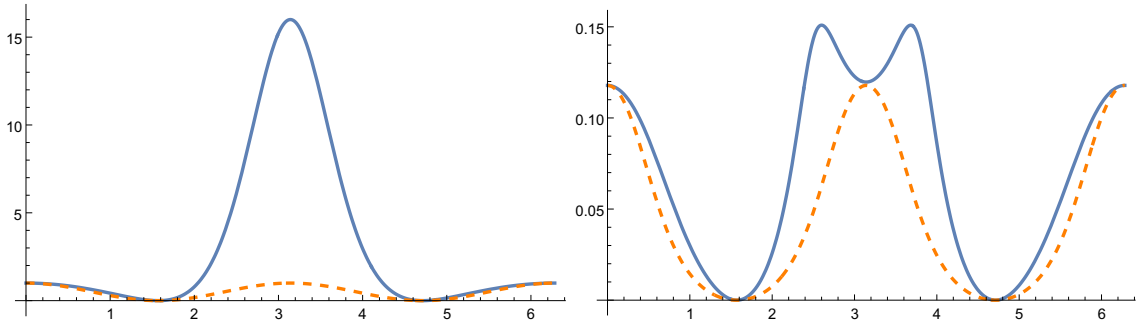

Figure 12. Left: Evolution of the tetrahedron volume as a function of true anomaly ν and eccentricity, e. Vertical axis shows the volume compared to its initial value at the perigee, $V(\nu)/V(0)$, where formation was initiated. Right: Changes in the normalized volume $(\mathbf{n}_{41}\cdot[\mathbf{n}_{42} \times \mathbf{n}_{43}]) = V(\nu)/r_{41}r_{42}r_{43}$. Horizontal axis: $\nu \in [0,2\pi]$. Dashed: $e = 0$; solid: $e = 0.6$.

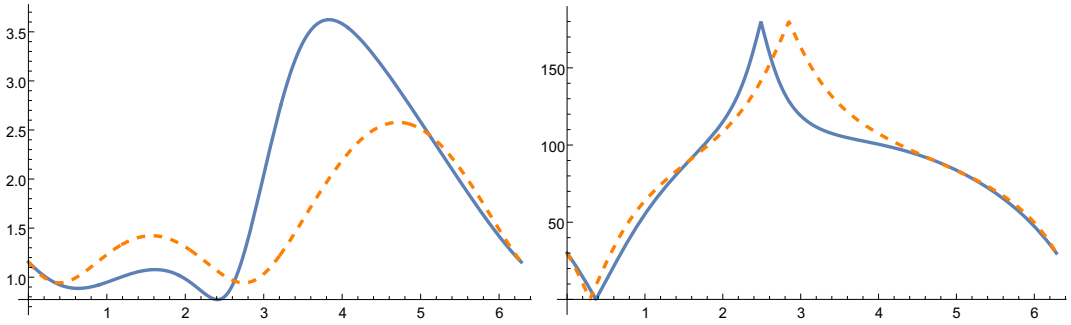

Figure 13. Left: Distance r_{41} as a function of ν and eccentricity, e. Vertical axis shows the distance compared to its initial value at perigee, $r_{41}(\nu)/r_{41}(0)$. Right: Pointing angle $\theta_{41}(\nu)$, as a function of ν and eccentricity, e). Vertical axis: angle in degrees. Horizontal axis is $\nu \in [0,2\pi]$. For both plots: dashed: $e = 0$, solid: $e = 0.6$.

We were able to evaluate the behavior of the relative vectors between the spacecraft. With $\mathbf{r}_4 = 0$, we have $\mathbf{r}_{4i} = \mathbf{r}_i$ while remaining vector differences are readily computed as $\mathbf{r}_{ij} = \mathbf{r}_j - \mathbf{r}_i$ allowing us to study the internal dynamics of the tetrahedral configuration via the displacement between individual spacecraft pairs. To appreciate the dynamics of the entire tetrahedral structure we may examine either of the vectors to infer the overall behavior and stability of the tetrahedral formation. Taking, for instance, $\mathbf{r}_{41}$, we model the range between the two vehicles as

$$r_{41} = \frac{\sqrt{3}}{2}\ell_0\left[\cos^2\nu + \left(\frac{1}{\sqrt{3}}\frac{r}{a(1-e)} - \left(1 + \frac{r}{a(1-e^2)}\right)\sin\nu\right)^2\right]^{\frac{1}{2}}. \tag{101}$$

Figure 13(left) shows the range evolution as the spacecraft move in their orbit, indicating that for $e = 0.6$, it periodically increases by ~ 3.83 times.

We considered the practical implications of the tetrahedron's dynamic behavior, especially in terms of gimbal articulation. As spacecraft move in their orbits, the tetrahedron's edges change causing the relative angles between the spacecraft may change by more than 80-deg. Such angular variations necessitate the development and deployment of gimbals that can achieve these wide articulations but also maintain stability throughout the entire angular range.

Our investigation highlighted a pivotal distinction between internal and external measurements. Traditional external references, prevalent in astrometry, exhibit limitations in precision. Given these constraints, our study advocated for the use of Sagnac observables, which are based on local measurements. This approach has the potential to surpass current methodologies, offering enhanced measurement accuracy without dependency on external reference systems.

5.2.1 Mission simulation

In described in detail in (Turyshev et al., 2024), we explored the feasibility of a tetrahedral constellation of four satellites in heliocentric orbit to precisely reconstruct the trace of the GGT. These satellites are designed to gauge inter-satellite distances and to clock the round-trip times and phases of signals coherently exchanged between them. Relying solely on inter-satellite distances poses challenges due to its ignorance of the constellation's rotational dynamics, which introduce fictitious forces. By integrating Sagnac-type observables, we can account for and rectify these rotational discrepancies.

The tetrahedral satellite constellation offers a promising avenue for precision gravitational measurements. In the quest to accurately measure variations in the gravitational field, particularly the trace trace[GGT], the configuration's potential becomes evident. Using data about the Sun's position and distance, our system—comprising satellites typically spaced 1,000 km apart and orbiting with a semi-major axis of 1 AU—shows capability to achieve a measurement precision approaching $O(10^{-24}\,s^{-2})$. Such precision provides a tangible means to probe for Galileonic deviations in the solar gravitational field, potentially significantly improving our current understanding.

Tetrahedral configurations of spacecraft on unperturbed heliocentric orbits allow for highly precise observations of small spatial changes in the gravitational field, especially those affecting the GGT. It was suggested that the resulting high sensitivity may be used to search for new physics that could manifest itself via deviations from general relativistic behavior yielding a non-vanishing trace of the GGT. We validated the feasibility of recovering the trace[GTT] with the sensitivity of $O(10^{-24}\,s^{-2})$ – the level where some of the recently proposed cosmological models may have observable effects in the solar system. We considered how a set of local measurements provided by precision laser ranging (to measure the inter-satellite ranges) and atom-wave interferometry (to correct for any local non-gravitational disturbances) can be used for that purpose.

Table 4. Select mission parameters of the GDEM mission used in the simulations.

Parameter	Symbol	Value
Semimajor axis	a	1 AU
Orbital eccentricity	e	0.6
Heliocentric velocity	$v_j \simeq \sqrt{\mu_\odot/a}$	29.78 km/s
Mean orbital frequency	$n \simeq \sqrt{\mu_\odot/a^3}$	1.99×10^{-7} s^{-1}
Heliocentric acceleration	$a_0 = \mu_\odot/a^2$	5.93×10^{-4} m/s^2
Inter-spacecraft range	r_{ij}	10^3 km
Inter-spacecraft range rate	$\dot{r}_{ij} \simeq n r_{ij}$	0.20 m/s
Relative spacecraft acceleration	$\ddot{r}_{ij} \simeq n^2 r_{ij}$	3.96×10^{-8} m/s^2

Table 5. Top level instrumental requirements for the GDEM mission.

Parameter	Symbol	Value
Laser ranging	δr_{4i}	10×10^{-12} m
Range-rates	$\delta \dot{r}_{4i}$	1×10^{-5} m/s
Line-of-sight accelerations	$\delta \ddot{r}_{4i}$	1×10^{-15} m/s^2
AI, as inertial sensor	δf_{4i}	1×10^{-15} m/s^2
Sagnac observable	$\delta\omega$	1.5×10^{-15} s^{-1}

We studied the dynamical behavior of a tetrahedral formation established by four spacecraft placed on nearby elliptical orbits around the Sun. For that, we developed analytical models for the relevant observables and studied the conditions for setting up an optimal tetrahedral configuration. We formulated the observational equations to measure the trace[GTT] relying only on the local observables that are available within the formation, such as those based on the laser ranging and the Sagnac interferometry.

We demonstrated that Sagnac observable is a mission enabling capability that allows to measure the angular frequency of the tetrahedral rotation with respect to an inertial reference frame with an accuracy that is much higher than that available from any other modern navigational techniques.

To validate the analysis and results, we developed simulation software. Implemented in HTML and JavaScript, the software offers a simple visualization of the evolving tetrahedron configuration while at the same time calculating the trace of the GGT, as well as the same trace, recovered from intersatellite range and generalized Sagnac observables.

In our simulation, the gravitational influence was limited to the Sun's field. While gravitational effects from other bodies in the solar system do exist, their impact on our results is negligible. This is due to the vacuum Poisson equation. Consequently, while the gravitational field influences the satellites' orbits, it does not directly affect the term trace[GTT]. This effect is only through the approximations previously discussed. The contribution from solar system bodies other than the Sun to these terms is minimal and can be considered insignificant for our simulation purposes.

The simulation code features a variety of preconfigured satellite constellations. Among these, a particularly notable orbit exhibits a high eccentricity, $e = 0.59$, and a perihelion distance of 0.6AU. This specific orbit could potentially represent a realistic experiment that might be conducted in the future. In addition to this orbit, our investigation covers a spectrum of orbital configurations, ranging from near circular to highly elliptical trajectories. This includes orbits with semi-major axes ranging from approximately 0.1 AU to as large as about 30 AU.

The simulation software models an orbital constellation comprising four satellites. These satellites' initial state vectors are derived from a nominal state vector but are purposefully perturbed.

Distances between satellites are a few thousand kilometers, with relative heliocentric velocities differing by a maximum of 0.1 m/s (see Table 3, Table 4).

To improve calculation accuracy, the software adopts a moving reference frame that aligns with the satellite's nominal, unperturbed orbit. In this frame, satellite positions are typically within a few tens of thousands of kilometers. This limitation enables the software to achieve sub-micron level positional accuracy using standard double-precision numerical formats. This method effectively addresses the challenge of maintaining millimeter-scale accuracy in a heliocentric coordinate system, which becomes more complex when satellites are several AUs away from the Sun.

For orbit calculations, the software incorporates a fourth order Runge-Kutta integrator. When simulating a satellite orbit at 1 AU from the Sun, it uses a 600-sec timestep. This specific timestep is chosen to balance the minimization of numerical errors with the efficiency of the simulation, ensuring accurate yet expedient orbit predictions.

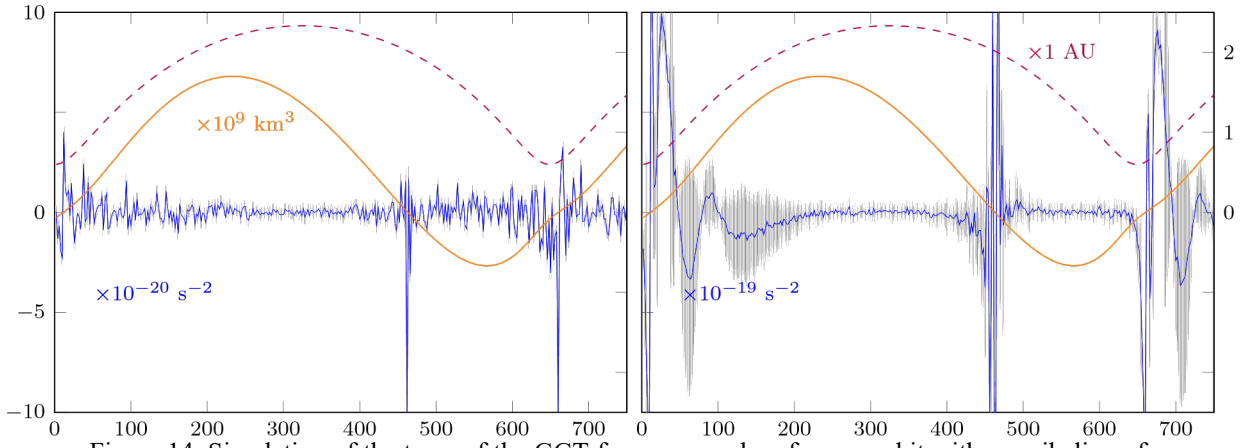

Figure 14. Simulation of the trace of the GGT for an example reference orbit with a perihelion of 0.6 AU and eccentricity e ~ 0.5909, with the satellites initially forming a tetrahedron with ~ 1,000 km edges. The constellation volume is also shown (orange solid line). Dashed purple line shows the heliocentric distance, referencing the secondary vertical axis. Horizontal axis: days since perihelion passage.

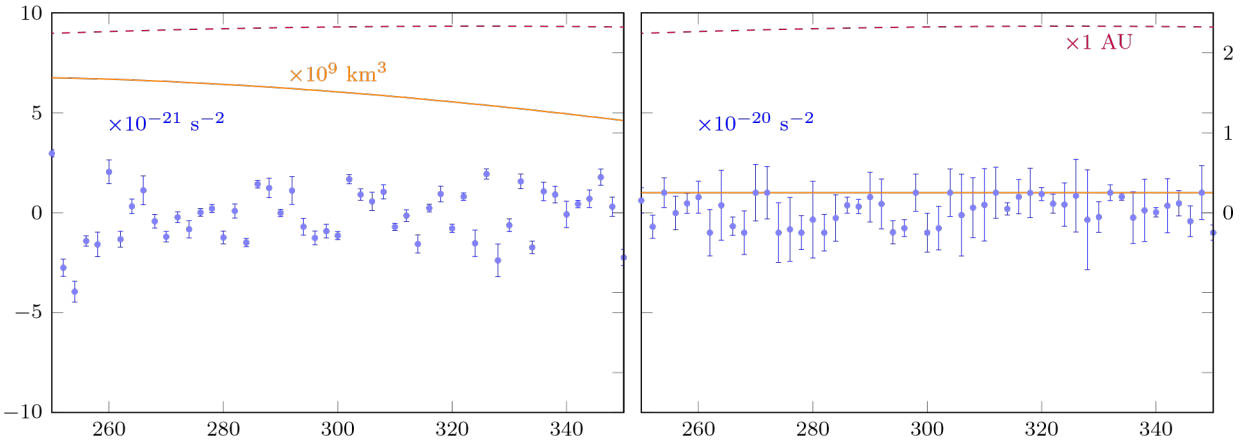

Figure 15. Details from the simulation shown in Figure from a region of maximum sensitivity. Horizontal axis: days.

The main loop of the software integrates both the numerical simulation and visualization components. The visualization updates occur at a lower frequency to optimize runtime performance, ensuring smooth animation. During each iteration in the main loop the software advances the satellite orbits using the Runge-Kutta integrator. It then integrates the reference orbit, updating the coordinate system origin for the subsequent iteration. Then, it calculates trace[GGT] in the inertial reference frame, serving as the "true" value of this trace, given the numerical constraints. Observables are derived, including the six inter-satellite ranges and the 12 generalized Sagnac observables.

The software then determines the coordinates of the four vertices in the TCS using the time-series range observables. The generalized Sagnac observables are leveraged to factor in rotation and pseudo-accelerations. The software then calculates numerical second derivatives from the coordinate time series to determine relative accelerations. These values are used to reconstruct the gravitational gradient tensor's trace in the TCS, representing the "observed" value. The software also factors in the second-order gravitational gradients. These steps are replicated for all four vertices. The software then averages the "true" and "observed" gravitational gradient tensor trace values across the vertices and computes the corresponding standard deviation.

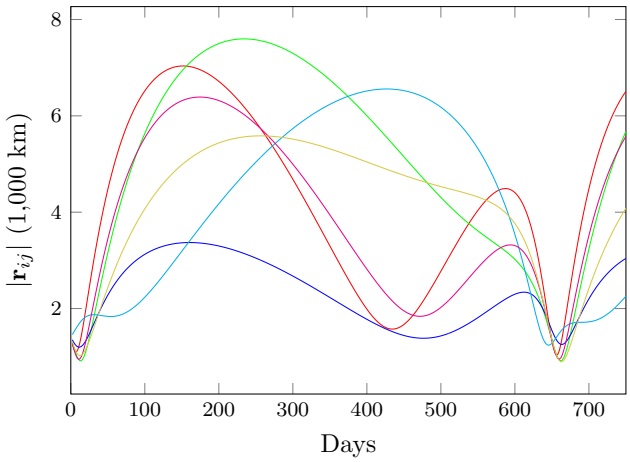

Figure 16. The six intersatellite ranges of the configuration introduced inFigure 15.

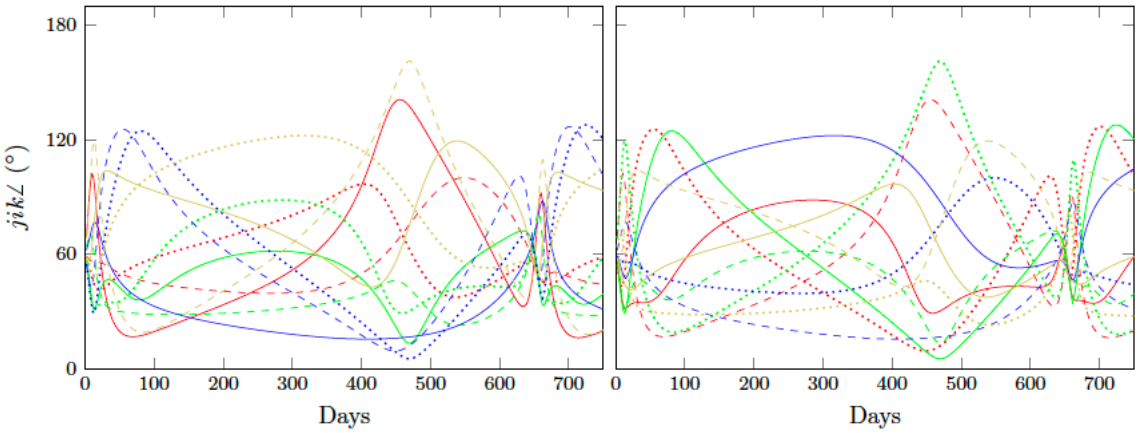

Figure 17. The twelve tetrahedron angles of the configuration introduced in Figure 15, grouped, using color, by vertex (left) and tetrahedron face (right).

Results of our simulations are shown in Figure 14 and Figure 15. Figure 14 (left) shows results for a specific orbit that has been selected for this study with a perihelion of ~ 0.6 AU and an eccentricity of $\varrho \simeq 0.5909$. In addition, the volume of the tetrahedron formed by the arrangement of the four satellites in space is depicted. This tetrahedral formation is crucial because it's the basis for the measurement methodology being discussed. When examining the data presented, it becomes evident that most of the computational results align well with the predicted accuracy for the trace of the GGT. However, there's a notable exception. Whenever the tetrahedron becomes "degenerate," meaning its three-dimensional shape collapses to a point where its volume is essentially zero, the calculations don't reproduce the expected trace of the GGT. This indicates the potential limitations or challenges of this measurement methodology under specific geometric conditions.

In contrast, Figure 14 (right) shows the values for the GGT that are derived from the actual ranges between satellites and the generalized Sagnac observables (see Table 5). This means we're looking at data derived from more direct measurements. Additionally, to improve the accuracy of this data, the approximate distance and directional angle to the Sun, as it's perceived in the TCS (a specific observational reference), are also considered. This inclusion is necessary because there are certain gradient contributions—specifically, those of the second order. For clarity in interpretation, gray error bars have been added to the graph. These bars represent the variability in the values obtained when the same calculation is repeated. Each repetition is anchored at a different vertex of the tetrahedron, and there are four such vertices, leading to four repetitions.

One can see that there is a clear correlation between the geometry of the tetrahedron and the sensitivity of measurements. Specifically, when the tetrahedron's volume collapses—effectively making it flat—the ability of the satellite constellation to detect perturbations in the GGT decreases. This geometric condition hence becomes a limitation or a challenge in the study. To further elucidate this behavior, Figure 16 zooms into specific segments of the constellation's orbit, focusing particularly on those segments where sensitivity to detect changes in the GGT is at its maximum. This view can help understand the conditions under which the methodology is most effective.

Additional details from this simulation are shown in Figure 16, in the form of the six intersatellite ranges. We can see that the ranges changes substantially during a full orbit, varying between ~1,000 and ~8,000 km. Such variations could be due to various factors like gravitational perturbations, inherent satellite propulsion, or design of the orbit. The range data indicates the dynamism of the satellite constellation during its operation.

Figure 17 shows two views of the tetrahedral angles (that is to say, the angular separation of a pair of satellites as seen from a third satellite). There are twelve such angles (three per tetrahedron vertex or, alternatively, three per tetrahedron face). Correspondingly, two views are presented: in one view, the angles are grouped using the same color per vertex, whereas in the other, the grouping is by face. We can see that the tetrahedron flexes substantially, with all twelve angles changing dramatically during a fall orbit. Both views reveal a significant amount of flexing in the tetrahedron throughout its orbit. The angles are not rigid but vary substantially, highlighting the tetrahedron's dynamic geometry as the satellites move.

These results are by no means unique to the specific configuration that we used for this simulation. In fact, this configuration performed quite well in comparison to potential alternatives. This is evident when observing the cyclical nature of the satellite constellation. After completing a full orbit, the satellites realign into a formation very close to their starting configuration. Such behavior underscores the resilience and reliability of the chosen configuration. However, the takeaways are clear: any ultimate mission that aims to use a tetrahedral configuration must account for the inherent flexibility of the tetrahedron and the variability in intersatellite distances. These factors aren't

mere nuances; they are integral to the mission design. Ensuring the optimal functionality of equipment onboard, communication between satellites, and accurate data collection hinges on understanding and leveraging this dynamical motion.

We note that this simulation is constrained, in part, by the limits imposed by double-precision arithmetic, which yields at most ~15.9 digits of precision for simple arithmetic operations. For complex calculations, errors accumulate (random walk) so we do not expect a relative accuracy much better than $\sim 10^{-14}$. This constrains our ability to recover the "true" value of the trace, and further constrains our ability to recover the "observed" value. Ultimately, a more accurate simulation may benefit from the use of extended precision arithmetic, which was not implemented in this prototype simulation.

In the simulation, trace [GGT] exhibits a nonzero value with a tight standard deviation of 10^{-24} s^{-2}. This standard deviation is computed by iterating over the 4 satellites, considering each as the origin point in the satellite fixed tetrahedral coordinate system (TCS) reference frame. The tightness of this standard deviation suggests that the deviation from zero is not due to random errors; rather, it indicates the presence of 2nd order tidal terms that have not been accounted for in the GGT. When these 2nd order terms are included in the model, the trace of the GGT comes significantly closer to zero. Similar improvements were observed when the relativistic terms were included.

We emphasize that once the Sagnac observables are fully incorporating, the estimated trace [GGT] value comes significantly closer to zero, offering a more accurate representation of the GGT. Therefore, the inclusion of the Sagnac-type measurement provides an important correction mechanism to improve the precision of the estimate. More broadly, in satellite constellations, determining relative accelerations requires accounting for the rotational dynamics of the reference frame. This involves determining the frame's angular velocity, achievable through Sagnac effect in the constellation's tetrahedral configuration. By analyzing these timings bidirectionally across three satellite triplets, the frame's three-dimensional angular velocity can be accurately derived, ensuring precise acceleration measurements.

As a result, based on simulations and mission analysis, we determine that achieving a sensitivity of 1×10^{-24} s^{-2} is feasible for the satellite configuration considered. This assessment considers the precise angular velocity measurement obtained through bidirectional Sagnac effect timing across the tetrahedral satellite constellation. The targeted sensitivity reflects the technical capabilities of the system, encompassing error analysis, system response, and operational thresholds in the specified rotational dynamics context.

5.2.2 Preliminary GDEM mission design

Through the simulations described in previous section, we were able to validate the design for The Gravity Probe and Dark Energy Detection Mission (GDEM) which is designed to search for deviations from the canonical Newtonian $1/r^2$ gravitational potential within the solar system's context. The mission employs a set of four spacecraft in tetrahedral configuration, each fitted with atom-wave interferometers. These spacecraft use high-precision laser ranging systems to interconnect, allowing simultaneous measurements of Doppler, absolute range, and Sagnac rotation to reduce gravitational gradients in four distinct directions. This design ensures the gravitational tensor's trace vanish irrespective of the tetrahedron's orientation.

The following are the key technical aspects for the development of the baseline GDEM architecture that will become a platform to challenge and expand our current understanding of fundamental physics:

- *Tetrahedral Configuration:* This geometric setup is vital. The tetrahedron ensures that gravitational effects are sampled in four non-coplanar directions, enabling the effective nullification (or detection) of tensor traces regardless of the tetrahedral orientation in space. This tetrahedral formation is established by the four-spacecraft following nearby elliptic orbits. This mission is enabled by the fact that it relies on a set of local differential measurements done at the orbital coordinate frame. Our analysis and simulations have shown that a proper tetrahedral with reasonable enclosed volume is critical to the measurement precision of the GGT trace. In the free flying approach without frequency formation maintenance, one would make sure the proper tetrahedral formation is recovered at the strategic orbit locations, preferrable near the perigee and apogee to maximize the detectable signal differences. Of course, this would be at the expense of available measurement times at these orbital locations. The other extremes would be taking advantage of maximum time of proper tetrahedral formation. A full simulation and optimization of such a maintenance-free configuration will be done in the follow-up studies.
- *Elliptical heliocentric orbit:* To optimize the conditions to detect the anticipated signal that behaves $\propto 1/\sqrt{r}$, the GDEM spacecraft will be placed on nearby elliptic heliocentric orbits that will allow to sample the Galileon field at various distances from the Sun. Based on the simulations of the Galileon field, there is an order of magnitude of the Galileon force variation in the solar system [White et al. 2020]. An elliptical orbit with varying distance from the Sun will allow the observation of such variation. This distance-dependent variation will reduce the systematics yielding stronger evidence for a GR violation, if observed. Based on the findings of the simulations and the measurement systematic vs signal trade-off, the primary concept is to have the measurement formation at 1AU as an optimal distance from the Sun where the GGT should be measured. Taking a 1 AU orbit around the Sun, we choose to have the elliptic orbit of semi-major axis of a=1 AU with an eccentricity of 0.6.
- *Precision Laser Ranging Systems:* These systems provide inter-spacecraft Doppler and distance measurements with very high measurements accuracy. These laser links are used for 1) Absolute distance measurements between the spacecraft to determine the tetrahedral geometry, particularly to meet the stringent geometric angles of the tetrahedral. 2) Laser interferometer link for Doppler for differential acceleration measurements like that of LISA and GRACE missions. The Doppler will also be used for Sagnac rotation to consider of the tetrahedral formation rotation in the solar gravity. The drag-free measurements are achieved through local spacecraft drag measurements through atomic test massed and atom interferometers. 3) Phase coherent links for the AI laser to be able to conduct the differential measurements with the common laser phase noises suppressed.

  Each of the spacecraft is equipped with three small telescopes having a precision gimbal capable of a wide angular articulation in two dimensions. The range of the angular articulation will also affect the tetrahedral formation geometry under which the laser links can be established, and measurements can be performed. The laser ranging system should be capable of reaching a LISA-class ranging sensitivity at the level of ~ 30 pm/√Hz. In addition, high frequency (~10 GHz) pseudo-ranging modulation will be applied to the ranging laser for absolute distance ranging. Here optical frequency comb based ranging scheme can help.
- *Atom Interferometers (AI):* There are three nearly orthogonal AIs to measure the non-gravity forces in all directions. In each AI implementation, ultracold atoms are generated onboard the spacecraft, via laser cooling and trapping. These ultracold atoms are then coherently transported (without heating) out of spacecraft to the open space vacuum via a moving optical lattice facilitated by the retroreflection mirror assembly at the end of the boom. When atoms reach the desired location and

velocity, both are controlled via optical frequencies of a moving optical lattice, interferometer sequence starts by applying AI light pulses, facilitated by the boom-mirror structure. At the end of the interferometer, two clouds of complementary spatial features that carry the acceleration information are coherently transported back to the spacecraft via the moving optical lattice. Then, the spatial distribution is imaged on cameras. The source generation can be shared among three AIs, to reduce SWaP, or be independent to reduce operation complexity. Multi-axis operations can be conducted simultaneously for independent sources, or sequentially for a shared source. There should be no impact on data processing. The notional parameters are listed in Section 4.3 to reach the target acceleration sensitivity.

5.3 Instrument Payloads

The GDEM aims to detect deviations from the Newtonian $1/r^2$ gravitational potential within the solar system. Utilizing a tetrahedral spacecraft configuration equipped with atom-wave interferometers, GDEM employs precision laser ranging systems for interconnected measurements, enabling the assessment of gravitational gradients in multiple directions. This design ensures the gravitational tensor's trace can be effectively nullified or detected, irrespective of the tetrahedron's spatial orientation. The mission's architecture is centered on a tetrahedral constellation of spacecraft, each embedded with atom-wave interferometers for precise, local differential measurements in the orbital coordinate frame.

5.3.1 Precision Laser Ranging Systems

The GDEM mission employs a sophisticated laser interferometer system inspired by the design principles of LISA and GRACE-FO yet tailored to meet its unique precision requirements. Each of the four functionally equivalent satellites houses an optical payload with three identical optomechanical arrangements that facilitate both the emission of a laser beam to the satellite directly opposite and the reception of the beam emitted from that counterpart. This dual functionality is crucial for maintaining the LISA-class ranging sensitivity of ~30 pm/√Hz necessary for the mission's objectives.

Similar to LISA, the GDEM utilizes continuous heterodyne laser interferometry for measuring the differential optical pathlength modulation along each arm of the satellite's triangular configuration. These measurements are vital for tracking minute distance changes between co-orbiting, drag-free test masses, ranging from picometers to nanometers, which are induced by subtle Galilean signals. The design ensures high accuracy by employing a stable 1064 nm laser with a power output of about 100 mW, with each spacecraft functioning as an active transponder that emits a high-power beam phase-locked to the incoming weak beam.

Additionally, the GDEM integrates Sagnac interferometry to detect angular velocity with unprecedented precision, akin to LISA standards. This capability is essential for characterizing the yearly rotation of the constellation. The Sagnac measurements, which rely on the interferometric mixing of emitted and return beams, are enhanced by using quarter wave plates and a polarization beam splitter to achieve the fine pointing specification of a few nrad/√Hz.

The mission also introduces a unique absolute ranging system that distinguishes it from other missions. This system is critical for achieving precise inter-satellite distance measurements over approximately 1,000 km, utilizing a 5 cm aperture telescope to balance the demands of payload size,

mass, and scientific requirements. The absolute ranging capability ensures that the measurement formation geometry can be sufficiently determined and the minute Galilean signals can be accurately differentiated from larger variations.

By integrating these advanced laser ranging, Doppler, Sagnac, and absolute ranging measurements within a single coherent system, GDEM sets a new standard in precision for space-based gravitational experiments. The focus on refining these systems to operate within the specified technical parameters ensures that GDEM not only meets but exceeds the precision and reliability required for its ambitious scientific goals.

5.3.2 Atom Interferometers (AI)

The AI system consists of three subsystems, the atomic physics package (APP), the laser and optical system (LOS), and the integrated control electronics (ICE). The APP includes atom source, interferometry, detection, and the supporting optomechanics including the booms. The LOS generates laser light of desired frequencies, power, and timing, and delivers light through optical fibers to the APP. The ICE interfaces between subsystems and communicates with the spacecraft. There are up to three AI systems for three-axis acceleration measurements. If the common-source architecture is chosen, there is only one AI system.

APP:

- *The vacuum enclosure:* The APP centers around a vacuum enclosure, which has a vacuum gate valve leading to the external of spacecraft. The enclosure is capable of maintaining ultra-high-vacuum at 1e-11 torr when the valve is closed. The valve will be open only when the external pressure is adequate, and the AI is ready to operate. The vacuum enclosure consists of three compartments. One for two-dimensional magneto-optical trap (2D-MOT), where the atom reservoir releases atoms to be precooled. The precooled atomic beam passes through a differential pumping hole to another compartment, where a 3D-MOT captures the flux and perform further cooling in all directions. MOT is facilitated by magnetic field gradient and laser beams, both can be switched on and off in a sequence. A third compartment is for shuffling ultracold atoms in and out of spacecraft, and for imaging detections. Electronics such as vacuum pump drivers, magnetic coil drivers, gate valve controller, reservoir controller, housekeeping sensor controllers, and camera controllers are included in the APP.
- *The boom and retroreflection mirror assembly:* A boom of >50 m extension is positioned right at the gate valve. A hollow retroreflector is attached at the end of the boom, to reflect the optical lattice beams and interferometer beams from the spacecraft back precisely disregarding boom pointing jitter. There is no active element at the end of the boom for AI operations. The clear aperture of the retroreflector is sufficiently large to accommodate AI/lattice beams of few cm diameter and potential boom pointing variations.

LOS:

- Notionally, the LOS is similar to CAL, BECCAL, or MAIUS. It consists of a master laser with its frequency stabilized to an atomic transition. The linewidth shall be < 1 kHz, and the long-term accuracy shall be better than 1e-11, considering the nominal gravity gradient of 1e-14/s^2 and the target trace sensitivity of 1e-24/s^2. Several secondary lasers are frequency-offset phase-locked to the master laser, such that they have the same linewidth and accuracy. The offset frequencies are in MHz to few 10GHz range, to be derived from the stable local oscillator from

the spacecraft. Laser frequency agility is provided by the offset frequency synthesizers. Most of the laser optical components are interconnected via optical fibers, to eliminate alignment drifts. Various fiber splitters, intensity modulators, shutters, and optical amplifiers are envisioned to be included in the LOS architecture. The control of all the active components is facilitated by LOS electronics, including thermal management and power conditioning. The sequence of operation is represented as a table of parameters provided by the ICE. The LOS takes the starting trigger from the ICE and then proceeds with the timing table while synchronized with the ICE master clock. It is envisioned that the required peak optical power in fiber to the APP is less than 1W.

ICE:

- The ICE digitally communicates with other subsystems and with the spacecraft. It acquires a stable timing reference from the spacecraft and provides the master clock for the AI system. The ICE generates timing sequences based on modes of operation, such as diagnostics or normal operation. The high-level sequence is sent to LOS for processing, while direct control of APP electronics is envisioned. Images from cameras are acquired and processed at ICE.

Physics protocol of operation:

- Each AI run starts by loading the 3D-MOT from the 2D-MOT. A cloud of 10^9 atoms at few μK is produced after the polarization-gradient cooling following the extinguishment of the 3D-MOT magnetic field gradient. An advanced cooling stage of < 1 s, such as BEC followed by delta-kick collimation, results in 10^8 atoms at < nK. This ultracold cloud is then moved to the detection chamber via an optical lattice, with a travel distance of few cm. This cloud is then moved outwards through the gate valve via an optical lattice formed by an outgoing beam and a retroreflected beam from the retroreflection mirror assembly at the end of the boom. Optical lattices are proven to be fast and not cause heating. In < 1 s, the cloud is positioned at the desired starting position and velocity. Both the position and velocity are determined by the optical frequencies of the lattice, which are well-controlled to <1e-11 uncertainty. The AI light-pulse sequence then starts. After the light pulse sequence, the resulting clouds are coherently pulled back to the detection chamber. Then, on-resonant light is shone on the clouds and the fluorescence scattering is captured on cameras. While the onboard computer processes the images, the next AI sequence starts.

To implement remote AI retroreflection, one can use carbon-fiber hollow truss technology developed at NASA. This allows to implement AI retroreflectors at distances of 50-100 meters from the spacecraft and presents several engineering approaches, each with its specific trade-offs.

One practical approach involves extending truss structures made from carbon-fiber directly from the spacecraft. This design offers stable and fixed positioning of the retroreflectors, enhancing measurement accuracy through a consistently maintained baseline. The rigidity of carbon-fiber is beneficial in minimizing structural vibrations and thermal expansions, which are crucial in maintaining measurement accuracy in the varied thermal environments of space. However, this approach increases the spacecraft's mechanical complexity and introduces potential points of failure, necessitating robust, reliable deployment mechanisms.

Alternatively, deploying a small satellite or a modular unit connected to the main spacecraft by a carbon-fiber truss to house the AI retroreflectors can be considered. This method isolates the

retroreflectors from the main spacecraft, reducing interference and allowing more flexible positioning. While increasing mission costs and complexity, it enhances the potential for precise control over the measurement environment by allowing independent orientation and stabilization of the retroreflectors.

Another option involves integrating retractable carbon-fiber booms that can extend to deploy the retroreflectors as needed. This design provides operational flexibility, allowing adjustments based on the mission phase and enabling the system to be stowed during launch or hazardous conditions. The deployment mechanisms for this approach must be exceptionally reliable to prevent failures and ensure consistent extension and retraction without introducing measurement errors.

The selection of carbon-fiber for these structures is due to its advantageous properties of low thermal expansion and high stiffness, essential for maintaining dimensional stability under space conditions. Integrating these systems with the spacecraft necessitates careful planning to ensure they do not adversely affect the spacecraft's center of mass, power budget, or thermal regulation.

For the GDEM, precise deployment accuracy is crucial, targeting alignment within millimeters to ensure the functionality of the AI retroreflectors. The mission design must also accommodate real-time operational adjustments based on live data feedback, with a drift in measurement accuracy limited to nanometers per square root hertz to meet the stringent requirements of space-based gravitational measurements.

The choice of implementation strategy for the AI retroreflectors in the GDEM will depend heavily on balancing mission-specific requirements with acceptable risk levels and operational priorities. Extensive testing and simulations are recommended to validate the structural integrity and operational reliability of the selected solution, ensuring it meets the high precision and reliability demands of the mission.

Measurement and Control Systems:

- *Detection and Measurement:* Utilize sensitive detectors to read the interference pattern resulting from the atomic wave packets. The system should be capable of detecting minute phase shifts corresponding to the targeted sensitivity.
- *Feedback Control:* Implement feedback control systems using the AI data to maintain drag-free conditions. This involves precise thrust control systems that can react to the detected accelerations and adjust the spacecraft's trajectory or attitude accordingly.

Environmental Isolation and Stability:

- *Vibration Isolation:* Ensure the AI system is well isolated from any external vibrations or mechanical disturbances, which could affect the measurements. This might involve passive or active isolation systems depending on the mission requirements.
- *Thermal Stability:* Maintain a stable thermal environment around the AI system to prevent temperature fluctuations from affecting the cold atoms or the interferometry setup.
- *Open Space Vacuum Operation:* The high sensitivity of AI gained by extended interrogation time in microgravity comes at the cost of the spatial extent. For beamsplitters n=200 and interrogation time T=10s, the atomic wavefunction will separate up to 24 m. It is not foreseeable that a spacecraft can accommodate several of such cylindrical shapes in various directions. The mitigation is to conduct AI directly in the open space vacuum, as opposed to in an UHV environment in an enclosure as in all terrestrial and space cold atom experiments. In this scenario, ultracold atoms will be generated onboard the spacecraft, coherently transported out of spacecraft using a moving optical lattice, manipulated with AI pulses, and then coherently

transported back to spacecraft for imaging readout. Shuttling the atoms is facilitated by an optical lattice formed by counterpropagating laser beams, where one beam comes from the spacecraft while the other retroreflected from a mirror at the end of a deployable boom. Since the AI will not be at the center of mass (CM) of the spacecraft, it will be conducted far enough away from the spacecraft such that mass distribution uncertainty will not introduce acceleration bias. When two AIs straddle the CM, the differential signal of the two AIs will reveal the CM acceleration while suppressing the gravity effect of the spacecraft itself.

One potential concern is the environmental effects on the AIs. Solar winds, interplanetary dusts, and electro-magnetic fields could be detrimental to AI. It is estimated that the nominal particle density at 1 AU is sufficiently low, such that interaction of ultracold atoms with undesired matter would cause negligible atom loss. Regarding the solar radiation, which can be modeled as blackbody radiation for this purpose, will ionize Rb atoms. It is calculated that about 1% of the ultracold atoms will be ionized during the $2T$=20s interferometer time, which has negligible impact on the sensitivity. A closer study on the interactions between these photo ions and the remaining neutral atoms show that ~25% of the neutral atoms will be in the collision paths. These collisions will change the trajectory of the impact atom and also introduce collision-energy dependent phase shift. We show analytically that the change of trajectory, which will be magnified for longer atom flight time, is strictly zero. We also show that the mean collisional phase shift is smaller than per shot AI sensitivity. We thus conclude that AI in open space vacuum at 1 AU are feasible.

5.3.3 Communication and Data Handling

For GDEM's transmission, equipping the spacecraft with robust communication systems capable of transmitting potentially gigabytes of data back to Earth daily is critical. This aspect ensures that the vast amounts of scientific data collected can be efficiently and reliably sent back for analysis.

Implement communication systems with sufficient bandwidth to handle the data volume. For AI in the operation mode, the readout images are processed onboard to provide a single acceleration measurement per AI run of few 10 s. For diagnosis during commissioning, full frame images would be desired, where 1MB per measurement would be required. Image compression or pre-processing would significantly reduce the data volume. This might involve high-frequency bands like X-band or Ka-band, which are commonly used for deep-space communication due to their high data rates. Effectively managing the large data volumes generated by the spacecraft's instruments, especially considering the constraints on bandwidth and the long distances involved in deep-space communication. Balancing the power and onboard resources dedicated to data transmission with other mission needs, ensuring that the communication system does not unduly drain the spacecraft's power or computational resources.

Advanced onboard processing in GDEM is to enables efficient, autonomous handling of complex data analysis and system monitoring tasks directly on the spacecraft. This capability is crucial for optimizing scientific data collection, enhancing mission responsiveness, and ensuring operational efficiency. GDEM will rely on processors capable of handling complex data analysis tasks onboard, with speeds and capacities sufficient for real-time or near-real-time processing needs.

5.4 CONOPS

5.4.1 Getting into orbit

Forming the tetrahedral configuration for the GDEM is a critical technical aspect of the mission, involving complex maneuvers and precise coordination among the spacecraft. This formation is essential for achieving the mission's scientific objectives, as it allows for the measurement of gravitational effects from multiple, non-coplanar directions.

Once launched on the same vehicle, the spacecraft will be deployed into space near each other. The initial phase of forming the tetrahedral configuration involves moving each spacecraft to its designated position in the formation. This maneuvering must be executed with high precision, as the accuracy of the tetrahedral shape will directly impact the quality of the science measurements.

Each spacecraft needs advanced autonomous navigation capabilities. These systems must accurately determine the spacecraft's position and velocity and calculate the required maneuvers to maintain the tetrahedral formation. Effective communication between the spacecraft is vital for coordinating maneuvers and maintaining the formation.

5.4.2 Formation maintenance

The GDEM mission requires an operational decision between adopting a totally free-flying configuration and a fuel-carrying configuration optimized for full data acquisition. A totally free-flying configuration would operate passively without active propulsion, significantly reducing the spacecraft's mass and simplifying its design. This approach would also potentially extend the mission duration based on the initial launch trajectory and passive stabilization techniques. However, this configuration comes with considerable limitations, particularly in data collection. Without the ability to adjust its trajectory actively, the spacecraft’s fixed path could lead to less optimal spatial coverage. More critically, the passive setup could result in the tetrahedral formation’s volume collapsing due to orbital dynamics, which would render the collected data noisy and less reliable. To address this, the experiment would need to be periodically halted, the spacecraft repositioned, and then the experiment restarted, which could significantly disrupt continuous data collection.

Conversely, a configuration that includes fuel for active propulsion would enhance the mission’s data collection capabilities by allowing precise orbital adjustments. This setup would not only increase spatial coverage but also enable the spacecraft to actively maintain the tetrahedral formation, preventing collapse and thus ensuring the integrity of the data. The capability to make dynamic adjustments would lead to richer and more comprehensive datasets. However, this active configuration would increase the mission’s complexity and costs due to the additional fuel storage and management systems required. The mission duration would also be constrained by the amount of fuel carried, with estimates suggesting that the mission's active operations could be extended by several months per kilogram of fuel, depending on propulsion efficiency.

In choosing the optimal configuration for GDEM, it is crucial to balance the scientific objectives against budget constraints and operational risks. If extensive, high-quality data collection from various spatial domains is a priority, the benefits of an active propulsion system might outweigh the higher costs and complexity. However, if the mission can achieve its objectives with more limited spatial coverage or aims to minimize cost and complexity, careful consideration must be given to the potential for data interruption in a passive setup. A potential compromise might involve a minimal propulsion capability, enough to make critical adjustments to prevent formation collapse and to reposition spacecraft as needed without significantly increasing the mission’s mass or operational complexity. Such an approach requires precise planning and optimization to ensure

that minimal fuel usage still permits essential mission maneuvers, extending the useful mission life while managing costs and complexities.

5.4.3 Constellation location measurements and data link

The essential feature during the flight into perihelion is DSN tracking and resultant guidance updates to (1) aim each spacecraft to the exact location and time of perihelion and, (2) to command the onboard trajectory management system to exit perihelion passage with the right state vector to reach the SGLF of the selected stellar system. So far this is routine operations.

As the spacecraft navigate their elliptical orbits, accurate tracking and guidance updates become essential. These updates, facilitated by the DSN, are crucial for ensuring that each spacecraft maintains its correct trajectory. The primary objective during this phase is to manage the onboard trajectory systems effectively. This involves continually adjusting each spacecraft's path to adhere closely to the intended orbit, thereby ensuring the precise positioning necessary for the mission's scientific objectives.

DSN will provide GDEM with essential support in terms of general formation maintenance and communication. However, DSN's ranging precision, which is ~1 meter, falls short of meeting the stringent tracking precision required for GDEM's scientific objectives. GDEM needs greater accuracy to precisely measure the minute variations in gravitational fields that GDEM aims to study.

While DSN is invaluable for maintaining contact with the spacecraft, providing updates, and receiving data, its tracking capabilities are not sufficient for the high-precision measurements central to GDEM's investigation of gravitational anomalies. Instead, GDEM must rely on more precise onboard instruments and systems specifically designed for this purpose. These systems are capable of achieving the necessary picometer-level precision in measuring distances and changes within the spacecraft formation, far beyond the capabilities of the DSN.

Throughout their journey along these elliptical orbits, the spacecraft will rely on their onboard systems to maintain the correct trajectory. This process involves constant monitoring and adjustments to correct any deviations from the planned path. The focus is to ensure that by the time the spacecraft reach the furthest point in their orbit, where the influence of Earth and the Sun on their trajectory diminishes, they are precisely where they need to be. Once in the correct trajectory, the spacecraft will operate in a more traditional manner, focusing on their primary mission of gravitational measurement.

5.4.4 Ground support and data analysis

The GDEM mission utilizes an advanced data processing system, designed to manage complex spacecraft operations and execute sophisticated scientific analyses. This system operates under a flexible architecture that adapts its autonomy based on the mission's changing requirements, crucial for optimizing resource allocation, enhancing data collection, and improving data analytics.

The data processing system is central to maintaining optimal spacecraft positioning and dynamically adjusting data collection processes to correct for any distortions that might affect the accuracy of scientific measurements. Operating under a Monitor-Analyze-Plan-Execute (MAPE) loop architecture, this system allows for independent yet coordinated decision-making across spacecraft. The computational demands are substantial, with processing capabilities expected to reach teraFLOPs to support real-time processing of large data volumes. Each spacecraft is equipped with several terabytes of data storage to manage the information collected between communication periods with Earth.

While the DSN provides essential support for GDEM, its capabilities in ground tracking and data transmission are tailored to general formation maintenance rather than precise scientific data collection. DSN's ground tracking offers a ranging precision of about 1 meter, which is adequate for basic navigational support and maintaining the spacecraft formation. However, this level of precision is insufficient for the primary scientific measurements of GDEM, which require picometer-level accuracy.

The role of DSN in GDEM extends to facilitating the downlink of raw data from the spacecraft to Earth. This raw data includes basic telemetry and initial measurement data, which is then processed into high-level scientific data on-board before transmission. The distinction between raw data and high-level scientific data is crucial, including i) all basic observational data and telemetry transmitted directly from the spacecraft to ground stations. Raw data is primarily used to monitor spacecraft health and operational status, and ii) handing high-level science data that implies that after initial processing onboard to filter out noise and irrelevant information, the data is further refined to meet the scientific goals of the mission. This includes detailed analyses of gravitational fields and other phenomena, which require more sophisticated processing algorithms that can handle the complex dynamics of the mission.

For GDEM, the high-level data is used for multiple scientific objectives (addressed below), including the detailed study of gravitational anomalies and the testing of theoretical physics models. The onboard processing systems use advanced algorithms and machine learning techniques to maximize data fidelity, ensuring that the information used for scientific discoveries is of the highest quality and precision.

5.5 Enabling Multiple Gravitational Science Products and Returns

The GDEM mission is primarily designed to the unknown dark energy force that violates the inverse square law. On the other hand, it becomes obvious that the precision differential gravity measurements in a non-planar constellation will produce a set of rich data and yield multiple gravitational science products and returns. Below we will give a summary of these diverse scientific outcomes:

5.5.1 Model agnostic use and analysis of ISL measurements

GDEM's use of ISL measurements as a tool to investigate deviations from Newton's law of gravitation is rooted in the precise determination of the gravitational attraction between masses at varying distances. Technically, this involves comparing the observed gravitational force between test masses at different separations to the theoretical predictions provided by Newton's law, which states that the force should diminish as the square of the distance between the masses.

To achieve this, GDEM will employ high-precision instrumentation capable of measuring minute changes in gravitational force or potential. This might involve techniques like atom interferometry, where clouds of ultra-cold atoms are used as test masses, providing extreme sensitivity to gravitational acceleration. By measuring the acceleration of these atoms over various distances, GDEM can test the $1/r^2$ nature of gravitational attraction with high precision.

The mission will measure the gravitational forces on a set of test masses over a range of heliocentric distances, looking for discrepancies from the expected $1/r^2$ behavior. Such discrepancies could manifest as additional forces, changes in the effective gravitational constant, or other anomalies. Detecting these would indicate new physical phenomena or modifications to gravity, such as those

predicted by theories of extra dimensions, modified gravity models, or the presence of exotic particles or fields.

The model-agnostic approach of GDEM means that its measurements are not specifically tailored to test any single theoretical prediction. Instead, the mission measurements can be sensitive to a wide range of possible deviations from Newtonian gravity, making it a versatile tool for testing the current understanding of gravity and searching for new phenomena. As new theories or models of gravity are developed, the data from GDEM can be re-analyzed or new measurement campaigns can be designed to test them, making the mission adaptable to the evolving landscape of gravitational physics. This flexibility is crucial for a field where theoretical innovation is ongoing and the true nature of gravity is still not fully understood.

5.5.2 Mid-band gravitational wave detection

GWs in the mid-frequency band addresses a critical gap between the frequency ranges covered by current ground-based and planned space-based detectors. Ground-based detectors like LIGO (Arm length of 4 km) and Virgo are sensitive to high-frequency gravitational waves, typically above 100 Hz, while space-based projects like LISA (arm length > $1x10^6$ km) are designed to detect low-frequency waves of mHz. For interferometers like LISA and LIGO of two-arm or triangle differential measurements, sweet spot in sensitivity scales like $\sim 1/L$. GDEM has the differential measurements are in four triangle planes simultaneously, equivalent to 4 LISA-like interferometers. It can naturally serve as GW detector with the necessary sensitivity. GDEM, with 1,000 km of arm length, would be most compelling operating in the mid-band ~0.03 – 1Hz. An initial consideration showed that each of the GDEM's LISA-like interferometer can reach a strain floor of $1x10^{-21}/\sqrt{Hz}$ at 0.1 Hz.

The mid-frequency band, ranging from approximately 0.01Hz to 1 Hz, remains largely unexplored by the current ground GWD and the planned space mission.

Detecting gravitational waves in this mid-band is crucial for several reasons:

1. *Intermediate-Mass Black Holes*: Observations in the mid-band are expected to be particularly sensitive to mergers involving intermediate-mass black holes (IMBHs), which are theorized to exist with masses between 100 and 10,000 solar masses. These objects are difficult to detect with electromagnetic observations, and their gravitational wave signatures would fall right into the mid-frequency band. Detecting these waves would not only confirm the existence of IMBHs but also provide insights into their formation and role in the evolution of galaxies and star clusters.
2. *Dense Star Systems:* The mid-band also includes gravitational waves emitted by dense star systems, such as white dwarf binaries or neutron stars in close orbits. These systems can provide precise tests of general relativity and insights into the extreme states of matter within neutron stars.
3. *Early Inspirals*: For supermassive black hole mergers, the early inspiral phase emits gravitational waves in the mid-band. Observing these early stages can provide a clearer picture of the dynamics and environments of these massive mergers, offering valuable data on the evolution of galaxies and the behavior of matter and spacetime in the most extreme conditions.

One of the intriguing prospects of GDEM as GW detector is the non-planar simultaneous measurement planes. This allows more comprehensive determination of polarizations and cross-correlations. LISA with its 3 arms is effectively two independent 2-arm interferometers. This allows

one to measure both polarizations, but nothing is gained by cross-correlating them. GDEM with its 4 arms allows us to use cross-correlation to dig out stochastic background (not just excess power). In principle this gives GDEM a very big advantage in searching for stochastic GWs from early universe. GDEM could reach down to $\Omega_{gw}(\mathrm{f}_0 = 0.1Hz) \sim 3 \times 10^{-13}$. The challenge will be the stochastic GW foreground from inspiraling BH-BH and NS-NS binaries which is estimated about two orders of magnitude in strength. Nevertheless, GDEM will be able to dig down somewhat deeper than this foreground since spectrum from binary foreground has a known shape, which is very different from very-early-universe sources. Possible early-universe stochastic sources would include GWs from a strongly first-order phase transition at $\sim 10^2$ Tev. GDEM would provide an opportunity to look for such phase transitions.

5.5.3 Dark matter detection

GDEM's capability to accurately measure gravitational effects plays a critical role in the potential detection of dark matter. Dark matter, an invisible substance that does not emit, absorb, or reflect light, is known to exert gravitational influence on visible matter, radiation, and the structure of the universe. Despite its elusive nature, dark matter's presence can be inferred from its gravitational effects on celestial bodies and the distribution of galaxies.

Here's how GDEM could contribute to dark matter detection and understanding:

1. *Gravitational Influence on Celestial Bodies*: Dark matter's gravitational pull affects the orbits of planets, moons, and other celestial bodies. By precisely measuring the orbits and motions of these bodies, GDEM could detect anomalies that suggest the presence of unseen mass, potentially attributable to DM. For example, if the observed orbital dynamics of objects in the outer solar system do not match predictions based on visible matter alone, this could indicate the influence of DM. GDEM's precise measurements could help map the distribution of this unseen mass and contribute to our understanding of its distribution within the solar system.
2. *Perturbations in the Gravitational Field:* Dark matter is expected to form large structures like halos, which can cause subtle perturbations in the gravitational field. GDEM's sensitive instrumentation could detect these perturbations as variations in the gravitational force or potential across different regions of space. By measuring the gravitational field with high precision, GDEM might detect the gravitational signature of DM structures or clumps. This could not only confirm the presence of DM but also provide insights into its clumping properties, density, and distribution.
3. *Constraints on Dark Matter Properties*: Precise gravitational measurements can provide constraints on the properties of dark matter, such as its mass, interaction cross-section, and distribution. By comparing observations with predictions from dark matter models, GDEM could help narrow down the range of viable theories or suggest new properties that dark matter must possess. Additionally, GDEM's measurements could be used to test alternative theories of gravity that aim to explain galactic rotation curves and other phenomena without invoking dark matter. By providing stringent tests of these theories, GDEM could help determine whether modifications to gravity or the presence of dark matter is a more plausible explanation for the observed gravitational effects.
4. *Dark Matter Direct Detection using Atom Interferometry*: For certain types of dark matter particle models (e.g., those that have very light masses and that interact with the Standard Model with a light mediator), GDEM would potentially directly detect dark matter. Dark matter particles could interact with the cold atom clouds within the atom interferometers aboard GDEM, leading to decoherence and phase effects. Because of its long baselines, interrogation times,

and placement in space, GDEM would be an ideal setup for this measurement. Indeed, recent work has shown that GDEM would have better constraints in certain parameter ranges than any existing limits on dark matter models like these (Du et al. 2022).

By focusing on the subtle gravitational signatures that dark matter is expected to produce, GDEM aims to contribute significantly to the detection and characterization of dark matter. Its precise measurements could help unravel the mystery of DM's nature and distribution, enhancing our understanding of its role in cosmic structure formation and the overall dynamics of the universe.

5.5.4 Tests of General Relativity

GDEM will provide an opportunity to test Einstein's theory of general relativity in the solar system. It may be used to test the foundations of relativistic gravitation on the solar system scales. It enables very powerful tests of long-range modifications of gravity. These measurements can help refine constraints on the range and coupling constant of Yukawa-type extensions of Newtonian gravity: effects due to such forces increase with distance, leading to a possible improvement by a factor of 100 compared to current results (Turyshev, 2008). Such an experiment can also help improve limits on the post-Newtonian parameters of generalized theories of gravitation, in particular Eddington's gamma-parameter, which measures the effects of spatial curvature.

Limits on the minimum acceleration a_0 and constraints on the interpolating function (g/a_0) of Modified Newtonian Dynamics (MOND) (Blanchet & Novak, 2011; Milgrom, 2014) can be refined, along with possible violations of the weak equivalence principle. Also, dark matter may influence the trajectories of spacecraft sufficiently far from the Sun (Belbruno & Green, 2022), thus providing conditions necessary for its detection and study.

With its acceleration sensitivity of 10^{-15} m/s^2, GDEM will be able to precisely measure gravity at large distances from the Sun would establish stringent limits on possible violations of Newtonian gravity while probing for the presence of dark matter in the outer solar system. It will be important for the validation of various theories of modified or massive gravity theories that are proposed as alternatives to dark matter or the cosmological constant. Experimental confirmation of new fundamental forces would provide an important insight into the physics beyond the Standard Model. These results will help bridge the presently extant gap between the data in the solar system and astronomical data obtained on scales that are several orders of magnitude larger, characterizing the dynamical gravitational behavior of star clusters and galaxies.

5.5.5 Detection of unknown terrestrial bodies

Another intriguing prospect of GDEM is the potential detection of unknown terrestrial bodies through their gravitational signatures. If there are undiscovered planets or large asteroids in the solar system, their gravitational effects on nearby objects or the overall gravitational field could be detected by GDEM. This could lead to the discovery of new celestial bodies within our own solar system, enhancing our understanding of its formation and evolution.

Over the past decade, robust scientific simulations have provided evidence suggesting the formation of a large Neptune-sized planet during the nascent stages of our solar system. The clustering of orbits for a group of extreme trans-Neptunian objects suggests the existence of an unseen planet of mass M ~5-10$M_\oplus$, the so-called *Planet 9*, at ~400-800 AU from the Sun (Batygin et al. 2019). Direct electromagnetic searches have not yet detected this *Planet 9*. The prevailing theory posits that approximately 4 billion years ago, concurrent with the era of giant planet migration, Planet 9 was ejected into a remote orbit of the Solar System.

This theory primarily draws support from observational data of the outermost Kuiper Belt Objects (KBOs). These distant KBOs exhibit highly elliptical orbits that are anomalously aligned within a similar plane. A notable feature of these orbits is an unexpected clustering in their arguments of perihelion. Such orbital characteristics are challenging to explain without postulating the gravitational influence of an unseen, substantial planetary body. Therefore, it is hypothesized that these orbital anomalies of the KBOs are the result of dynamic interactions with the proposed Planet 9.

Current models suggest that Planet 9, if it indeed exists, is likely situated near the galactic plane, directionally aligned with the constellation of Orion. Its orbit is theorized to be at an extreme distance from the Sun, ranging between 400-800 AU, with translates into acceleration 1.1×10^{-13} m/s^2 on GDEM spacecraft. With its acceleration sensitivity of $\sim 1\times 10^{-15}$ m/s^2, GDEM will be able to not only detect the presence of Planet 9, but also its position in the distant regions of the solar system.

As a result, GDEM's detailed gravitational field measurements within the solar system have far-reaching implications. From probing the internal structures of planets and the Sun to testing fundamental physics and potentially uncovering new celestial bodies, the mission is poised to significantly enhance our knowledge of the solar system's dynamics and composition.

6 SUMMARY AND RECOMMENDATIONS

Today physics stands at the threshold of major discoveries. Growing observational evidence points to the need for new physics. As a result, efforts to discover new fundamental symmetries, investigations of the limits of established symmetries, tests of the general theory of relativity, searches for gravitational waves, and attempts to understand the nature of dark matter and dark energy are among the main research topics in fundamental physics today (Turyshev et al., 2007).

The remarkable recent progress in observational cosmology has subjected the general theory of relativity to increased scrutiny by suggesting a non-Einsteinian scenario of the Universe's evolution. From a theoretical standpoint, the challenge is even stronger---if gravity is to be quantized, general relativity must be modified. Furthermore, recent advances in the scalar-tensor extensions of gravity, and brane-world gravitational models, along with efforts to modify gravity on large scales, are motivating new searches for experimental signatures of very small deviations from general relativity on various scales, including on the spacecraft-accessible distances in the solar system. These advances are motivating searches for very small deviations from Einstein's theory, at the level of three to five orders of magnitude below the level currently tested by experiment.

This progress was matched by the major improvements in measurement technologies. Today, a new generation of high-performance quantum sensors (e.g., ultra-stable atomic clocks, accelerometers, gyroscopes, gravimeters, gravity gradiometers) is surpassing previous state-of-the-art instruments, demonstrating the high potential of these techniques based on the engineering and manipulation of atomic systems. New quantum devices based on ultra-cold atoms will enable fundamental physics experiments testing quantum physics, physics beyond the Standard Model of fundamental particles and interactions, special relativity, gravitation and general relativity.

The Gravity Probe and Dark Energy Detection Mission (GDEM) is motivated and stands to benefit from this progress, thus providing us with a unique opportunity to explore the limits of fundamental physics. Our GDEM study conducted during NIAC Phase II has demonstrated at a conceptual level the scientific and technical feasibility of directly detecting Galileon signals of the dark energy field within the solar system. This mission, if realized, would not only shed light on the nature of dark energy but also provide critical data for testing gravity field theories beyond Newtonian

gravity. It has the potential to advance the search for ultra-light fields of dark matter and facilitate gravitational wave detections in the mid-band frequency spectrum.

However, bringing the GDEM concept to fruition presents substantial technical challenges, arguably surpassing those of missions like LISA in terms of laser ranging, drag-free control, and spacecraft formation flight. One of the main challenges lies in suppressing gravity effects by ten orders of magnitude, which is central to the direct detection of dark energy. The proposed strategy of measuring the trace of the field force gradient tensor offers a way to eliminate gravity effects in principle, shifting the focus to controlling and reducing systematic errors in the measurements. Further improvements in measurement sensitivity could be achieved by reducing high-order systematics from gravity effects with correction coefficient measurements. Additionally, controlling systematics from the measurement instrument itself is crucial, which is expected to be more manageable in the microgravity environment of space, aided by common mode rejection schemes used.

The mission architecture design plays a significant role in reducing measurement systematics. For instance, modulating the dark energy signal to a higher frequency could mitigate errors due to biases and drifts, which are common in DC measurements. This modulation could be achieved through a better understanding of the spatial variations of the dark energy signal in the solar system and designing mission measurement orbits accordingly.

A significant part of the study involves simulating the dark energy field to understand how it is affected by massive bodies in the solar system. The nonlinear nature of Galileon fields makes numerical simulations challenging, often leading to instability or artifacts. The study has so far focused on analytical solutions around spherical bodies and avoided regions close to planets where the Sun's influence dominates the Galileon signal. Exploring regions of signal enhancement in multi-body settings and natural signal modulations are part of the ongoing research. Developing a reliable three-dimensional numerical simulation package for arbitrary mass distribution will aid in refining the mission concept, requirements, and expected scientific return.

Key technologies enabling the GDEM concept include atomic test masses operated as atomic interferometers in free space vacuum, away from spacecraft. These interferometers provide the necessary measurement stability for such an endeavor. While most required operation schemes for atom interferometers have been demonstrated in research labs, high-flux, high-speed BEC production remains to be achieved. Demonstrating atom interferometer operation in free space vacuum may require a technology demonstration mission, possibly at a cis-lunar gateway.

Laser ranging interferometry, like that used in LISA, is crucial for differential gravity measurements. This technology, already demonstrated in GRACE-FO mission, requires even higher precision for dark energy measurement. The high precision of absolute ranging measurements at the micrometer level, routinely done in laboratories, will need to be validated over long distances.

The GDEM mission concept for the direct detection of dark energy, particularly for the cubic Galileon of the Sun, is scientifically sound and technically feasible based on current estimations. It identifies areas of technology that need advancement or demonstration for mission realization. GDEM promises not just to validate or disprove the cubic Galileon theory but also to contribute significantly to our understanding of fundamental physics, astrophysics, and cosmology.

It is worth emphasizing that the GDEM mission concept is envisioned and timed to mature alongside and complement current and upcoming observational missions like Euclid and the Roman Space Telescope. As these telescopes expand our understanding of the universe, particularly in dark matter and dark energy, GDEM aims to fill in critical gaps with its unique capabilities in measuring the GGT. To align with these missions, GDEM will focus on specific phenomena or

regions that are inaccessible or not optimally covered by them, thereby pushing the envelope of our understanding of gravity and cosmic evolution. This approach ensures that GDEM not only contributes to but also significantly extends the scientific legacy of current space-based observatories.

In alignment with the recent 2023 Biological and Physical Science Decadal Survey report and the recommended PFaST (Probe Fabric of Space and Time) campaign, GDEM is positioned to advocate and implement advanced quantum sensors in space as well as meet the science objectives. Enabling quantum technologies, particularly atom-wave interferometers operating at sensitivities around $\sim 10^{-15}$ m/s^2/$\sqrt{\text{Hz}}$, are at the forefront of precision measurement and fundamental physics research. By integrating these quantum sensors, GDEM will not only pursue its primary scientific objectives but also serve as a testbed for technology maturation, paving the way for future missions and incremental scientific discoveries. The mission's adherence to the recommendations of the BPS decadal report ensures its relevance and impact within the wider scientific community.

Addressing high-risk items and technological challenges is a critical component of GDEM's development. Identified risks from Phase II studies, particularly in 1) implement and operate high precision atom interferometers in open space vacuum, and 2) the precision laser ranging systems and the long-term operational stability of Sagnac interferometers, require focused research and development to advance their readiness levels. Collaborative efforts with industry and academia will be key to innovating and refining these technologies. There are many upcoming opportunities that space atom interferometers to being matured, from today's NASA BPS Cold Atom Laboratory on ISS to its follow-on by BECCAL, a bilateral NASA-DLR collaboration, to the NASA Earth Science Quantum Gravity Gradiometer (QGG) technology pathfinder mission being planned, to post-ISS NASA CLDs (commercial Low Earth Orbit destinations), as well as many other similar mission developments from space agencies in Europe and around the world. The more ambitious GDEM mission can leverage and build on these progresses. Furthermore, a robust risk mitigation strategy, including alternative approaches and redundancy plans, will ensure GDEM mission's resilience and success. By systematically addressing these technical challenges and aligning with broader scientific initiatives, GDEM stands to make substantial contributions to our understanding of gravitational physics and the fundamental forces shaping our universe.

In conclusion, the comprehensive studies and analyses conducted for the GDEM during our NIAC Phase II effort have validated its feasibility and underscored its potential to significantly advance our understanding of gravitational physics. The mission is well-aligned with current scientific objectives in astrophysics and cosmology, complementing and extending the capabilities of existing and planned observational missions. It is also well aligned to answer key scientific questions for the Fundamental Physics Program in NASA BPS. The key technologies required for GDEM, including precision laser ranging systems, atom-wave interferometers, and Sagnac interferometers, either already exist or are in active development, promising a high degree of technical readiness and reliability in the decade. The mission's innovative approach, coupled with the ongoing advancements in space technology, positions GDEM as a viable and valuable mission. It is poised to open new frontiers in our quest to understand the universe's fundamental forces, making it an exciting and promising venture in space science and exploration. As we look forward to the mission's progress and eventual launch, GDEM represents a significant step forward in our continuous journey to unravel the mysteries of the cosmos.

7 Acknowledgement

We would like to express our gratitude to our many colleagues who have either collaborated with us on this report or given us their wisdom. We specifically thank Viktor T. Toth who provided us with very valuable comments, encouragement, support and stimulating discussions while this report was in preparation.

Finally, we are especially thankful to NASA Innovative Advanced Concepts (NIAC) for their support for our work in the pursuit of an exciting objective – using the SGL for direct high-resolution imaging and spectroscopy of a potentially habitable exoplanet.

The work described here was carried out at the Jet Propulsion Laboratory, California Institute of Technology, under a contract with the National Aeronautics and Space Administration.

8 Institution Required Disclaimer

This report contains Pre-Decisional Information -- For Planning and Discussion Purposes Only

9 References and Citations

Adelberger, E.G., B. R. Heckel and A. E. Nelson, "Tests of the gravitational inverse square law," Annual Review of Nuclear and Particle Science, vol. 53, pp. 77-121, 12 (2003).

Andrews, M., Y.-Z. Chu, and M. Trodden, Phys. Rev. D 88, 084028 (2013).

Armano, M., H. Audley, J. Baird, P. Binetruy, M. Born, D. Bortoluzzi, E. Castelli, A. Cavalleri, A. Cesarini, A. Cruise, K. Danzmann, M. Deus Silva, I. Diepholz, G. Dixon, R. Dolesi, L. Ferraioli, V. Ferroni, E. Fitzsimons, M. Freschi, L. Gesa, F. Gibert, D. Giardini, R. Giusteri, C. Grimani, J. Grzymisch, I. Harrison, G. Heinzel, M. Hewitson, D. Hollington, D. Hoyland, M. Hueller, H. Inchauspé, O. Jennrich, P. Jetzer, N. Karnesis, B. Kaune, N. Korsakova, C. Killow, J. Lobo, I. Lloro, L. Liu, J. López-Zaragoza, R. Maarschalkerweerd, D. Mance, N. Meshksar, V. Martín, L. Martin-Polo, J. Martino, F. Martin-Porqueras, I. Mateos, P. McNamara, J. Mendes, L. Mendes, M. Nofrarias, S. Paczkowski, M. Perreur-Lloyd, A. Petiteau, P. Pivato, E. Plagnol, J. Ramos-Castro, J. Reiche, D. Robertson, F. Rivas, G. Russano, J. Slutsky, C. Sopuerta, T. Sumner, D. Texier, J. Thorpe, D. Vetrugno, S. Vitale, G. Wanner, H. Ward, P. Wass, W. Weber, L. Wissel, A. Wittchen and P. Zweifel, "Beyond the Required LISA Free-Fall Performance: New LISA Pathfinder Results down to 200.167em0.167emHz," Physical Review Letters, vol. 120, 2 (2018).

Batygin K., Adams K. F., Brown M. E., Becker J., Phys. Reps., 805, 1 (2019)

Barrett, B., L. Antoni-Micollier, L. Chichet, B. Battelier, T. Lévèque, A. Landragin and P. Bouyer, "Dual matter-wave inertial sensors in weightlessness," Nature Communications, vol. 7, 12 (2016).

Becker, D., M. D. Lachmann, S. T. Seidel, H. Ahlers, A. N. Dinkelaker, J. Grosse, O. Hellmig, H. Müntinga, V. Schkolnik, T. Wendrich, A. Wenzlawski, B. Weps, R. Corgier, T. Franz, N. Gaaloul, W. Herr, D. Lüdtke, M. Popp, S. Amri, H. Duncker, M. Erbe, A. Kohfeldt, A. Kubelka-Lange, C. Braxmaier, E. Charron, W. Ertmer, M. Krutzik, C. Lämmerzahl, A. Peters, W. P. Schleich, K. Sengstock, R. Walser, A. Wicht, P. Windpassinger and E. M. Rasel, "Space-borne Bose–Einstein condensation for precision interferometry," Nature, vol. 562, pp. 391-395, 10 (2018).

Berezhiani, Z., F. Nesti, L. Pilo, and N. Rossi, 2009, 083 (2009).

Berman, P.R., and V. Kharchenko, Atom interferometry, AIP, 1997.

Belbruno, E., and J. Green, MNRAS 510, 5154 (2022).

Blanchet, L., and J. Novak, Mon. Not. R. Astron. Soc. 412, 2530 (2011).

Copeland, E.J., M. Sami and S. Tsujikawa, "Dynamics of Dark Energy," International Journal of Modern Physics D, vol. 15, pp. 1753-1935, (2006).

Creminelli, P., and F. Vernizzi, "Dark Energy after GW170817 and GRB170817A," Physical Rev. Letters, vol. 119, 12 (2017).

Crisostomi, M., and K. Koyama, "Vainshtein mechanism after GW170817," Physical Review D, vol. 97, 1 (2018).

Chiow, S.-w., and N. Yu, "Multiloop atom interferometer measurements of chameleon dark energy in microgravity," Physical Review D, vol. 97, p. 044043 (2018).

Chiow, S.-w., J. Williams and N. Yu, "Laser-ranging long-baseline differential atom interferometers for space," Physical Review A, vol. 92, 12 (2015).

Chiow, S.-w., T. Kovachy, H.-C. Chien and M. A. Kasevich, "102ℏkLarge Area Atom Interferometers," Physical Review Letters, vol. 107, 9 (2011).

Chiow, S.-w., J. Williams and N. Yu, "Noise reduction in differential phase extraction of dual atom interferometers using an active servo loop," Physical Review A, vol. 93, p. 013602 (2016).

Chiow, S.-w., and N. Yu, "Compact atom interferometer using single laser," Applied Physics B, vol. 124, 5 (2018).

Chiow, S.-w and Yu, N., “”, submitted (2024)

Du, Y., C. Murgui, K. Pardo, Y. Wang, K.M. Zurek, "Atom Interferometer Tests of Dark Matter," Physical Review D, **106** (9), id.095041 (2022).

Elder, B., J. Khoury, P. Haslinger, M. Jaffe, H. Müller and P. Hamilton, "Chameleon dark energy and atom interferometry," Phys. Rev. D, vol. 94, no. 4, p. 044051, 8 (2016).

Estey, B., C. Yu, H. Müller, P.-C. Kuan and S.-Y. Lan, "High-Resolution Atom Interferometers with Suppressed Diffraction Phases," Physical Review Letters, vol. 115, 8 (2015).

Gao, D.-F., J. Wang and M.-S. Zhan, "Atomic Interferometric Gravitational-Wave Space Observatory (AIGSO)," Communications in Theoretical Physics, vol. 69, p. 37, 1 (2018).

Graham, P.W., J. M. Hogan, M. A. Kasevich, S. Rajendran and R. W. Romani, "Mid-band gravitational wave detection with precision atomic sensors," 6 11 (2017), https://arxiv.org/abs/1711.02225.

Pitjeva, E.V., "Determination of the Value of the Heliocentric Gravitational Constant ($GM_{\odot}$) from Modern Observations of Planets and Spacecraft," Journal of Physical and Chemical Reference Data, vol. 44, p. 031210, 9 (2015).

Peters, A., K. Y. Chung and S. Chu, "High-precision gravity measurements using atom interferometry," Metrologia, vol. 38, p. 25 (2001).

Rudolph, J., W. Herr, C. Grzeschik, T. Sternke, A. Grote, M. Popp, D. Becker, H. Müntinga, H. Ahlers, A. Peters, C. Lämmerzahl, K. Sengstock, N. Gaaloul, W. Ertmer and E. M. Rasel, "A high-flux BEC source for mobile atom interferometers," New Journal of Physics, vol. 17, p. 065001, 6 2015. Sereno, M., and P. Jetzer, "Solar and stellar system tests of the cosmological constant," Physical Review D, vol. 73, 3 (2006).

Hamilton, P., M. Jaffe, P. Haslinger, Q. Simmons, H. Müller and J. Khoury, "Atom-interferometry constraints on dark energy," Science, vol. 349, pp. 849-851 (2015).

Haslinger, P., M. Jaffe, V. Xu, O. Schwartz, M. Sonnleitner, M. Ritsch-Marte, H. Ritsch and H. Müller, "Attractive force on atoms due to blackbody radiation," arXiv preprint arXiv:1704.03577, 2017.

Hogan, J. M., D. M. S. Johnson, S. Dickerson, T. Kovachy, A. Sugarbaker, S.-w. Chiow, P. W. Graham, M. A. Kasevich, B. Saif, S. Rajendran and others, "An atomic gravitational wave interferometric sensor in low earth orbit (AGIS-LEO)," General Relativity and Gravitation, vol. 43, pp. 1953-2009 (2011).

Hogan, J.M., and M. A. Kasevich, "Atom-interferometric gravitational-wave detection using heterodyne laser links," Physical Review A, vol. 94, 9 (2016).

Hiramatsu, T., W. Hu, K. Koyama and F. Schmidt, "Equivalence principle violation in Vainshtein screened two-body systems," Physical Review D, vol. 87, 3 (2013).

Hu, J., A. Urvoy, Z. Vendeiro, V. Crépel, W. Chen and V. Vuletić, "Creation of a Bose-condensed gas of87Rb by laser cooling," Science, vol. 358, pp. 1078-1080, 11 (2017).

Joyce, A., B. Jain, J. Khoury and M. Trodden, "Beyond the cosmological standard model," Physics Reports, vol. 568, pp. 1-98 (2015).

Jaffe, M., P. Haslinger, V. Xu, P. Hamilton, A. Upadhye, B. Elder, J. Khoury and H. Müller, "Testing sub-gravitational forces on atoms from a miniature in-vacuum source mass," Nature Physics, vol. 13, pp. 938-942 (2017).

Kasevich, M., and S. Chu, "Atomic interferometry using stimulated Raman transitions," Physical review letters, vol. 67, p. 181 (1991).

Ketterle, W., D. S. Durfee and D. M. Stamper-Kurn, "Making, probing and understanding Bose-Einstein condensates," 2, 4 (1999), https://arxiv.org/abs/cond-mat/9904034.

Kalaydzhyan, T., and N. Yu, "Extracting dark matter signatures from atomic clock stability measurements," Physical Review D, vol. 96, 10 (2017).

Kalaydzhyan, T., and N. Yu, "Searching for Stochastic Background of Ultra-Light Fields with Atomic Sensors," Universe, vol. 4, p. 99, 9 2018.

Kovachy, N., P. Asenbaum, C. Overstreet, C. A. Donnelly, S. M. Dickerson, A. Sugarbaker, J. M. Hogan and M. A. Kasevich, "Quantum superposition at the half-metre scale," Nature, vol. 528, pp. 530-533, 12 (2015).

Kovachy, T., J. M. Hogan, A. Sugarbaker, S. M. Dickerson, C. A. Donnelly, C. Overstreet and M. A. Kasevich, "Matter Wave Lensing to Picokelvin Temperatures," Physical Review Letters, vol. 114, 4 (2015).

Milgrom, M., Scholarpedia 9, 31410 (2014).

Müller, H., S.-w. Chiow and S. Chu, "Atom-wave diffraction between the Raman-Nath and the Bragg regime: Effective Rabi frequency, losses, and phase shifts," Physical review A, vol. 77, p. 023609, 2008.

Sakstein, J., "Tests of Gravity with Future Space-Based Experiments," arXiv preprint arXiv:1710.03156, 2017.

Turyshev, S. G., U. E. Israelsson, M. Shao, N. Yu, A. Kusenko, E. L. Wright, C. W. F. Everitt, M. Kasevich, J. A. Lipa, J. C. Mester, et al., Int. J. Mod. Phys. D 16, 1879 (2007)

Turyshev, S.G., Ann. Rev. Nucl. Part. Sci. 58, 207 (2008).

Turyshev, S.G., Chiow, S-w., Yu, N., "Searching for new physics in the solar system with tetrahedral spacecraft formations," Phys. Rev. D **109**, 084059. https://doi.org/10.48550/arXiv.2404.02096. (2024).

While, Nicholas C., Troian, Sandra M., Jewell, Jeffrey B., Cutler, Curt J., Chiow, Sheng-wey, and Yu, Nan, "Robust numerical computation of the 3D scalar potential field of the cubic Galileon gravity model at solar system scales," Nicholas C. White, Sandra M. Troian, Jeffrey B. Jewell, Curt J. Cutler, Sheng-wey Chiow, and Nan Yu, Phys. Rev. D. 102, 024033, arXiv:2003.02648 [physics.comp-ph]. (2020).

Yu, Nan, "Direct probe of dark energy interactions with a Solar System laboratory," NIAC Phase 1 Final Report (2018). https://ntrs.nasa.gov/api/citations/20190002500/downloads/20190002500.pdf.

10 Appendix: List of Acronyms

List of Acronyms used in the Proposal:

AI	Atom Interferometer
AU	Astronomical unit
BCRS	Barycentric Coordinate Reference System
BEC	Bose Einstein Condensate
BECCAL	Bose Einstein Condensate Cold Atom Laboratory
BPS	Biological and Physical Sciences
CAL	Cold Atom Laboratory
CLD	Commercial Low Earth Orbit destination
CONOPS	Concept of operations
DLR	German Space Agency
GDEM	Gravity Probe and Dark Energy Detection Mission
GGT	Gravity gradient tensor
GR	general theory of relativity
LISA	Laser Interferometer Space Antenna
LRI	Laser ranging interferometer
ISL	Inverse square law
ISS	International Space Station
JPL	Jet Propulsion Laboratory
mas/uas/nas	milli-arcsecond / micro-arcsecond / nano-arcsecond
NASA	National Aeronautics and Space Administration
PSF	point-spread function
QGG	Quantum Gravity Gradiometer
RTG	Radioisotope Thermal Generator
s/c	spacecraft
SME	Subject matter expert
SNR	signal-to-noise ratio
TRL	Technology Readiness Level
UV	Ultraviolet